



venterra

Helping wind power grow

Kriegers Flak II North – Integrated 3D GeoModel



ENERGINET

Client	Energinet
Document Ref.	24004-REP-002-03
Project Title	Kriegers Flak II North
Date	04/09/2024

Project Title:	Kriegers Flak II North
Project Reference	24004-REP-002-03
Report Title:	Kriegers Flak II North –Integrated 3D GeoModel
Document Reference	24004-REP-002-03
Client Report Reference	24004-REP-002-03

Client:	Energinet
Ultimate Client:	Energinet
Confidentiality	Client Confidential

REVISION HISTORY

Rev	Date	Reason for Issue	Originator	Checker	Reviewer	Approver
[00]	02/08/2024	Draft	JM, EM, GM, MG	TB	GMcA,TJ	LT
01	07/08/2024	Draft, Geotechnical Parameters included	JM, EM, GM, MG	AL	TJ	LT
02	26/08/2024	Updated to address client comments	JM, EM, GM, MG	TB	GMcA,TJ	GMcA,TJ
03	04/09/2024	Updated to address client comments	JM, EM, GM, MG	TB	JQ	TJ

DISCLAIMER

Gavin & Doherty Geosolutions Ltd (GDG), part of the Venterra Group, has prepared this report for the sole use of Energinet (hereafter the “Client”) in accordance with the terms of a contract between the Client and GDG. No other warranty, expressed or implied, is made as to the professional advice contained in the report or any other services provided by GDG. Any party other than our Client that relies upon this report in whole or in part does so at their own risk. GDG assumes no liability or duty of care to any third party in respect of or arising out of or in connection with this report and/or the professional advice contained within.

This report is the copyright of GDG. All rights reserved.

TABLE OF CONTENTS

Chapter	Page
Table of Contents	3
Executive Summary	12
1 Introduction	14
1.1 Purpose and Scope of Work	14
1.2 Limitations and Exclusions	14
1.3 Geodetic Information	15
1.4 Vertical Datum	15
1.5 Summary of Previous Studies and Site-Specific Reports	15
2 The Site	17
3 Method Description and Deliverables	18
4 Geological Background and Previous Studies	20
4.1 Preliminary Ground Model (GEOxyz, 2024)	20
4.2 Geotechnical Site Investigation (Gardline, 2024)	21
4.3 Regional Geological Background	21
4.3.1 Regional Geological History	21
4.3.1.1 Pre-Quaternary	21
4.3.1.2 Quaternary	25
4.3.2 Expected Seabed Sediments	33
4.4 Conceptual Geological Model	33
5 Integrated 3D GeoModel Development	37
5.1 Geophysical Survey - Interpretation Refinement	39
5.1.1 UHRS Data Quality Grading	39
5.2 Geotechnical Data Summary	41
5.3 Geotechnical Data Integration	42
5.4 Velocity Model Revision	46
5.5 Gridding and Depth Conversion	49
5.5.1 Gridding	49
5.5.2 SEGY Depth Conversion	50
6 Discussion Of Spatial Integrated 3D GeoModel	52
6.1 Seafloor Interpretation	52
6.1.1 Multibeam Echosounder Bathymetry and Slope	52
6.1.2 Side Scan Sonar	55
6.1.3 Seafloor Lithology	58
6.1.4 Seafloor Morphology	60
6.1.5 Seafloor Objects	62
6.1.6 Magnetic Anomalies	63
6.2 Sub-seafloor Interpretation	64
6.2.1 Seismic Unit I (SU I) - Marine Sediments	69
6.2.1.1 Geophysical Description	69
6.2.1.2 Spatial Distribution	69
6.2.1.3 Geotechnical Description	71
6.2.1.4 Interpretation	71

6.2.2	Seismic Unit III (SU III) – Glaciolacustrine	74
6.2.2.1	Geophysical Description	74
6.2.2.2	Spatial Distribution	74
6.2.2.3	Geotechnical Description	76
6.2.2.4	Interpretation	76
6.2.3	Seismic Unit IV (SU IV) – Glacial	80
6.2.3.1	Geophysical Description	80
6.2.3.2	Spatial Distribution	80
6.2.3.3	Geotechnical Description	82
6.2.3.4	Interpretation	82
6.2.4	Seismic Unit V (SU V) – Chalk	85
6.2.4.1	Geophysical Description	85
6.2.4.2	Spatial Distribution	85
6.2.4.3	Geotechnical Description	85
6.2.4.4	Interpretation	86
6.2.5	Geological Units Summary	89
6.3	Soil Zonation	91
6.4	Geotechnical Unitisation	94
6.5	Integrated 3D GeoModel Uncertainty	94
6.6	Statistical Correlation of GI with Geophysical Data	97
7	Geotechnical Parameters	98
7.1	General	98
7.2	Geotechnical Soil Parameters	98
7.3	Recommended Parameter Bounding Framework	99
7.4	Interpretation Strategy	100
7.5	Selection of CPT Classification Method	100
7.5.1	General	100
7.5.2	Soil Classification Based on CPT Data	101
7.6	Summary of Laboratory Tests	102
7.7	Geotechnical Properties	103
7.8	Engineering Properties	105
7.9	Cone Penetration Test Parameters	105
7.9.1	General	105
7.9.1.1	Relative Density	107
7.9.2	Static Undrained Shear Strength	107
7.9.3	Remoulded Undrained Shear Strength	107
7.9.4	Sensitivity	108
7.9.5	Stress History and Consolidation	108
7.9.5.1	Overconsolidation Ratio	108
7.9.6	Coefficient of Lateral Earth Pressure at Rest	109
7.9.7	Effective Stress Parameters	110
7.9.7.1	General	110
7.9.8.1	P-S logging	111
7.9.8.2	Seismic CPT	111
7.9.8.3	CPT Data	111

7.9.8.4	Small Strain Shear Modulus	111
7.9.8.5	Strain at 50% Peak Deviator Stress	111
7.10	Rock Parameters	112
7.10.1	General	112
7.10.2	RQD	112
7.10.3	Point Load Tests	112
7.10.4	Unconfined Compressive Strength	112
7.10.5	Intact Youngs Modulus	113
8	Hazards And Geohazards	114
8.1	Seafloor Hazards	114
8.1.1	Boulders and Debris	114
8.1.2	Depressions	115
8.1.3	Seafloor Scarring	115
8.1.4	Slope	115
8.1.5	Wrecks	115
8.1.6	Cables/Pipes	116
8.1.7	Other	116
8.2	Sub-Seafloor Hazards	116
8.2.1	Boulders and Coarse Sediments	116
8.2.2	Shallow Gas	116
8.2.3	Channels and Channel Infill	118
8.2.4	Faults and Faulting	118
8.2.5	Glacial Features	119
8.2.6	Low Strength Sediments	119
8.2.7	Shallow Bedrock	119
9	Risk Register	120
10	Recommendations	122
10.1.1	Desk Studies	122
10.1.2	Data Re-processing	122
10.1.3	Further Survey and Investigations	122
11	Conclusions	124
12	References	127
13	Appendices	130
	Appendix A – Charts and Digital Deliverables	130
	Appendix B - Seismic Cross Sections	131
	Appendix C - Unitised Geotechnical Parameters	131
	Appendix D - Risk Register	131
	Appendix E – Geotechnical Cross Sections	131

LIST OF TABLES

Table 1-1 - Geodetic parameters	15
Table 4-1 - Shallow geological units (GEOxyz, 2024)	20
Table 4-2 - Regional Quaternary stratigraphy and seismic facies	30
Table 4-3 - Conceptual geological model summary	34
Table 5-1 - Revised seismic interpretation of the geophysical data	39
Table 5-2 - Correlation between seismic and geotechnical tops	45
Table 5-3 – Geotechnical and seismic data offsets	45
Table 5-4 - Velocity model parameters	47
Table 5-5 - Final velocity model	49
Table 6-1 - Sediment classification based on MBES backscatter analysis	60
Table 6-2 - Overview of the interpreted units	66
Table 6-3 - Geological units summary	90
Table 6-4 - Defined provinces	91
Table 6-5 - Ground conditions and design challenges at each Province	93
Table 6-6 - Geomodel uncertainties	95
Table 6-7 - Statistical correlation between GI and geophysical data	97
Table 7-1 - Geotechnical soil and rock parameters determined	98
Table 7-2 CPT classification	102
Table 7-3 - Types and number of tests available at time of reporting (Gardline, 2024)	103
Table 7-4 - Measured and derived CPT parameters	106

LIST OF FIGURES

Figure 1-1 - Danish Offshore Wind Farms (www.ens.dk)	14
Figure 2-1 - The proposed Kriegers Flak II Northern OWF site overview (Flanders Marine Institute, 2023)	17
Figure 4-1 - Geological schematic, general arrangements of units (GEOxyz, 2024)	20
Figure 4-2 - Regional setting, modified from Graversen (2009). AOI – Area of Interest	22
Figure 4-3 - Pre-Quaternary deposits (lithology) and faults (EMODnet, 2024)	23
Figure 4-4 - Pre-Quaternary deposits (age) and faults (EMODnet, 2024)	23
Figure 4-5 - Pre-Quaternary deposits (age) and faults (DGU, 1992; GEUS, 2024)	24
Figure 4-6 - Top pre-Quaternary surface elevation (Binzer, et al., 1994; GEUS, 2024)	25
Figure 4-7 - Ice margin evolution (Pedersen, 1998; GEUS, 2024)	26
Figure 4-8 - Danish region palaeogeography from 18 to 12 ka BP; modified from GEUS (2022; 2023)	27
Figure 4-9 - Danish region palaeogeography from 11.5 to 7 ka BP; modified from GEUS (2022; 2023)	28
Figure 4-10 - Quaternary deposits age (EMODnet, 2024)	32
Figure 4-11 - Quaternary deposits lithology (EMODnet, 2024)	32
Figure 4-12 - Seabed sediments – Folk 7 (EMODnet, 2024)	33
Figure 4-13 - Conceptual geological model	36
Figure 5-1 - IGM development workflow	38
Figure 5-2 - UHRS line paths and data quality grades	41
Figure 5-3 - Geotechnical site investigation locations overview (Gardline, 2024)	42
Figure 5-4 - Comparison of pre (a) and post (b) geotechnical interpretation integration, extracted from SBP line ‘0048_A_KN_GO5_L030’ at location KFII_N_13_BH	44
Figure 5-5 - Comparison of pre (a) and post (b) geotechnical interpretation integration, extracted from SBP line ‘A_KN_L022_UHR_T_MIG_STK’ at location KFII_N_23_BH	44
Figure 5-6 - Seismic unit velocity model	48

Figure 6-1 - Hillshaded MBES bathymetry	52
Figure 6-2 - MBES derived slope	53
Figure 6-3 - Areas of increased slope angle	54
Figure 6-4 - Bathymetry with hillshade	54
Figure 6-5 - Side scan sonar (GEOxyz, 2024)	55
Figure 6-6 - Seafloor features identified as potential wrecks as shown by the SSS data	56
Figure 6-7 - Circular objects identified on SSS and backscatter data	57
Figure 6-8 - Bathymetry profiles through the observed features	57
Figure 6-9 - Overview of the seabed lithology classification and extents (GEOxyz, 2024; Gavin and Doherty Geosolutions Ltd., 2024)	58
Figure 6-10 - MBES backscatter (GEOxyz, 2024)	59
Figure 6-11 - Overview of seabed features (GEOxyz, 2023; refined by Gavin and Doherty Geosolutions Ltd., 2024)	61
Figure 6-12 - Example of undulated seabed and other seabed features	62
Figure 6-13 - Example of seafloor contacts picked on SSS and MBES bathymetry	63
Figure 6-14 - Magnetic contacts and offshore infrastructure (HELCOM, 2018)	64
Figure 6-15 - Schematic diagram showing seismic unit distribution west to east in the survey area	68
Figure 6-16 - Top of Unit I elevation (mMSL)	70
Figure 6-17 - Unit I vertical thickness isochore	70
Figure 6-18 - Interpretation of SBP line '0003_A_KN_GO5_L052'	72
Figure 6-19 - Interpretation of SBP line '0048_A_KN_GO5_L030' with GI location KFII_N_13_BH	73
Figure 6-20 - Top of Unit III elevation (mMSL)	75
Figure 6-21 - Unit III vertical thickness isochore	75
Figure 6-22 - Interpretation of SBP line '0097_A_KN_GO5_L046A'	78
Figure 6-23 - Interpretation of SBP line '0057_A_KN_GO5_L016' with GI location KFII_N_DCPT24	79
Figure 6-24 - Top of Unit IV elevation (mMSL)	81
Figure 6-25 - Unit IV vertical thickness isochore	81
Figure 6-26 - Interpretation of SBP line 'A_KN_L023_UHR_T_MIG_STK'	83
Figure 6-27 - Interpretation of UHRS line 'A_KN_L022_UHR_T_MIG_STK' with GI location KFII_N_23_BH	84
Figure 6-28 - Top of Unit V elevation (mMSL)	85
Figure 6-29 - Interpretation of SBP line 'A_KN_L008_UHR_T_MIG_STK'	87
Figure 6-30 - Interpretation of UHRS line 'A_KN_L036_UHR_T_MIG_STK' with GI location KFII_N_DCPT16	88
Figure 6-31 Geotechnical zonation provinces	92
Figure 7-1 - Roberston (2009) classification	101
Figure 7-2 - Schneider et al (2008) classification	101
Figure 8-1 - Section of line '1437_C_KN_G06_L509V' seafloor targets interpreted as boulders	115
Figure 8-2 - Section of line '0041_A_KN_GO5_L033' showing partial acoustic blanking	117
Figure 8-3 - Section of line '1185_C_KN_G06_L721V' showing a possible flare	117
Figure 9-1 - Risk matrix	121

LIST OF ABBREVIATIONS

Abbreviations	
Abbreviation	Description
ALARP	As Low As Reasonably Practicable
BE	Best Estimate
BH	Borehole
BP	Before Present
CIUc, CIDc, CAUc	Consolidated Triaxial
CPT	Cone Penetrometer Testing
CPTU	Cone Penetrometer Testing with Pore Water
DSS	Direct Simple Shear
EEZ	Exclusive Economic Zone
EMODnet	European Marine Observation and Data Network
EPSG	European Petroleum Survey Group
GDG	Gavin and Doherty Geosolutions
GEUS	Geological Survey of Denmark and Greenland
GI	Geotechnical Investigation
GM	Ground Model
GRS	Grid Reference System
HE	High Estimate
HF, LF SSS	High, Low Frequency Side Scan Sonar
IGM	Integrated 3D GeoModel
LE	Lower Estimate
LL	Liquid Limit
MAG	Magnetometer
MBES	Multibeam Echosounder
mBSF	Metres Below seafloor
MCS	Multi-Channel Seismic
MD	Measured Depth
MLV	Miniature Lab Vanes
MSL	Mean Sea Level
OCR	Overconsolidation Ratio
OWF	Offshore Wind Farm
PGM	Preliminary Ground Model
PL	Plastic Limit
PLT	Point Load Test (Point Load Index)
PP	Pocket Penetrometers
PSD	Particle Size Distribution
pUXO	Potential UXO
SBP	Sub Bottom Profiler
SCPT	Seismic Cone Penetration Test
SCS	Single-Channel Seismic
SQL	Structured Query Language
SSS	Side Scan Sonar
TC	Thermal Conductivity
TV	Torvane
TWTT	Two-way Travel Time

Abbreviations	
Abbreviation	Description
UCS	Unconfined Compressive Strength
UHRS	Ultra-High Resolution Seismic
UTM	Universal Transverse Mercator
UU	Unconsolidated Undrained Triaxial
UXO	Unexploded Ordnance

GLOSSARY OF TERMS

Glossary of Terms	
Item	Description
Artefact	A non-geological feature present in hydrographic or geophysical data because of data acquisition and/or processing. E.g. busts – where adjacent survey data are not vertically aligned giving the false impression of a step in the surface being represented
Cone Penetrometer Testing	This testing measures Tip Resistance, Sleeve Friction, Pore Pressure of a sensor lowered into the ground. Calculations with these values can give indications of sediment classification.
Diamict/Diamicton	A sediment that is unsorted to poorly sorted and contains particles ranging in size from clay to boulders, suspended in an unconsolidated matrix of mud or sand.
Folk Substrate Classification	A scheme for classifying seafloor sediment types
Geological Unit	A volume of sediments/rock with similar petrographic and lithological characteristics.
Isochore	Isochore are grids that represent the vertical thickness of a layer or unit in metres; not to be confused with the depth of a unit interface that is presented as metres below seafloor.
Isochron	Isochrons are grids that represent the vertical thickness of a layer or unit in Two-way travel time.
Kingdom	Seismic data interpretation software
Multi-Channel Seismic	A seismic survey system that typically uses one or many towed high-power sources to transmit low frequency acoustic signals into the sub-seafloor where its reflections are detected by receivers along a towed streamer. These systems can provide good penetration below seabed at high resolution.
Multibeam Echosounder	This sensor transmits an acoustic signal to the seafloor, time taken allows for Bathymetry (depth) to be calculated. The Backscatter (signal strength) measures reflectance and can give indications of seafloor texture and sediment grain size. Seafloor Slope can also be derived from the Bathymetry data.
Seismic Facies	Seismic facies can be defined as a group of seismic amplitude variations with characteristics that differ distinctly from those from other facies. Seismic facies is the manifestation of the underlying geologic facies or structural feature in the seismic-amplitude data.
Seismic/Seismostratigraphic Unit	A volume of sediments/rock with similar seismic facies.
Side scan Sonar	This is a towed sonar system that transmits an acoustic signal at an angle to the seafloor, perpendicular to the path of the sensor through the water. The reflected signal received by the system allows seafloor features and targets to be detected through variations in reflectance and acoustic shadows. Each section of data is layered and combined to form a side scan mosaic.
Single-Channel Seismic	A shallow seismic survey system that uses one towed high-power source to transmit relatively low frequency acoustic signals into the sub-seafloor where its reflections are detected by a single receiver.

Glossary of Terms	
Item	Description
	These systems can provide relatively good penetration below seafloor at relatively lower resolution.
Sub-Bottom Profiler	A shallow seismic survey system that typically uses a hull-mounted low-power source to transmit very high frequency acoustic signals into the sub-seafloor where its reflections are detected by a single receiver. Parametric systems, such as Innomar, are often employed to provide improved sub-seafloor resolution, footprint and penetration below seafloor.
Till	A sediment that is characteristically unsorted and unstratified and is not usually consolidated. Most Till consists predominantly of clay, silt, and sand, but with pebbles, cobbles, and boulders scattered through the Till.

EXECUTIVE SUMMARY

Gavin & Doherty Geosolutions Ltd (GDG) as part of the Venterra Group, was commissioned by Energinet to produce an Integrated 3D GeoModel (IGM) for the proposed Krieger's Flak II Northern Offshore Wind Farm (OWF) site as part of the Danish Offshore Wind 2030 project for the Danish government. This comprised the preparation of a conceptual geological model, that formed the basis of the IGM through the refinement and integration of newly acquired geophysical (GEOxyz, 2024), and geotechnical (Gardline, 2024) data. An independent interpretation of the geotechnical data was performed and then integrated with the refined seismic interpretation to constrain the model and tie in interpreted seismic units with geotechnical unit top markers.

The recent geophysical and geotechnical surveys have a variable coverage of the site per sensor type. Bathymetry and side scan sonar datasets have full coverage (acquired at 62.5 m line spacing), with magnetometer acquired at a 50 m line spacing. The Sub-bottom profiler data have a high density across the site, spaced at approximately 60 m, whilst the ultra-high resolution seismic data were acquired at approximately 250 line spacing. Multiple geotechnical investigation methods were used across 20 locations, though only six locations had recovered borehole samples. These methods included composite boreholes, sampling boreholes, borehole CPTU's, seabed CPTU's, and seabed SCPTU's. The varying line spacing and spread of investigation locations presents limitations expected with this phase of investigation.

The bathymetry data show that the site area has a regional seabed slope dipping eastward as the seabed elevation ranges from -21.5 m in the northwest to -34.87 m relative to mean sea level, at the eastern extents. In the western half of the site, areas of outcropping glacial sediments are associated with boulder fields, creating rugged terrain. Bedforms including ripples and sandwaves were not predominantly observed in the northwestern part of the site. In the central and southeastern part of the site, the seabed is heavily scarred from anthropogenic activity. Various seabed hazards were identified. These include but are not limited to boulders and debris, depressions (pitted seabed with possible pockmarks), as well as five wrecks, potentially including three additional ones. One pipeline and five cables crossing the site were identified in acoustic data. Subsurface hazards include an unidentified cable crossing, magnetometer targets, glacial features such as till deposits and evidence of potential subglacial channels within the glacial/glaciolacustrine unit.

The IGM comprised four seismic units that consist of Holocene and Pleistocene deposits overlying Upper Cretaceous Chalk bedrock that are correlated with five geotechnical units (including a total of 11 subunits). The seismic units consist of up to 2.2 m in thickness of surficial, marine sediments (seismic Unit I) overlying transitional deposits, late glacial and glaciolacustrine sediments (seismic Unit III). Seismic Unit III (up to 7.0 m in thickness) overlies the glacial seismic unit Unit IV, which reaches up to 45.2 m in thickness. This unit corresponds to a complex sequence of multiple deposits associated with at least three glaciations. Each subunit is likely to correspond to a different till member, with each being separated by minor unconformities corresponding to erosional surfaces or ice-contact surfaces. The variable lithology of this unit coupled with limited borehole locations represents a significant geohazards, especially in areas where paleochannels have been recognized and where the

multiple subunits are well preserved. This seismic unit overlies the Upper Cretaceous chalk bedrock Unit V. The boundary between unlithified and lithified chalk was often described in geotechnical data but could not be tracked across the whole site in seismic.

Seismic Unit II represents the transition between Unit I and Unit III (corresponding to the post-glacial transition deposits) and shares similar geotechnical properties with both geotechnical units Ib and IIIa1. The unit does not contrast with the overlying and underlying units and was observed across the whole site in seismic data but could not be identified in the geotechnical until later stage in the project. Because this unit shares geotechnical properties with geotechnical units Ib and GU IIIa1, it has limited impact on design.

The acquisition, interpretation, and integration of the geophysical and geotechnical datasets has provided improved reliability of this second stage of the IGM, though uncertainties remain, which without further investigation will present risks to future developments on the site. Repeated geophysical surveys are recommended to rule out temporal seabed changes, whilst optimised, site-specific seismic surveys with reduced line spacing will provide more certainty in the interpretation of the seismic units and reduce the need for large inline gridding extrapolation.

Geotechnical zonation was performed to represent broadly similar ground conditions laterally and vertical across the site. Soil provinces were defined following the subseafloor interpretation, seismic unitisation, geotechnical unitisation, integration of the available geophysical and geotechnical data.

Geotechnical units represent similar geotechnical properties e.g. clay or sand. Geotechnical unitisation was performed considering the seismostratigraphic unitisation, IGM and factual data. Unitised geotechnical parameter profiles were determined for the geotechnical units identified at the site. Geotechnical parameter bounding was performed using either statistical and /or engineering judgement.

1 INTRODUCTION

1.1 PURPOSE AND SCOPE OF WORK

Denmark intends to further expand its offshore wind energy along with associated infrastructure. The Danish government (Danish Energy Agency) has allocated new offshore wind farm sites, as shown in Figure 1-1. The government has directed Energinet (Client) to commence site characterisation activities in the form of geophysical and geotechnical site investigation campaigns, and subsequent data interpretation, integration and visualisation. This is done under the project name “Danish Offshore Wind 2030”.



Figure 1-1 - Danish Offshore Wind Farms (www.ens.dk)

Gavin & Doherty Geosolutions Ltd (GDG) part of the Venterra Group were commissioned by Energinet (the Client) to undertake geophysical and geotechnical consultancy services with respect to site characterisation, and Integrated 3D GeoModel (IGM) development for the proposed Kriegers Flak II Northern and Southern OWF sites.

This report details the IGM and the integration of geophysical and geotechnical datasets to refine the existing Preliminary Ground Model (PGM) (GEOxyz, 2024) developed by GEOxyz based on the most recent geophysical survey and geotechnical site investigation performed by GEOxyz for the northern site. (GEOxyz, 2024) and Gardline (Gardline, 2024). The southern site was reported on separately in report “24004-REP-003-02-Integrated_3D_GeoModel_Report” (Venterra, 2024).

1.2 LIMITATIONS AND EXCLUSIONS

This section will outline the limitations and exclusions associated with the IGM:

- A decision was made by the client to not proceed with interpreting some newly identified horizons. This is discussed in Sections 5.1 and 6.2. If there is a future change to the known ground conditions and geomodel, this is not the liability of Venterra.
- The supplied data (geophysical) was provided with several processing artefacts (for example, tide reduction, signal processing, depth conversion) that each impacted the work performed as part of this IGM. Every effort has been made to produce this IGM to the highest standard, though some of these artefacts create remaining uncertainties within the mode. Venterra are not liable for the resultant geomodel uncertainties based on the input data. Where processes were impacted, these have been discussed in their relevant report section.
- The associated uncertainties in the geomodel are presented in greater detail in Section 6.5.
- Unexploded Ordnance (UXO) is not included within the scope of work for this IGM and UXO related risks or recommendations have not been provided.

1.3 GEODETIC INFORMATION

The project geodetic and projection parameters are summarised in Table 1-1 below:

Table 1-1 - Geodetic parameters

Geodetic parameters	
Parameter	Value
Projection:	ETRS89 / UTM zone 33N
Projection Type:	European Terrestrial Reference System 1989 ensemble
Central Meridian:	15
Latitude of Origin:	0
False Easting:	500,000
False Northing:	0
Scale Factor:	0.9996
Unit:	m
EPSG:	25833

1.4 VERTICAL DATUM

The vertical datum is Mean Sea Level (MSL). All elevations referenced in the text relate to MSL if not otherwise specified.

1.5 SUMMARY OF PREVIOUS STUDIES AND SITE-SPECIFIC REPORTS

In 2022, the Geological Survey of Denmark and Greenland (GEUS) was commissioned by the Danish Energy Agency to undertake a geological screening study for both the proposed Kriegers Flak II Northern and Southern OWF sites (GEUS, 2022). The study aimed to inform on site conditions for future investigations via the production of a conceptual geological model for the respective sites, based on available data at the time.

In 2023, GEUS produced an additional desk study report for the seabed geological conditions for the proposed Kriegers Flak II Northern and Southern OWF sites as well as proposed cable

routes, at the request of Energinet (GEUS, 2023). This study built upon the work of the existing report (GEUS, 2022) by integrating geological conditions for the proposed cable route.

In 2023, Energinet commissioned GEOxyz to perform a hydrographic and geophysical site investigation (GEOxyz, 2024), the findings of which are outlined in Section 4.1. The resulting preliminary ground model outlined an early-stage geological model for the site and was unconstrained by geotechnical data inputs.

In 2023, Gardline performed a geotechnical data acquisition survey that included in situ and laboratory testing (Gardline, 2024), the results of which are outlined in Section 4.2. The aim of this investigation was to understand the site's ground conditions and to be integrated with the available geophysical datasets for the IGM.

2 THE SITE

The proposed Kriegers Flak II Northern OWF site is in the Danish sector of the southwest Baltic Sea, east of the Fakse Bay and Møn Island (Figure 2-1), in water depths ranging between -20.0 and -35 mMSL. The areal extent of the site is 99 km². The site is approximately 17.5 km at its maximum length, from the northern most point to the southeast corner, and approximately 11 km at its maximum width, from the southwest boundary to the northeast boundary.

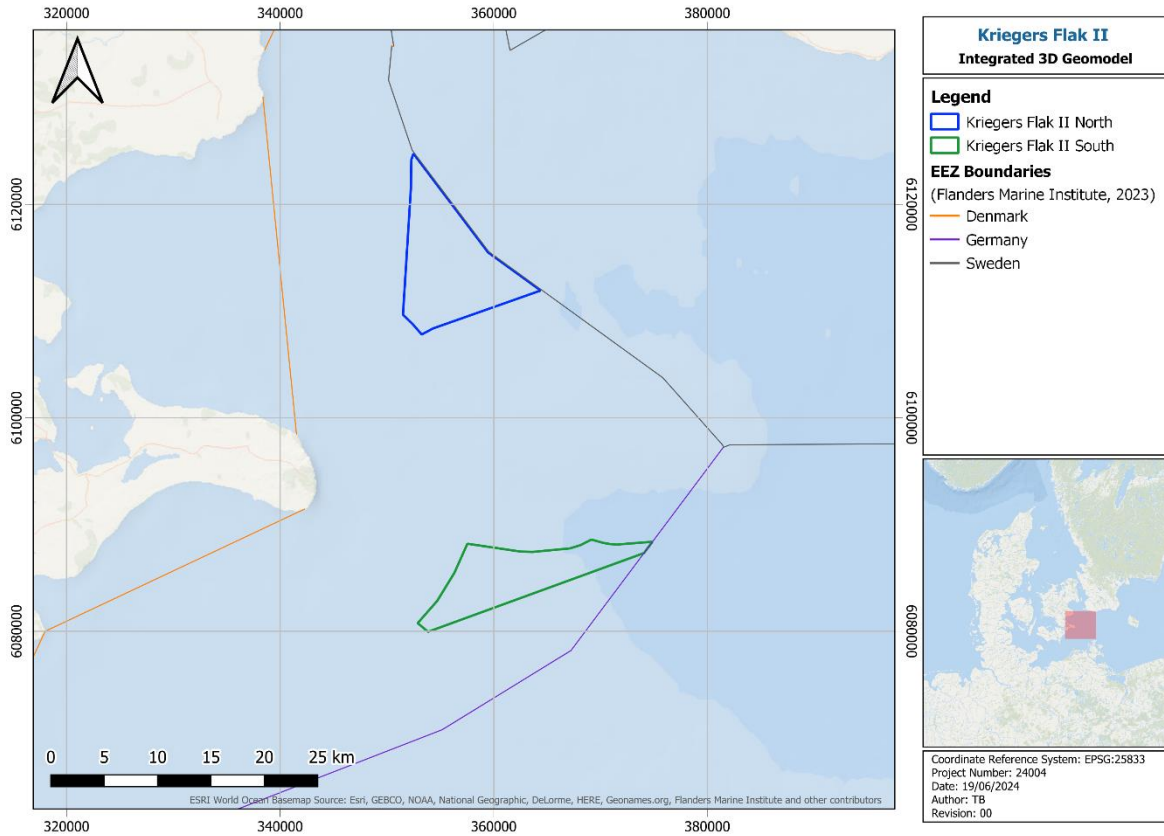


Figure 2-1 - The proposed Kriegers Flak II Northern OWF site overview (Flanders Marine Institute, 2023)

3 METHOD DESCRIPTION AND DELIVERABLES

This IGM consists of an update of the existing PGM carried out by GEOxyz in 2023 (GEOxyz, 2024), and relies on the recently acquired project-specific hydrographic and geophysical data from their Site Investigation and its interpretation, and also inclusion of the results from the geotechnical campaign performed by Gardline (Gardline, 2024). The IGM aims to inform understanding of the geology, geotechnical properties, and potential geohazards found/expected in the proposed Kriegers Flak II Northern OWF site.

An interpretation of the seafloor lithology, seafloor features, seafloor targets, seismic units and targets were provided by the contractor (GEOxyz, 2024). As part of the IGM development, Venterra focused on the following:

- Revising and updating the seafloor assessment. This will include a review of Multibeam Echosounder (MBES) and Side Scan Sonar (SSS) data for seafloor morphology, seafloor hazards, obstructions. Additional information on how seafloor features were identified and classified can be found in Sections 6.1.1 to 6.1.6.
- Updating the seafloor sediment classification to standard typology using MBES, SSS, and backscatter datasets, and available seafloor sampling data from Van Veen and Hamon grab samples (including new geotechnical data). Section 6.1.3 provides more detail into how different datasets were used to reassess the seafloor lithology distribution.
- Reviewing seismic units, attributed to geological units, through revision and reinterpretation of seismic data and building on the work of the PGM. The revision of the seismic interpretation followed the principles highlighted in Section 5.1, item 2. Details on how individual units and additional sub-seafloor features were characterized and separated are found in Section 5. A full description of the methodology employed to generate depth converted grids from the interpreted horizons is presented in Section 5.5.
- Reviewing geotechnical tops, interpreted from the geotechnical data, in the context of the IGM and correlating them with geological units interpreted from geophysical data. An overview of how the geotechnical data were integrated with the IGM can be found in Section 5.3.
- Investigating and applying potential improvements to the velocity model and depth conversion of seismic data, including utilisation of geotechnical velocity data where possible. An overview of the methodology employed for the velocity modelling is found in Section 5.4.
- Delineating and discussing areas of uncertainty.
- Identifying any observed and potential hazards and geohazards that may present risk to the development and longevity of the OWF and need to be taken into consideration during the design, construction, operational and decommissioning stages.

A risk register for the site were generated and is provided in Appendix D. The identified risks are discussed and graded by likelihood of occurrence and severity (pre-mitigation) based on

the criteria defined in Section 9 and an overall risk level has been determined from the risk matrix presented in the same section.

The seismic interpretation and geotechnical integration were carried out in Kingdom suite (SQL version 2019, Kingdom version 2022) and are provided in a master copy of the software (TKS format).

In addition to the above, the IGM digital data were collated in a GIS package with associated metadata and as a 3D GIS model (HTML format) to allow ease of distribution and visualisation of results.

4 GEOLOGICAL BACKGROUND AND PREVIOUS STUDIES

4.1 PRELIMINARY GROUND MODEL (GEOXYZ, 2024)

A PGM was produced by GEOxyz following their geophysical campaign for both the proposed Kriegers Flak II Northern and Southern OWF sites. A Schematic diagram and summary of their preliminary geological units is presented below. For further details, please refer to the full report (GEOxyz, 2024).

GEOxyz’s geological schematic (Figure 4-1) shows their interpretation of the arrangement of units within the northern site. A detailed summary is provided in Table 4-1. The key surfaces identified are the top of Unit III (H20/H05/seabed) which GEOxyz describe as being the top of potentially over consolidated deposits, and H30, the top of the bedrock.

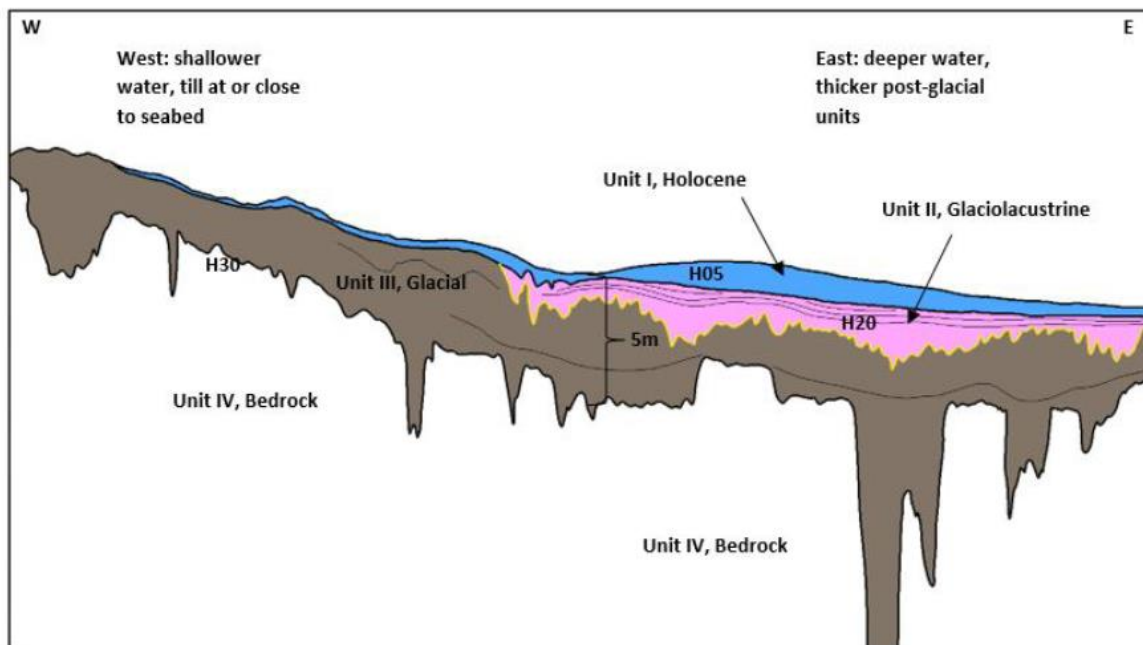


Figure 4-1 - Geological schematic, general arrangements of units (GEOxyz, 2024)

Table 4-1 - Shallow geological units (GEOxyz, 2024)

Shallow geological units				
Unit	Upper Surface	Lower Surface	Main Soil Description	Depositional Environment
I, H, Holocene	Seabed	H05	Silty, sandy CLAY with thin veneer of SAND at seabed	Post-glacial marine
II, LG, Late Glacial	Seabed/H05	H20	Variable, includes intervals of laminated CLAY, SAND-prone packages	Glaciolacustrine
III, GL, Glacial	H05/H15	H30	Variable, CLAY-prone, locally over consolidated	Glacial with localised direct ice contact, sandier outwash intervals
IV, BR, Bedrock	H20/H30	-	Chalk	Ancient shallow marine

4.2 GEOTECHNICAL SITE INVESTIGATION (GARDLINE, 2024)

An offshore geotechnical investigation campaign was performed by Gardline using the MV Kommandor Susan between 7 April and 27 August 2023, comprising:

Kriegers Flak II North

- 28 seabed Cone Penetration Tests with pore pressure measurements (CPTU), including bump-over locations;
- 12 CPTU boreholes;
- 6 Combined CPTU/sample boreholes;
- 2 P-S logging boreholes;
- Offshore geotechnical laboratory classification and strength testing.

Kriegers Flak II South

- 19 seabed Cone Penetration Tests with pore pressure measurements (CPTU), including bump-over locations;
- 2 seabed Seismic Cone Penetration Tests (SCPT);
- 12 CPTU boreholes;
- 5 Combined CPTU/sample boreholes;
- 2 P-S logging boreholes;
- Offshore geotechnical laboratory classification and strength testing.

Retrieved samples were preserved and transported to an onshore geotechnical laboratory for classification, strength and stiffness testing. The onshore laboratory test results were not available at the time of report submission. Please refer to the final factual results report for further details (Gardline, 2024).

4.3 REGIONAL GEOLOGICAL BACKGROUND

4.3.1 REGIONAL GEOLOGICAL HISTORY

4.3.1.1 PRE-QUATERNARY

The sites are located on the western margin of the Arkona Basin in the southwest Baltic Sea, on the West European Platform. The latter is separated from the Fennoscandian/Baltic Shield and the East European Platform by the west-northwest-east-southeast Sorgenfrei-Tornquist Zone (part of the larger Tornquist Zone), a Palaeozoic lineament. Besides this regional structure to the north of the Arkona Basin, the sites lie east of the Norwegian-Danish Basin and the Ringkøbing-Fyn High, and west of the Bornholm Basin (Figure 4-2).

The movement along Sorgenfrei-Tornquist Zone evolved from dextral strike-slip to extension throughout its stages of reactivation during the Triassic, Jurassic, and Early Cretaceous, culminating with Late Cretaceous to Early Paleogene inversion related to the Alpine

compression (Erlström & Sivhed, 2001; Mogensen & Korstgård, 2003; Graversen, 2004; Graversen, 2009). Graversen (2004) also mentions an earlier episode of inversion affecting the region during the Jurassic – Early Cretaceous. The whole region is affected by faults either following the west-northwest-east-southeast trend of this lineament, or in northwest-southeast and northeast-southwest directions (Figure 4-2). The local area, within and in the vicinity of the sites, is predominantly affected by northwest-southeast and northeast-southwest faults, as shown in Figure 4-3, Figure 4-4 and Figure 4-5 (EMODnet, 2024; GEUS, 2024).

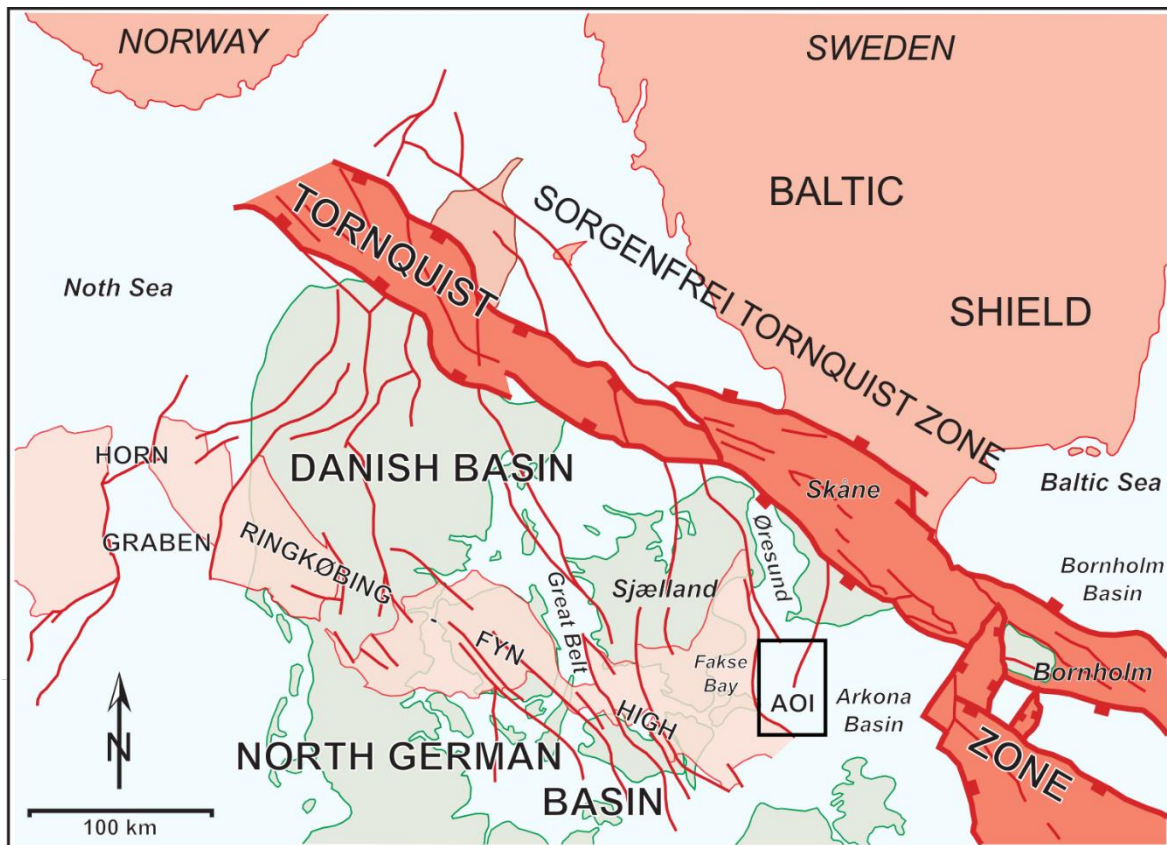


Figure 4-2 - Regional setting, modified from Graversen (2009). AOI – Area of Interest

In terms of stratigraphy, the basin area consists of Palaeozoic to Cenozoic rocks overlying Precambrian basement (Rosentau, et al., 2017). The Mesozoic to Cenozoic sedimentary infill is varied across the region, thinning from up to 10 km in the Norwegian-Danish Basin depocenter to less than 3 km along the Ringkøbing-Fyn High and within the Arkona Basin (Vejbæk & Britze, 1984; GEUS, 2024).

The lithologies expected to subcrop in the area of interest are Upper Cretaceous carbonates from the Chalk Group and Paleogene (Danian) limestone (Rosentau, et al., 2017; GEUS, 2022; 2023; 2024). The Upper Cretaceous subcrops in the entirety of the southern site. The extent of the Upper Cretaceous and Paleocene in the northern site differs between the map sources. According to the EMODnet (2024) map, the Chalk Group covers more than half of the northern site (Figure 4-3). However, from the GEUS (2024) map, the Upper Cretaceous deposits are confined to the very south-western corner of the northern site (Figure 4-4).

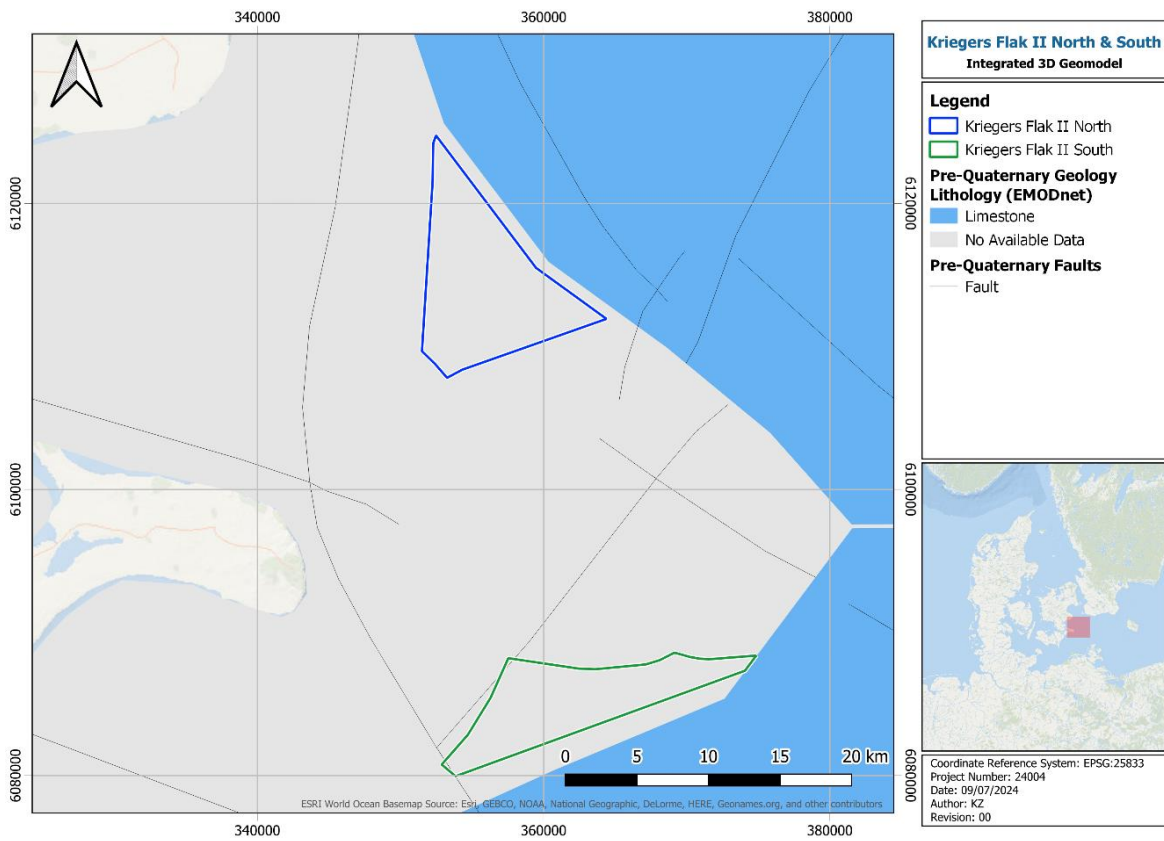


Figure 4-3 - Pre-Quaternary deposits (lithology) and faults (EMODnet, 2024)

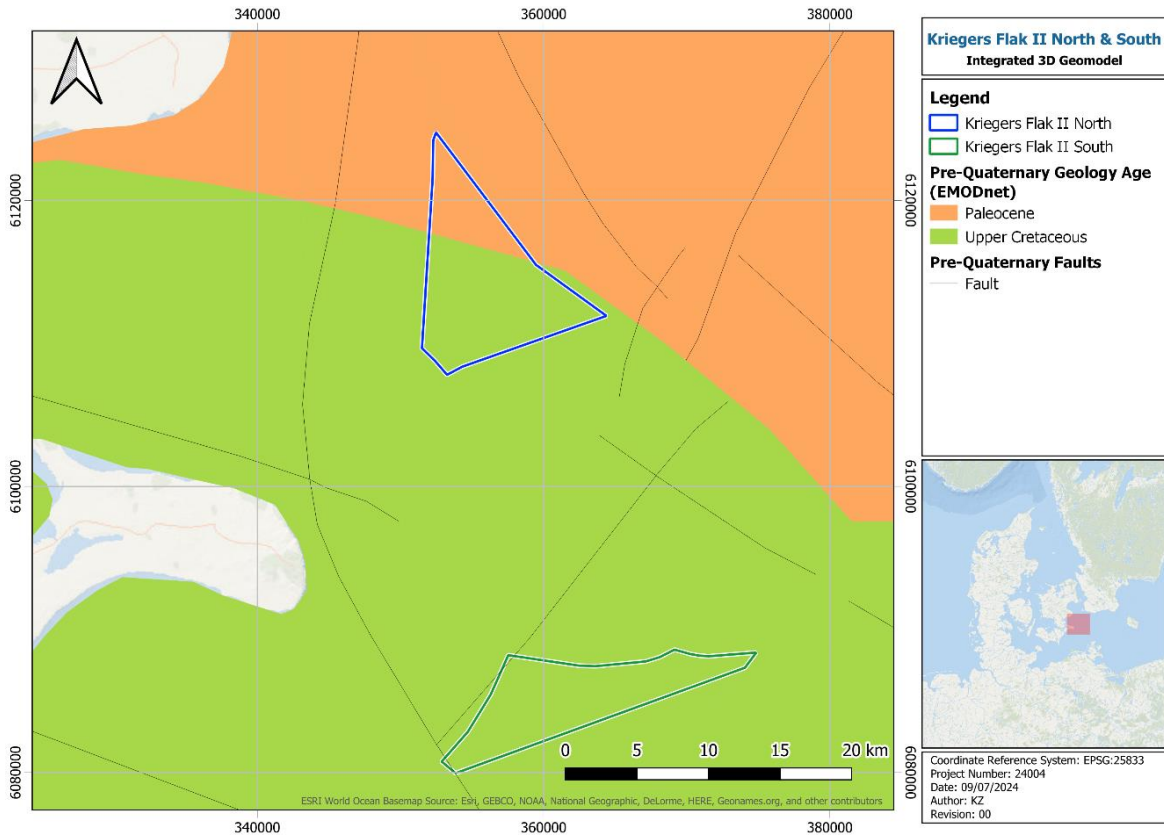


Figure 4-4 - Pre-Quaternary deposits (age) and faults (EMODnet, 2024)

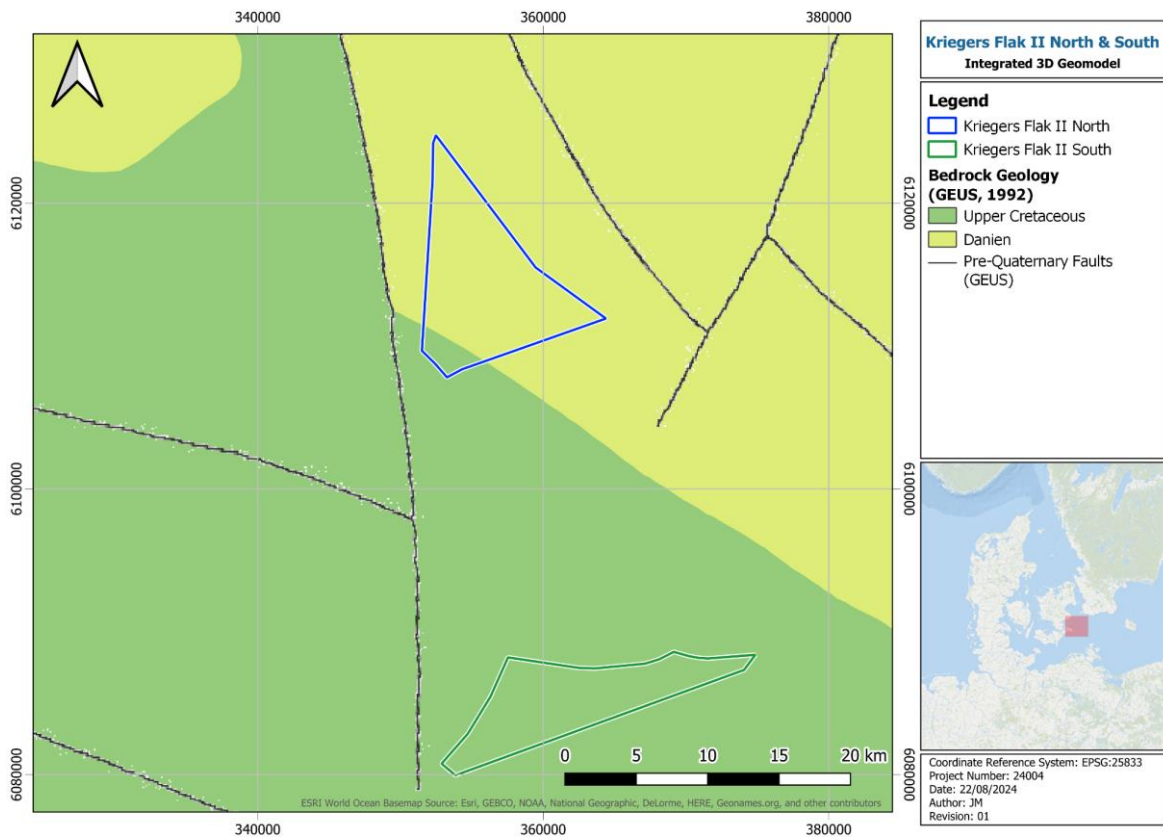


Figure 4-5 - Pre-Quaternary deposits (age) and faults (DGU, 1992; GEUS, 2024)

A map with the elevation of the top of the pre-Quaternary deposits has been generated by Binzer et al. (1994) and made available by GEUS (2024). Although this does not cover the full extent of the Arkona Basin, it can still be used to infer expected elevations. In the eastern part of the Arkona Basin the top of the pre-Quaternary was documented between -25 and -75 m relative to sea level, whereas in the west it is expected to shallow to between 0 and -50 m relative to sea level (Figure 4-6).

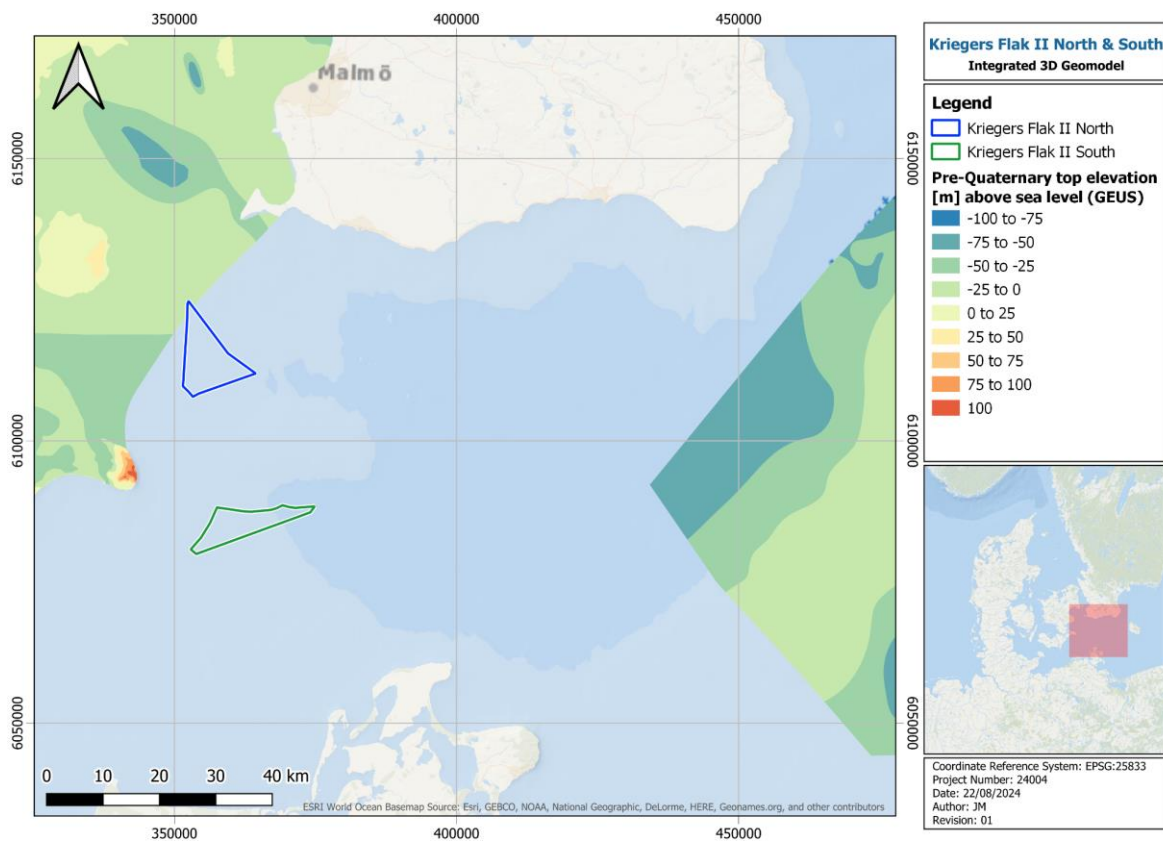


Figure 4-6 - Top pre-Quaternary surface elevation (Binzer, et al., 1994; GEUS, 2024)

4.3.1.2 QUATERNARY

The Cretaceous and Paleogene strata at each site are overlain by Quaternary deposits. These deposits show marked variability related to the palaeogeographic evolution registered by the Baltic Basin throughout this period. During the Saalian and Weichselian, the Baltic Sea region was affected by four glaciation events with the latest seeing the maximum extent of the Scandinavian Ice Sheet occurring at 22 ka before present (BP); (Figure 4-7). As the ice retreated, the Baltic Basin underwent a series of paleogeographic changes, documented in literature as the Baltic Ice Lake, Yoldia, Ancylus, and Littorina stages, during which the region alternated between the deposition of (glacio)lacustrine and transitional to marine sediments.

As the ice margin retreated from Zealand (Sjælland) through the Øresund and to the central part of Skåne and west of Bornholm at around 15 ka BP, the Baltic Ice Lake developed in front of the ice sheet, communicating with the Kattegat region through the Great Belt (Figure 4-8). The lake had several stages of damming documented, separated by regression events (Jensen, et al., 2002). The last stage of the Baltic Ice Lake occurred at around 12 k BP, had several minor channels draining it through the Great Belt and the Øresund (Figure 4-8), and was separated from the sea in central Sweden by a land bridge (Jensen, et al., 2002; Expedition 347 Scientists, 2014). Shortly after this, a connection was established between the lake and the ocean at 11.5 – 11.7 ka BP, through central Sweden, resulting in the formation of the Yoldia Sea (Figure 4-9). This stage of the Baltic Basin was short-lived as continued uplift of south-central Sweden due to ice unloading interrupted the ocean connection and led to the formation of the Ancylus Lake at around 10.2 ka BP (Figure 4-9). Continued sea level rise led

to the Littorina transgression and the formation of the Littorina Sea (Figure 4-9) at 8-7 ka BP (Emeis, et al., 2002; Jensen, et al., 2002; Expedition 347 Scientists, 2014).

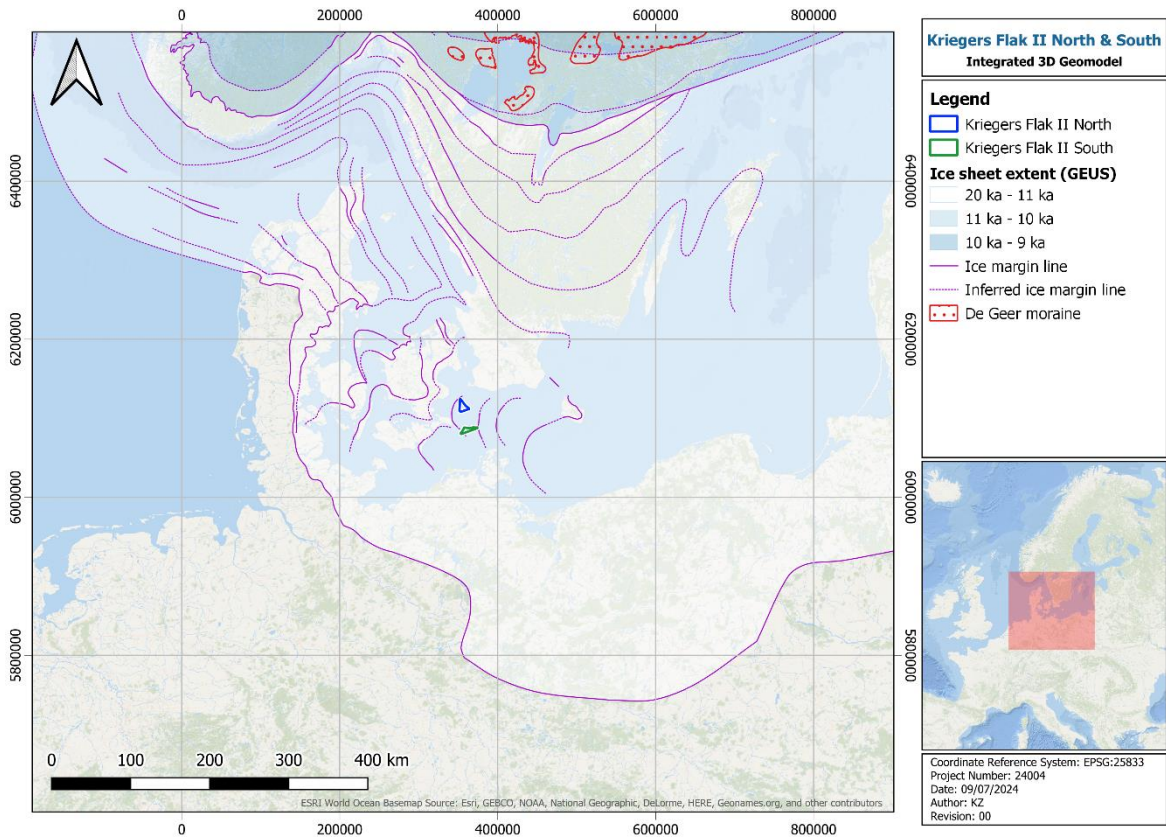


Figure 4-7 - Ice margin evolution (Pedersen, 1998; GEUS, 2024)

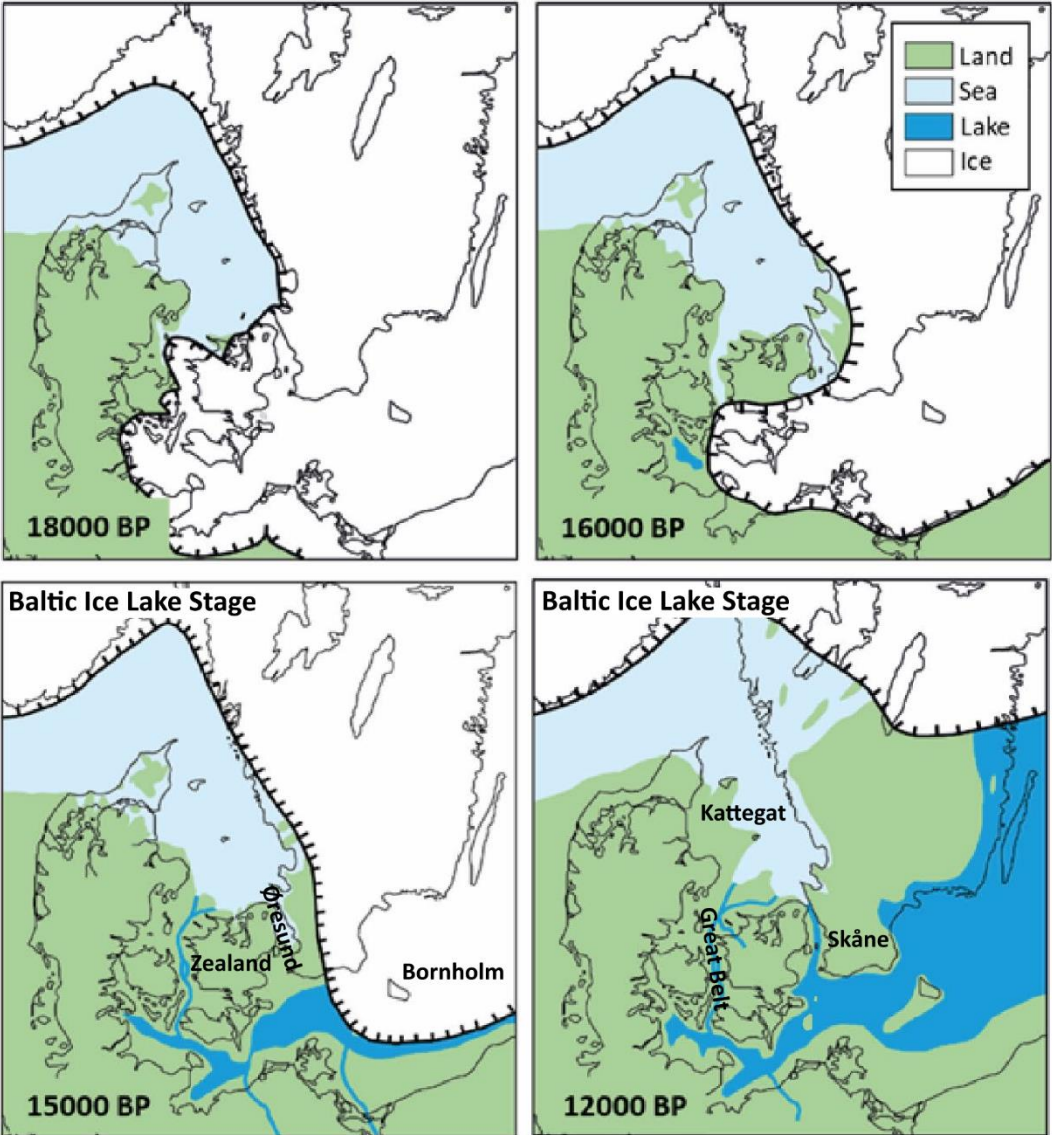


Figure 4-8 - Danish region palaeogeography from 18 to 12 ka BP; modified from GEUS (2022; 2023)

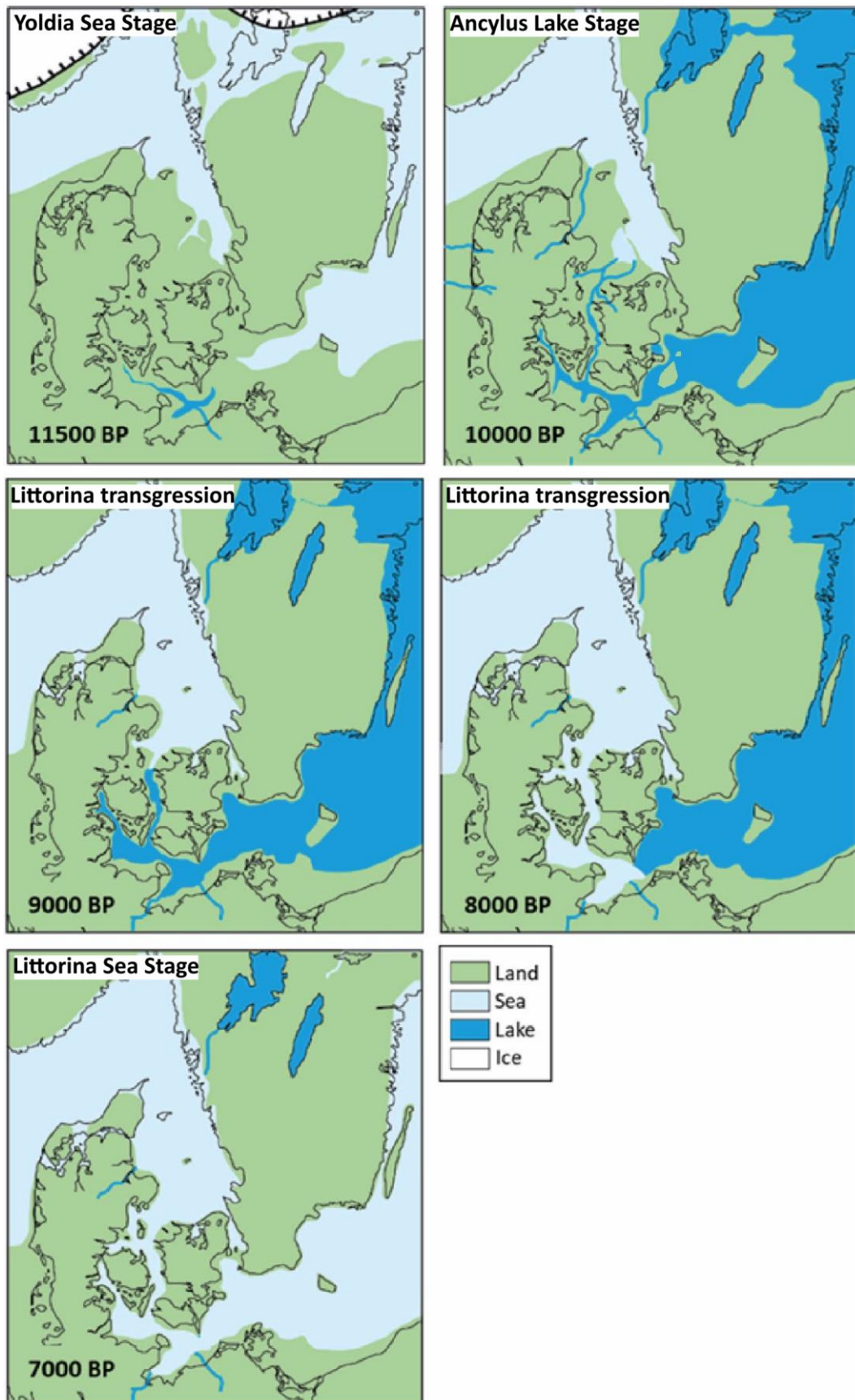


Figure 4-9 - Danish region palaeogeography from 11.5 to 7 ka BP; modified from GEUS (2022; 2023)

The nature and distribution of the Quaternary sediments deposited throughout these stages across the southwest Baltic Sea have been documented by several studies. The Arkona and the Bornholm basins have a similar reported stratigraphy (Table 4-2) consisting of tills overlain by varved and/or homogeneous clays and silty clays (Jensen, et al., 2017; GEUS, 2022). Local variations are observed in the Fakse Bay (Table 4-2) where the deglaciation was accompanied by the deposition of lagoon and coastal/barrier clay, silt, sand, gravel, and peat, and south of Møn, where late glacial coastal beach barrier sandy deposits that display progradational geometries from west to east, were documented (Jensen & Nielsen, 1998; GEUS, 2022; GEUS, 2023). Within the northern site, documented Quaternary shallow sediments include Holocene sand and mud across most of the site and Weichselian sand in the west (EMODnet, 2024), as shown in Figure 4-10 and Figure 4-11. Within in southern site, Holocene sand is reported across most of the site, with sand and mud present in the east (EMODnet, 2024).

Based on the top pre-Quaternary map (Binzer, et al., 1994) and current bathymetry of the area, the thickness of the Quaternary deposits are expected to vary between a few metres to 40 m in the Fakse Bay, up to 30 m in the eastern part of the Arkona Basin, and between a few metres and 60 m in the Bornholm Basin. In addition to this, the maps of Lemke (1998) presented in the reports of GEUS (2022; 2023) provide additional information on the thickness of Quaternary deposits and/or depths to intra-Quaternary interfaces within the Arkona Basin. Based on their analysis, the top of the till reaches 65 m below sea level in the central part of the basin, shallowing to 45 m in the southern site and to 25 m further north (their maps do not cover the northern site). Late glacial clays have documented thicknesses of up to 12 m in the central part of the basin, shallowing to 4 m or less towards the two sites, while proximal sandy coastal deposits are interpreted on the western margin of the basin with an estimated thickness of 30 m, as reported by GEUS (2022; 2023). Holocene muds have interpreted thicknesses of up to 12 m in the central part of the basin, shallowing to less than 3 m in the vicinity of the two sites

Table 4-2 - Regional Quaternary stratigraphy and seismic facies

Regional Quaternary stratigraphy and seismic facies											
Baltic Basin Stage	Environment	Bornholm Basin (Jensen, et al., 2017; GEUS, 2022)				Arkona Basin (Moros, et al., 2002; Mathys, et al., 2005)				Fakse Bay (Jensen & Nielsen, 1998; GEUS, 2022)	
		Unit	Member	Lithology	Seismic Facies	Unit	Unit	Lithology	Seismic Facies	Local Environment	Lithology
Littorina Sea	Post-glacial marine	I	a	organic rich CLAY	low amplitude, concave and onlapping parallel reflections	F	VI	greenish silty MUD	high amplitude reflection with onlapping geometries	coastal	SAND and GRAVEL
			b								
			c								
Ancylus Lake	Post-glacial transition	II	a	laminated CLAY	close spaced parallel reflection with decreasing amplitude upwards, strong upper reflection	E	V	silty grey CLAY	high amplitude reflection with onlapping geometries	lagoon and coastal /barrier	PEAT +/- SILT and CLAY; SAND and GRAVEL
b			homogenous CLAY	C							
Yoldia Stage						B	IV	red-brownish homogeneous silty CLAY	high amplitude reflection with onlapping geometries		
Baltic Ice Lake II	Glacio-lacustrine	III	a	rhythmic CLAY	parallel internals	All	III	red-brownish varved CLAY with dropstones	sub-parallel reflection with high amplitudes; transparent to chaotic	lagoon and coastal /barrier	SILT and CLAY; SAND and GRAVEL
			b	homogenous CLAY	homogenous						
Baltic Ice Lake I					c	rhythmic CLAY					

Regional Quaternary stratigraphy and seismic facies											
Baltic Basin Stage	Environment	Bornholm Basin (Jensen, et al., 2017; GEUS, 2022)				Arkona Basin (Moros, et al., 2002; Mathys, et al., 2005)				Fakse Bay (Jensen & Nielsen, 1998; GEUS, 2022)	
		Unit	Member	Lithology	Seismic Facies	Unit	Unit	Lithology	Seismic Facies	Local Environment	Lithology
									in the north and east		
-	Glacial	IV	a	SAND (outwash deposits)	high amplitude upper reflection (unconformity), internally chaotic	-	II	DIAMICTON	sub-parallel low amplitude reflections	-	-
			b	DIAMICTON (till)							
-	<i>Sedimentary bedrock</i>	V		LIMESTONE and calcareous SHALE	-	-	I	-	-	-	-

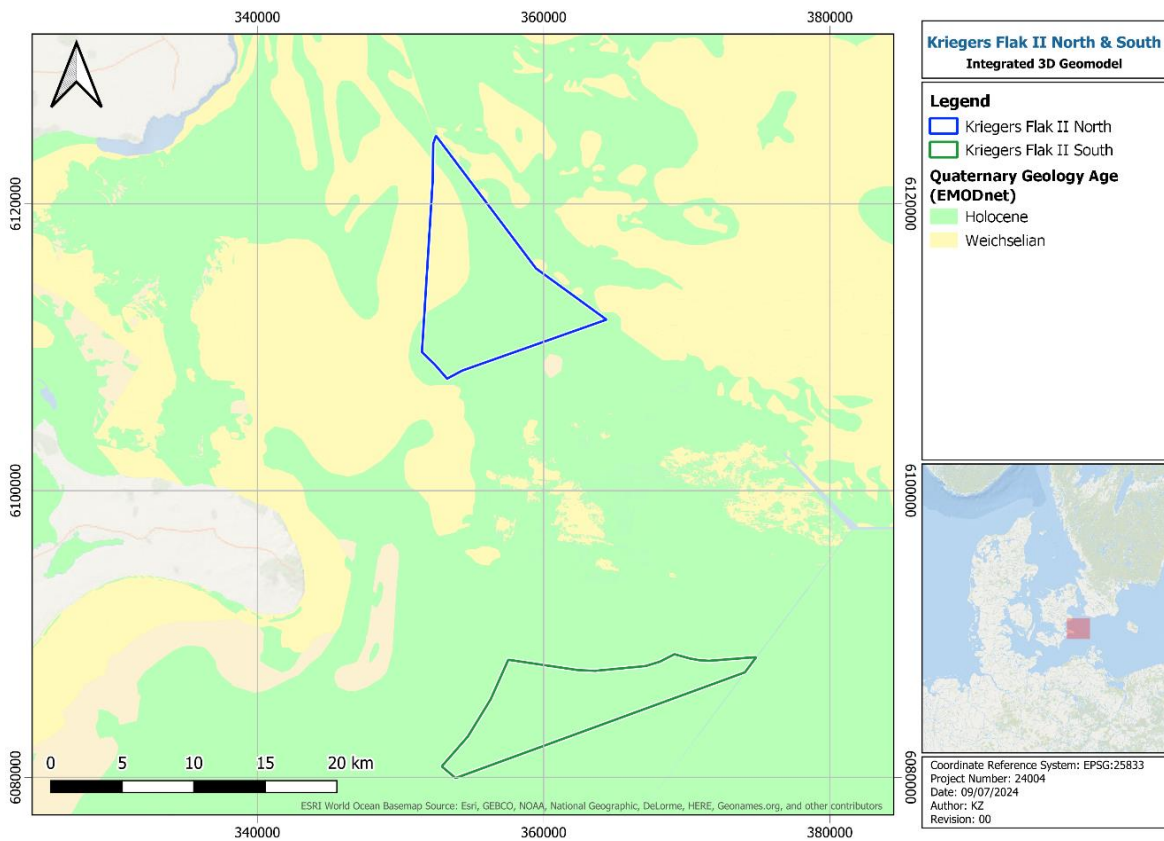


Figure 4-10 - Quaternary deposits age (EMODnet, 2024)

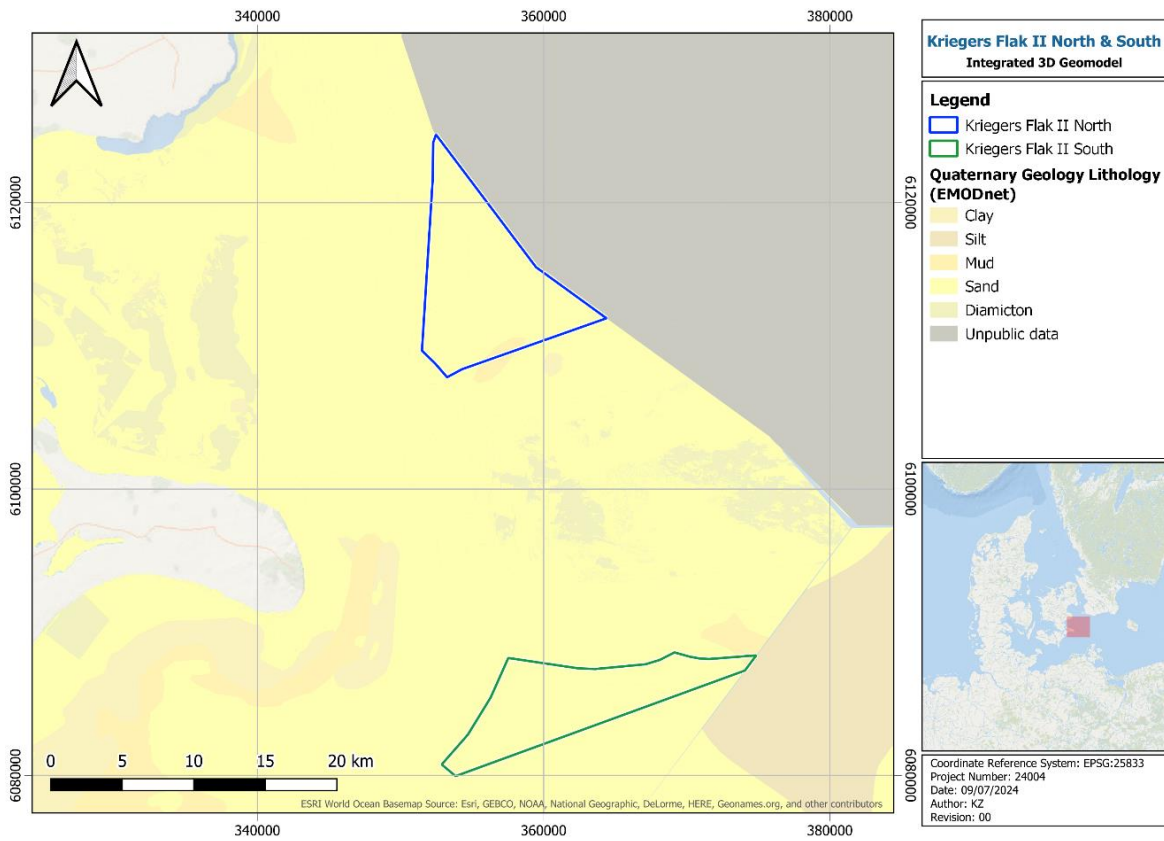


Figure 4-11 - Quaternary deposits lithology (EMODnet, 2024)

4.3.2 EXPECTED SEABED SEDIMENTS

The seabed sediments expected within the northern site have been extracted from EMODnet (2024) Folk 7 map (Figure 4-12). This shows mixed sediments in the western part of the site and muddy sand in the remainder of the site, with only an isolated area of mud reported in the southern part of the site. A similar seabed sediment distribution is reported by GEUS (2024). However, the area classified as mixed sediment by EMODnet is documented as diamicton (till) by GEUS.

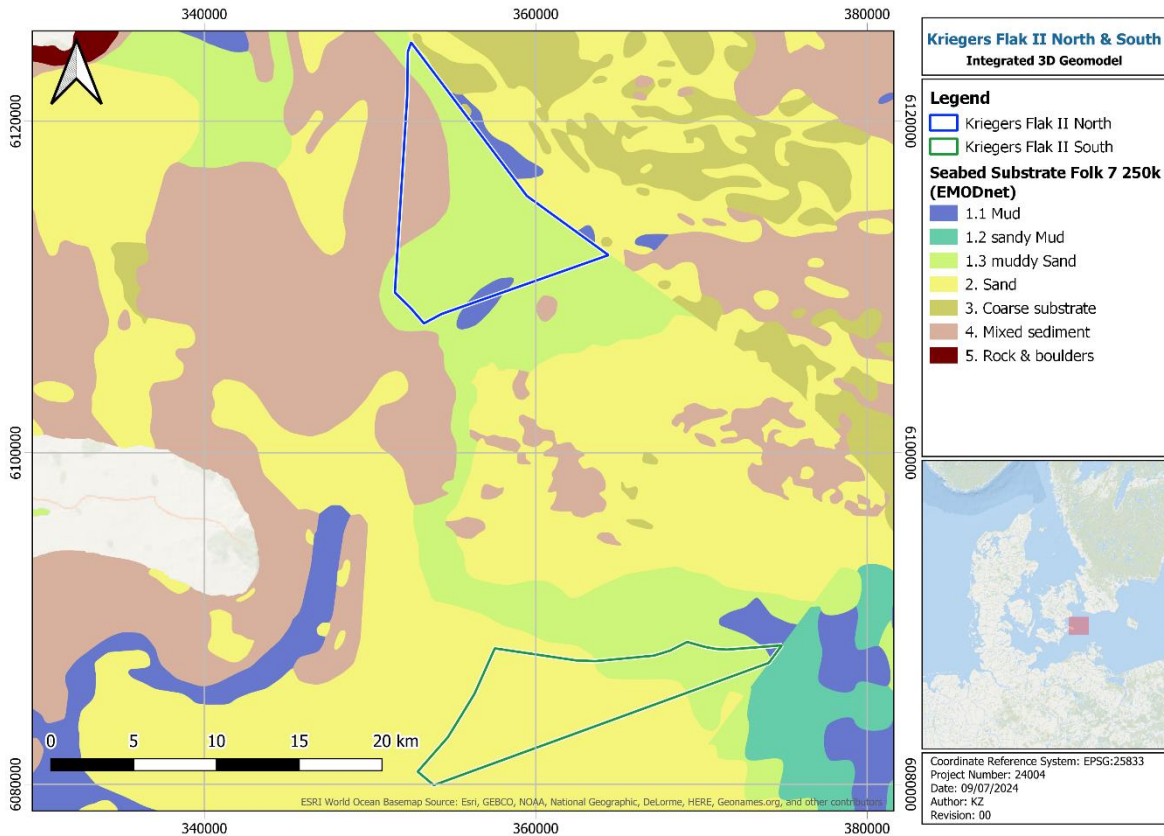


Figure 4-12 - Seabed sediments – Folk 7 (EMODnet, 2024)

4.4 CONCEPTUAL GEOLOGICAL MODEL

A conceptual geological model is presented for the site in Table 4-3 and Figure 4-13. The model consists of four seismic units (I, III, IV and V). Unit I consists of Holocene marine sands and clays, overlying a more variable Unit III. Unit III is of late glacial/glaciolacustrine origin, composed of low strength clays and silty sands and has been subdivided based on the variable seismic facies observed (discussed in more detail in Section 6.2.2). Underlying Unit III is Unit IV, the glacial unit consisting of clay and sand tills of Pleistocene (Weichselian) origin. Underlying Unit IV is Unit V, consisting of unlithified chalk (Dm/Dc, unit Va) and lithified chalk (A1-B4, unit Vb), of Upper Cretaceous origin.

Figure 4-13 illustrates the typical vertical stratigraphy of the units identified and their associated internal seismic facies. Section 6.2 and Section 7 provide further detail on the seismic unitisation, geotechnical data integration and the variability of these units across the site as well as the associated geotechnical parameters.

Table 4-3 - Conceptual geological model summary

Conceptual geological model summary				
Seismic Unit	Geotechnical Unit	Age	Geotechnical Description	Depositional Environment
Unit I (SU I)	GU Ia	Holocene	Loose to medium dense SAND	Marine
	GU Ib		Very low to low strength CLAY	
Unit III (SU III)	GU II	Pleistocene (Weichselian)	GU II was not picked as part of the seismostratigraphic unitisation but can be observed from both the geophysical and geotechnical data. This unit consists of very silty, sandy to very sandy, low to medium plasticity, very low to medium strength CLAY/SILT	Post Glacial/ Glaciolacustrine
	GU IIIa1		Silty to very silty, slightly sandy, medium to high plasticity, very low to low strength CLAY	
	GU IIIa2		Dense to very dense well sorted silty SAND	
	GU IIIb1		Medium dense to dense silty SAND with closely to widely spaced thin beds of clay	

	GU IIIb2		Sandy, slightly gravelly, medium to extremely high strength Clay	
Unit IV (SU IV)	GU IVa	Pleistocene (Weichselian)	CLAY TILL, very silty, very sandy, slightly gravelly, low plasticity, calcareous, micaceous, sand is fine to coarse, gravel is fine to coarse, subangular to subrounded, of mixed lithology (Extremely high strength)	Glacial
	GU IVb		SAND TILL, fine to coarse, poorly sorted, clayey, very silty, very gravelly, calcareous (Dense to very dense), with fine to coarse gravel size chalk nodules, highly calcareous	
Unit V (SU V)	GU Va	Upper Cretaceous	CHALK (Dm/Dc), unlithified (H1), white (N9), highly calcareous (Very high to extremely high strength) with rare fine to coarse gravel and stone sized fragments of chert, very strongly indurated (H5), non-calcareous (Very strong to extremely strong)	Marine (sedimentary bedrock)
	GU Vb		CHALK (A1-B2), slightly indurated (H2), unfractured to slightly fractured (S1-S2), highly calcareous (Extremely weak to very weak), with rare fine to coarse gravel sized pockets and extremely closely to closely spaced thin to thick laminae of marl, highly calcareous, and rare fine gravel to stone size fragments of chert, very strongly indurated (H5), dark grey to black (N3-N1), non-calcareous (Very strong to extremely strong)	

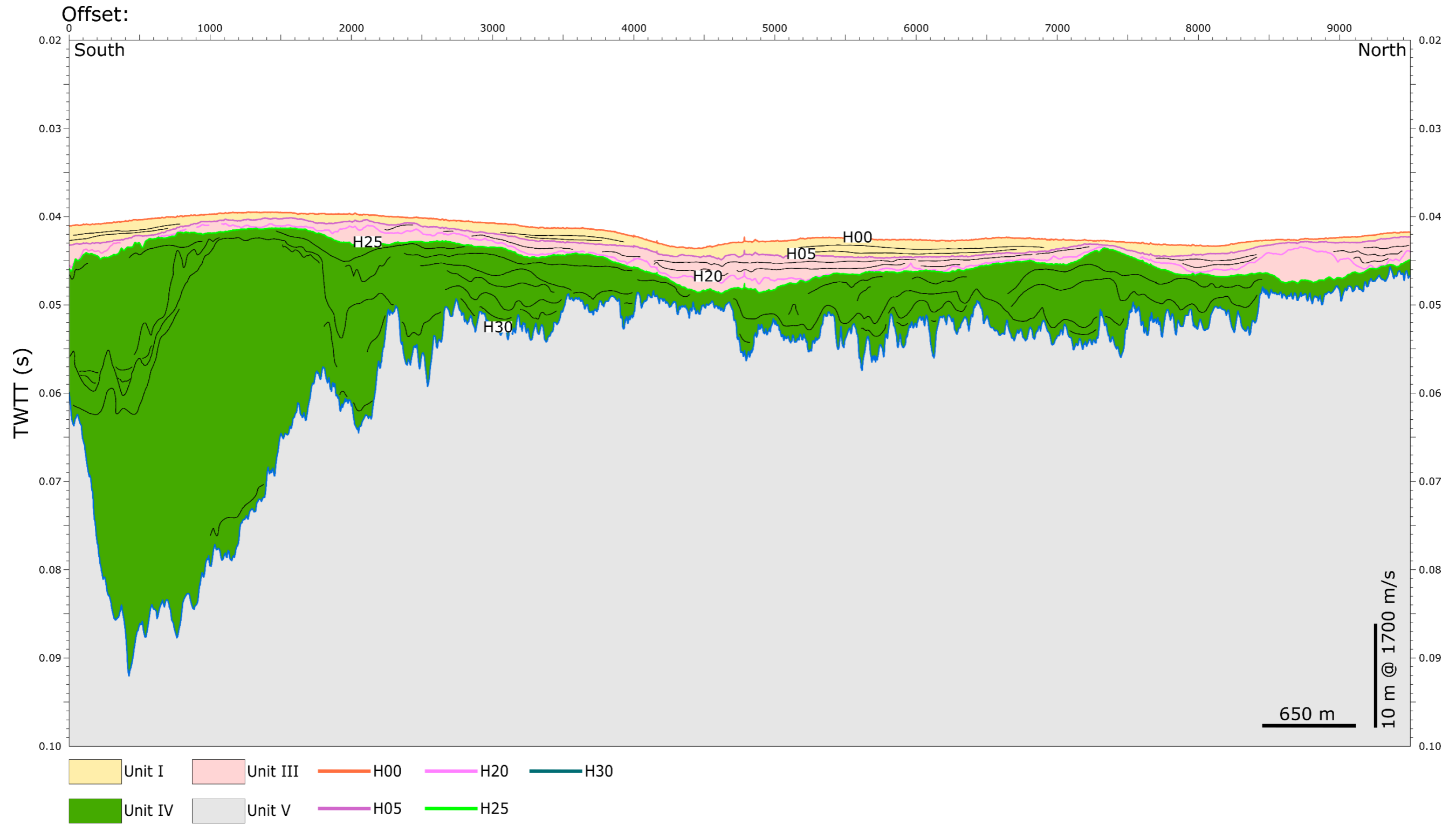


Figure 4-13 - Conceptual geological model

5 INTEGRATED 3D GEOMODEL DEVELOPMENT

This section comprises a summary of the main steps undertaken to develop the IGM. These included a revision of the provided geophysical survey interpretation, a review of the acquired geotechnical data and their integration in the IGM, a review of the velocity model, and an overview of how the final grids were generated and depth converted.

Seafloor lithology, seafloor contacts, and seismic unit grids have been revised from the interpretation originally provided by the contractor (GEOxyz, 2024). The revision of the seismic interpretation, presented as elevation and thickness grids in Sections 6.2.1 to 6.2.4, included changes in the extent of individual seismic units, picked Two-Way Travel Time (TWTT) of the base or top horizon, and/or changes in the depth distribution following depth conversion. Magnetic targets and buried contacts have remained as per the original contractor delivery (GEOxyz, 2024).

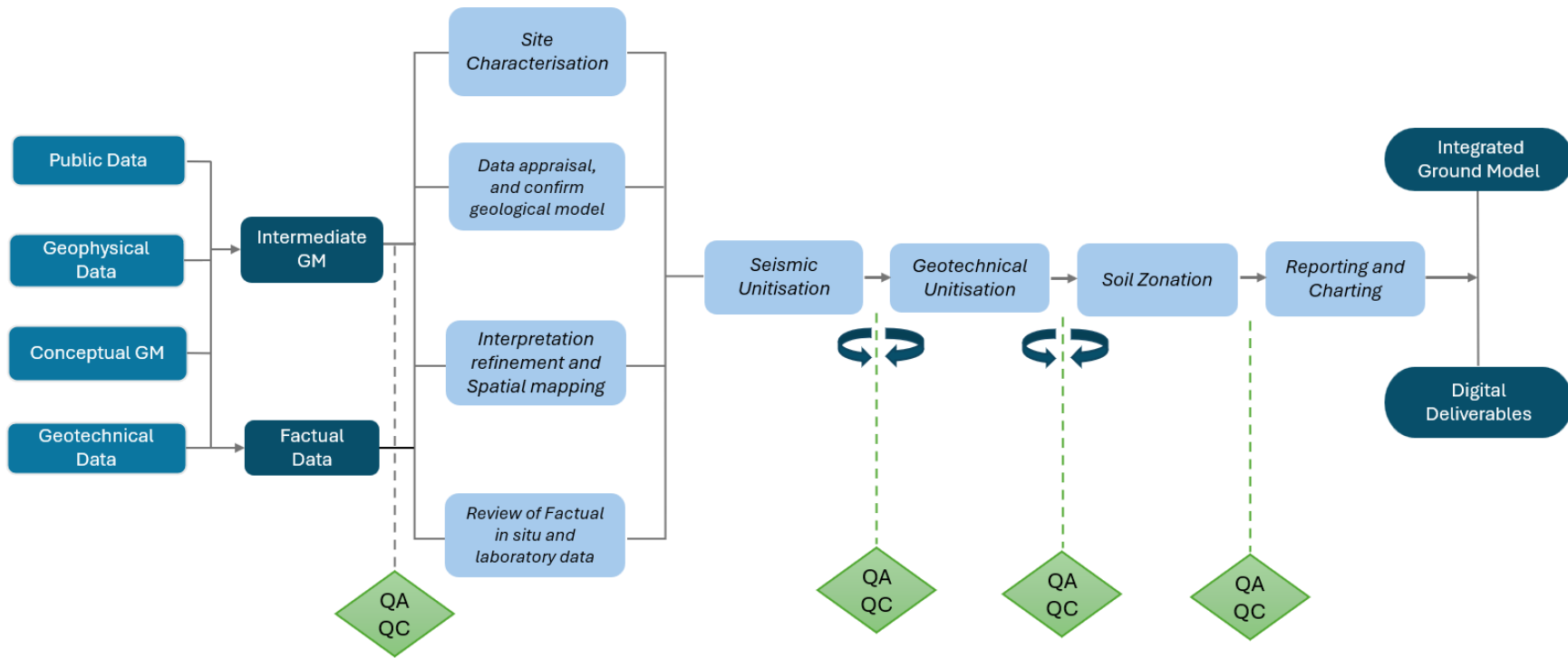


Figure 5-1 - IGM development workflow

5.1 GEOPHYSICAL SURVEY - INTERPRETATION REFINEMENT

- 1) Review seafloor data to identify any areas that will need refined interpretation.
- 2) Review seismic interpretation to identify any areas that will need refinement. This includes ensuring that the interpretation:
 - a) represents an update to the archived preliminary ground model (GEOxyz, 2024) based on Venterra’s interpretation of the data in conjunction with the available geotechnical data.
 - b) is reliable between SBP and 2D-ultra-high resolution seismic (SCS and MCS) datasets.
 - c) shows minimal mis-ties (vertical differences in interpretation where seismic lines intersect).
 - d) makes geological sense given the information available.
- 3) Identify additional horizons for interpretation. A summary of the revised seismic interpretation is provided in Table 5-1.
- 4) Review geotechnical data to highlight if there are any concerns with the reliability of in-situ or lab tests which may affect the IGM.
- 5) Review the velocity model and time-to-depth conversion of the seismic data interpretation, which was derived from the 2D multichannel ultra-high resolution seismic processing carried out by the contractor, and ensure that the model accounts for real variations in the seismic velocities, as far as the data supports, in particular by reviewing any possible integration of geotechnical data into the velocity model. This is discussed in Section 5.4.

Table 5-1 - Revised seismic interpretation of the geophysical data

Revised seismic interpretation of the geophysical data		
Seismic Reflector	Corresponding Seismic Unit	Comments (following client approval)
H00	Top of Unit I - Marine	Horizon refined
H05	Base of Unit I - Marine	Horizon refined and extent updated
H20	Internal of Unit III – Glaciolacustrine	Horizon refined and extent updated
H25	Top of Unit IV – Glacial	Horizon interpreted
H30	Top of Unit V - Chalk	Horizon refined based on limited available geotechnical data.

5.1.1 UHRS DATA QUALITY GRADING

The UHRS data were graded for their data quality, the results of which are presented in Figure 5-2 and chart 24004-OVR-001-02-00, in Appendix A.

The following data quality grades were utilised:

Good (G):

- Seabed is clear and continuous

-
- The depth of penetration, data resolution, and effective attenuation of the ghost and multiple signals is sufficient to allow interpretation of the data, with minimal artefacts.
 - The data have been correctly tidally reduced with no significant offsets between lines.
 - The signal has been effectively filtered and gains are well balanced across the record with a lack of remnant ambient and mechanical noise.

Fair (F):

- Seabed is clear and continuous
- The depth of penetration, data resolution, and attenuation of the ghost and multiple signals limits the interpretability of the data locally, though it is generally good.
- The applied tidal reduction is suitable with local variations.
- The signal filtering and gain balancing is generally good, with minimal noise present.

Poor (P):

- Seabed is unclear and/or discontinuous.
- The depth of penetration, data resolution, and attenuation of the ghost and multiple signals is poor, affecting the continuity of reflectors and the interpretability of the data.
- Tidal reduction and static corrections are variable and affect the continuity of the data.

The data require further filtering and balancing of gains to improve the record and remove the remnant noise that impacts interpretability.

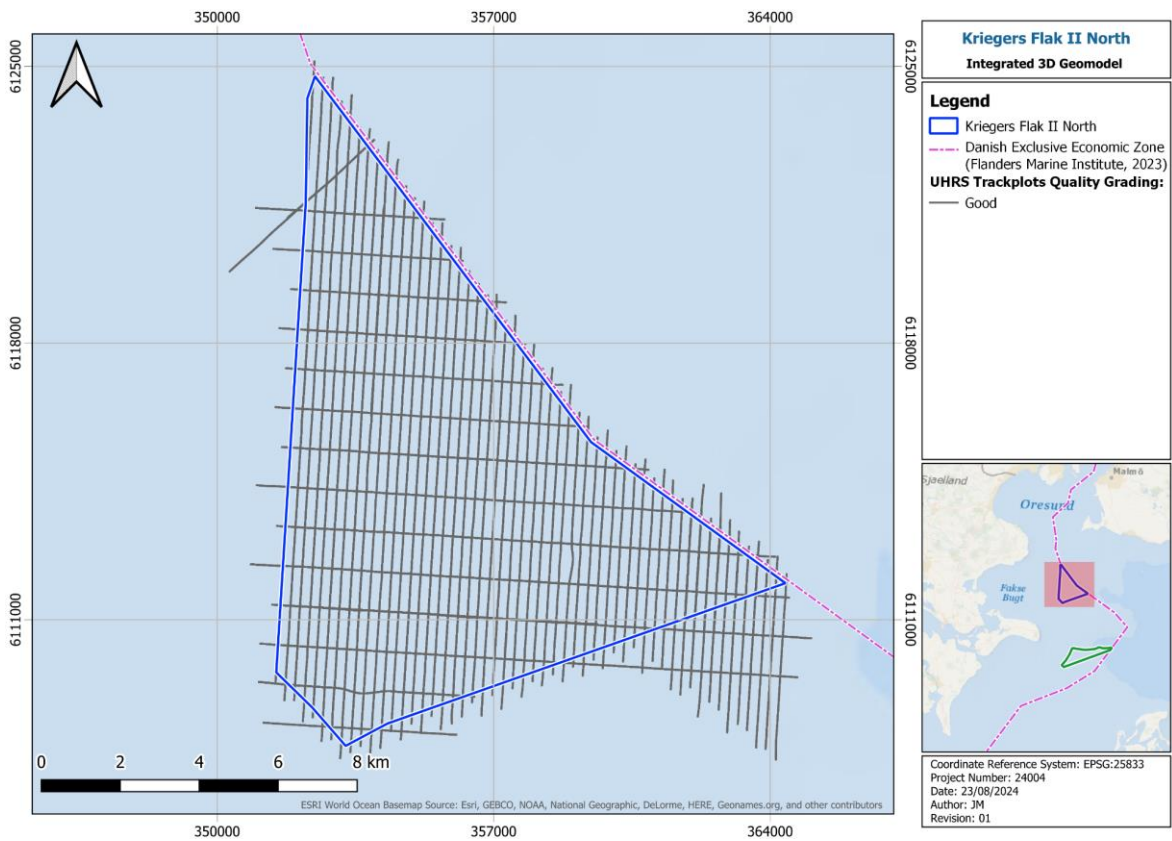


Figure 5-2 - UHRS line paths and data quality grades

5.2 GEOTECHNICAL DATA SUMMARY

Figure 5-3 shows the Geotechnical Investigation (GI) locations. Section 4.2 summarises the geotechnical testing performed at the site.

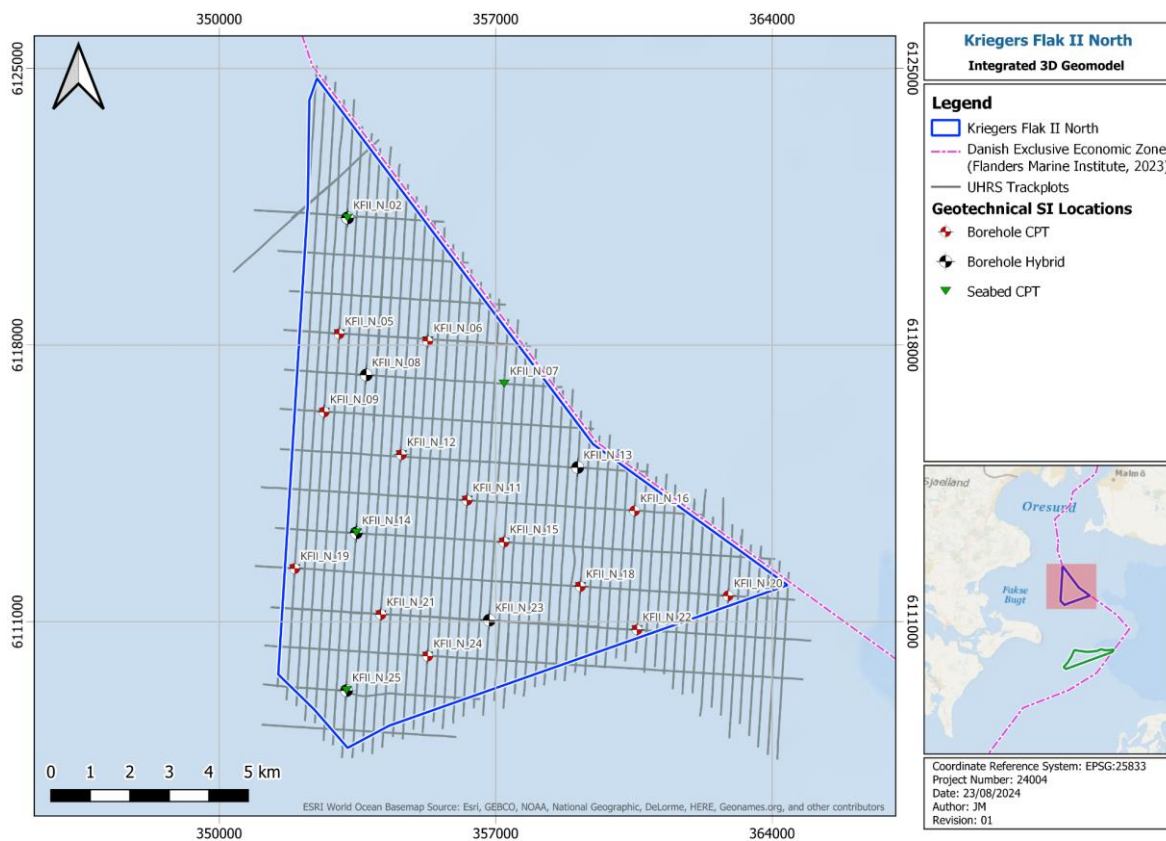


Figure 5-3 - Geotechnical site investigation locations overview (Gardline, 2024)

5.3 GEOTECHNICAL DATA INTEGRATION

At this stage, the IGM is primarily led by the interpretation of geophysical data. To verify it, the seismic interpretation and gridded seismic horizons were compared against the preliminary geotechnical tops that are interpreted from notable and spatially consistent variations in the available ground truthed geotechnical data – from CPT and BH log and sample testing measurements.

The integration of geotechnical data proceeded as follows:

- To avoid bias, geotechnical data was interpreted in isolation with no consideration for existing interpreted seismic units. For this,
 - CPT and BH data were projected along depth-corrected pseudo-sections.
 - Significant changes in measurement properties were identified in each GI location, generally representing a change in sediment type.
 - Corresponding sediment type boundaries were matched between GI locations and denoted geotechnical tops.
- Geotechnical tops were then compared against seismic data and interpreted seismostratigraphic horizons in Kingdom. Initially, this was done using the GEOxyz provided velocity model to convert the tops to TWTT to overlay on seismic data. Subsequently, when available, the improved velocity model was used.

- Where correlations did not immediately provide confirmation of reliable interpretation, the horizons were reinterpreted, and reliability of interpretation improved. On occasion, the seismic horizon was clear but associated geotechnical top was not sharply defined, possibly presenting a more gradual change of geotechnical parameters. In this case, the geotechnical top was reassessed and ultimately revised to align with the seismic interpretation more closely.
- In order to ensure the most consistent interpretation of both contributing datasets, multiple workshops between the geotechnical and geophysical interpreters were undertaken, resulting in multiple iterations of the interpretation
- Based on the analysis of the geotechnical data, a total of 11 geotechnical tops were identified. The geotechnical unitisation was developed considering the physical and mechanical geotechnical behaviour of the soil i.e. drained, undrained or mixed. Therefore, for a single seismostratigraphic unit, more than one geotechnical unit may be assigned to describe the soil behaviour.

Examples of seismic interpretation revision through geotechnical integration are shown in Figure 5-4 and Figure 5-5. In example location KFII_N_13_BH (Figure 5-4), initial H00 picks from GEOxyz were revised. Horizon H20 interpreted by GEOxyz (GEOxyz, 2024) was revised as H25 following the integration of geotechnical markers (clay till). Interpretation of H20 was then revised accordingly following H25 interpretation. In example location KFII_N_23_BH (Figure 5-5), H00 interpretation was missing and has been fully interpreted as part of the IGM. Horizon H30 was revised following the integration of geotechnical markers, which showed that the previous version of H30 from GEOxyz (GEOxyz, 2024) was associated with till deposits. The reflectors listed in Table 5-1 were refined based on the methodology above.

To summarise, the seismic units discussed in Section 6.2 were correlated with five interpreted geotechnical tops. The relationship between these interpretations is shown in Table 5-2. Statistics intended to quantify reliability of interpretation on the correlation between seismic units and geotechnical tops are presented in Section 6.6, with a more detailed table showing the integration in Table 6-2.

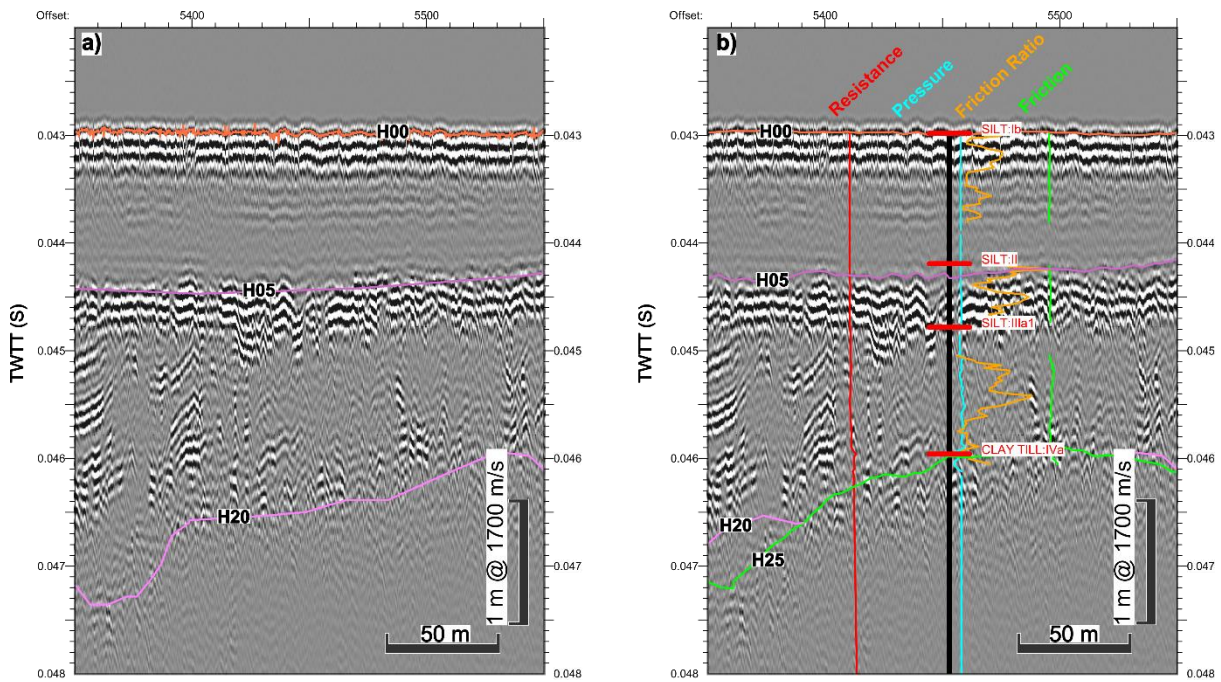


Figure 5-4 - Comparison of pre (a) and post (b) geotechnical interpretation integration, extracted from SBP line '0048_A_KN_GO5_L030' at location KFII_N_13_BH

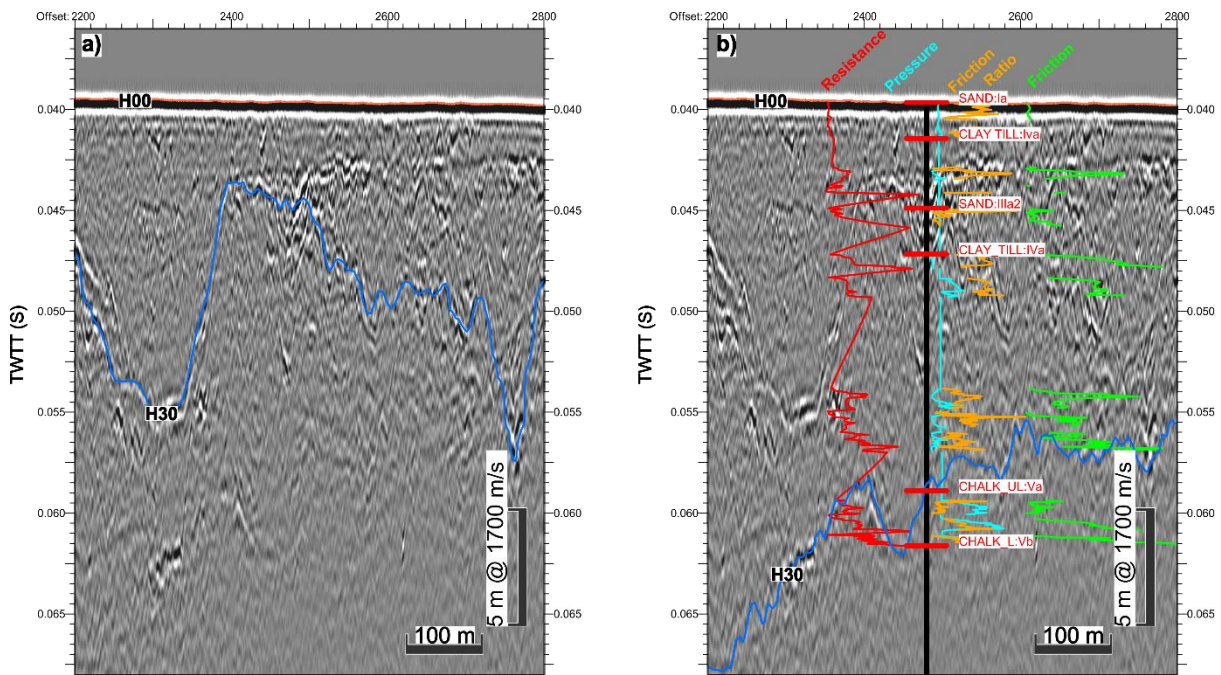


Figure 5-5 - Comparison of pre (a) and post (b) geotechnical interpretation integration, extracted from SBP line 'A_KN_L022_UHR_T_MIG_STK' at location KFII_N_23_BH

Table 5-2 - Correlation between seismic and geotechnical tops

Correlation between seismic and geotechnical tops	
Seismic Top	Geotechnical Unit
Seafloor/ Top Unit I	Ia
Top Unit III	IIIa1
Top Unit IV	IVa
Top Unit V	Va

The geotechnical data are not always perfectly co-located with a corresponding seismic line (UHRs or SBP). During the integration, the geotechnical data were projected onto the nearest seismic lines. For larger distances between the geotechnical data and the seismic, there is a greater chance of uncertainty, and as such, inconsistencies remain when correlating the geotechnical tops with the geophysical interfaces. A summary of the distance between each geotechnical location and the closest UHRs seismic line is provided in Table 5-3.

Table 5-3 – Geotechnical and seismic data offsets

Geotechnical and seismic data offsets						
ID	Easting (m)	Northing (m)	Type	Penetration (m)	Line Name	Line Offset (m)
KFII_N_02_CPT	353246.59	6121222.05	SCPSEA	5.29	A_KN_L005_UHR_T_MIG_STK	28.8
KFII_N_02_BH	353246.26	6121215.74	Borehole Hybrid	1.1	A_KN_L005_UHR_T_MIG_STK	28.9
KFII_N_02_BH_A	353250.51	6121217.51	Borehole Sampling	70.68	A_KN_L005_UHR_T_MIG_STK	33
KFII_N_05_CPT_A	353036.87	6118290.45	SCPSEA	3.08	A_KN_L005_UHR_T_MIG_STK	3.7
KFII_N_05_CPT_B	353039	6118295.12	SCPSEA	4.62	A_KN_L005_UHR_T_MIG_STK	5.5
KFII_N_05_DCPT	353034.7	6118282.12	Borehole CPT	20	A_KN_X011_UHR_T_MIG_STK	0.1
KFII_N_06_CPT_A	355278.3	6118108.56	SCPSEA	5.12	A_KN_L014_UHR_T_MIG_STK	2
KFII_N_06_CPT_B	355281.14	6118112.95	SCPSEA	3.56	A_KN_L014_UHR_T_MIG_STK	0.5
KFII_N_06_DCPT_A	355276.86	6118099.92	Borehole CPT	18.79	A_KN_L014_UHR_T_MIG_STK	2.9
KFII_N_07_CPT_A	357213.61	6117025.35	SCPSEA	2.52	A_KN_L022_UHR_T_MIG_STK	0.4
KFII_N_08_BH	353720.63	6117241.52	Borehole Hybrid	70.5	A_KN_L008_UHR_T_MIG_STK	0.6
KFII_N_09_CPT	352659.64	6116305.95	SCPSEA	2.28	A_KN_X009_UHR_T_MIG_STK	2.7
KFII_N_09_CPT_A	352661.98	6116310.23	SCPSEA	5.76	A_KN_L004_UHR_T_MIG_STK	2.4
KFII_N_09_DCPT	352655.69	6116306.53	Borehole CPT	13.1	A_KN_X009_UHR_T_MIG_STK	2.9
KFII_N_11_CPT	356275.75	6114076.3	SCPSEA	4.56	A_KN_L019_UHR_T_MIG_STK	2.5
KFII_N_11_CPT_A	356277.67	6114081.07	SCPSEA	4.64	A_KN_L019_UHR_T_MIG_STK	0.9
KFII_N_11_DCPT	356275.85	6114072.14	Borehole CPT	15.4	A_KN_L019_UHR_T_MIG_STK	2.2
KFII_N_12_CPT	354608.99	6115229.34	SCPSEA	1.56	A_KN_L012_UHR_T_MIG_STK	8.8
KFII_N_12_CPT_A	354611.87	6115233.51	SCPSEA	1.88	A_KN_L012_UHR_T_MIG_STK	11.6
KFII_N_12_DCPT	354609.52	6115224.97	Borehole CPT	12.06	A_KN_L012_UHR_T_MIG_STK	9.6
KFII_N_13_BH	359075.79	6114901.62	Borehole Hybrid	70.6	A_KN_X008_UHR_T_MIG_STK	3.6
KFII_N_14_BH	353469.23	6113244.47	Borehole Hybrid	70.8	A_KN_L008_UHR_T_MIG_STK	6.4
KFII_N_14_CPT	353469.56	6113250.98	SCPSEA	2.6	A_KN_L008_UHR_T_MIG_STK	6.5
KFII_N_14_CPT_A	353471.99	6113255.45	SCPSEA	2.6	A_KN_X006_UHR_T_MIG_STK	2.2
KFII_N_15_CPT	357210.3	6113015.93	SCPSEA	2.54	A_KN_L023_UHR_T_MIG_STK	5
KFII_N_15_CPT_A	357212.69	6113020.8	SCPSEA	2.66	A_KN_X006_UHR_T_MIG_STK	2.3

KFII_N_15_DCPT	357210.73	6113012.24	Borehole CPT	11.3	A_KN_L023_UHR_T_MIG_STK	5.6
KFII_N_16_DCPT	360515.84	6113805.12	Borehole CPT	15.02	A_KN_X007_UHR_T_MIG_STK	7.5
KFII_N_18_CPT	359143.15	6111893.17	SCPSEA	7.02	A_KN_X005_UHR_T_MIG_STK	1.1
KFII_N_18_CPT_A	359144.57	6111897.31	SCPSEA	9.77	A_KN_L031_UHR_T_MIG_STK	3.4
KFII_N_18_DCPT	359142.41	6111888.95	Borehole CPT	20.8	A_KN_L031_UHR_T_MIG_STK	1.8
KFII_N_19_CPT	351910.62	6112347.42	SCPSEA	1.74	A_KN_X005_UHR_T_MIG_STK	2
KFII_N_19_CPT_A	351912.78	6112351.55	SCPSEA	1.72	A_KN_L002_UHR_T_MIG_STK	1.9
KFII_N_19_DCPT	351910.61	6112343.14	Borehole CPT	12.54	A_KN_L002_UHR_T_MIG_STK	3.6
KFII_N_20_DCPT	362883.75	6111653.04	Borehole CPT	15.5	A_KN_X005_UHR_T_MIG_STK	1.5
KFII_N_21_CPT	354090.41	6111181.32	SCPSEA	1.82	A_KN_L011_UHR_T_MIG_STK	8.4
KFII_N_21_CPT_A	354092.8	6111184.93	SCPSEA	2.76	A_KN_L011_UHR_T_MIG_STK	6.2
KFII_N_21_DCPT	354090.83	6111177.65	Borehole CPT	14.98	A_KN_L011_UHR_T_MIG_STK	7.8
KFII_N_22_CPT	360576.37	6110800.73	SCPSEA	3.36	A_KN_L037_UHR_T_MIG_STK	2.5
KFII_N_22_CPT_A	360578.53	6110805.63	SCPSEA	3.36	A_KN_X004_UHR_T_MIG_STK	0
KFII_N_22_DCPT	360577.16	6110797.13	Borehole CPT	17.5	A_KN_L037_UHR_T_MIG_STK	3.4
KFII_N_23_BH	356836.03	6111035.91	Borehole Hybrid	71.3	A_KN_L022_UHR_T_MIG_STK	1.5
KFII_N_24_CPT	355276.35	6110132.19	SCPSEA	2.94	A_KN_L016_UHR_T_MIG_STK	5.1
KFII_N_24_CPT_A	355278.77	6110136.83	SCPSEA	3.74	A_KN_L016_UHR_T_MIG_STK	3
KFII_N_24_DCPT	355276.3	6110127.6	Borehole CPT	20.96	A_KN_X003_UHR_T_MIG_STK	0.5
KFII_N_25_BH	353221.87	6109254.26	Borehole Hybrid	70.7	A_KN_L008_UHR_T_MIG_STK	2
KFII_N_25_CPT	353218.59	6109259.89	SCPSEA	1.74	A_KN_L008_UHR_T_MIG_STK	5.6
KFII_N_25_CPT_A	353220.8	6109264.56	SCPSEA	2.22	A_KN_L008_UHR_T_MIG_STK	3.7

5.4 VELOCITY MODEL REVISION

Initial velocity model proposed by GEOxyz relied on a constant velocity of 1600 m/s in the sub-seabed, for the SBP dataset. For the 2D UHRS dataset, constant velocities of 1600 m/s for units above GEOxyz Unit III “shallow Quaternary sediments” and 1800 m/s to GEOxyz Unit III “relatively ancient rock” were applied for the Time-Depth (T-D) conversion of the interpreted horizons. According to GEOxyz report (GEOxyz, 2024), the T-D conversion of SEG Y data was performed accounting for water column velocity, constant velocity for the SBP dataset and a two-layer model, with constant velocities, for the UHRS dataset. Upper and lower limits of the interval velocities correspond to grids in time TWTT.

Following reception of the datasets, new T-D charts were implemented for the northern and southern site. For the display of geotechnical markers in the seismic section in time, initial T-D charts used a constant velocity of 1700 m/s.

Along with the progress of the seismic interpretation, a more detailed velocity model using constant interval velocities has been introduced to account for the variable lithologies. Based on literature and geological knowledge, intervals of possible empirical velocities were attributed to each lithology (Table 5-4).

Table 5-4 - Velocity model parameters

Velocity model parameters		
Lithologies	Inferred Velocity Value (m/s)	Possible Range (m/s)
Shallow (marine) sand	1650	1600 - 1650
Shallow (marine) silt	1650	1550 - 1650
Post-glacial sand	1700	1600 - 1700
Post-glacial clay	1700	1650 - 1750
Till (clay, sand, silt)	1800	1700 - 1900
Chalk	2200	2000 - 2500

Following continuous revision of the seismic interpretation against geotechnical marker in time domain, constant interval velocities in the different lithologies were revised for each location.

MD TVD TVD Seismic Subsea | Interval Velocity Average Velocity

Formation Tops

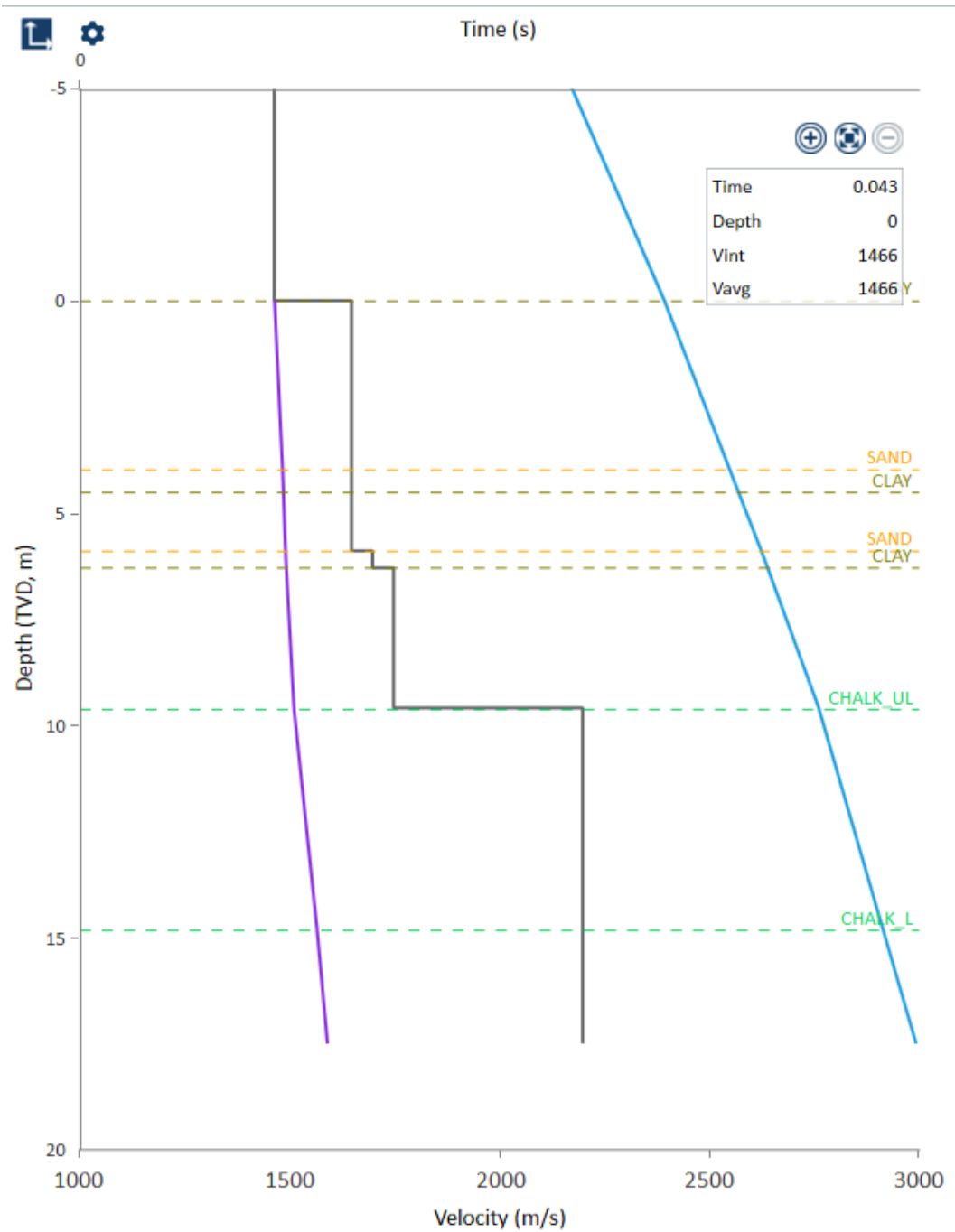


Figure 5-6 - Seismic unit velocity model

The final velocity model is based on the integration of the different lithologies per seismic units and the tie between the interpreted seismic horizons and geotechnical markers. For units with a single lithology and/or relatively homogenous sediments, a constant interval velocity was defined. For complex seismic units displaying multiple lithologies, spatially variable but constantly vertical, interval velocities were calculated based on the tie between seismic and geotechnical markers. Because of vertical uncertainties between the seismic and geotechnical markers, the calculated interval velocities for such units were rounded to nearest quarter. The

resulting spatially variable constant interval velocities were gridded and imported as a velocity grid to be used during the gridding process (Section 5.5.1, e).

For the northern site, only constant interval velocities were used (Table 5-5).

Table 5-5 - Final velocity model

Final velocity model	
Unit	Velocity (m/s)
Marine - Unit I	1650
Post glacial - Unit III	1700
Glacial - Unit IV	1750
Chalk - Unit V	2200

5.5 GRIDDING AND DEPTH CONVERSION

5.5.1 GRIDDING

Following the integration of the geotechnical interpretation and the completion of seismic reinterpretation, in Kingdom, the following methodology was employed:

- a) Picked horizons, in TWTT, for all seismic units, excepting H20, were gridded using the Flex Gridding algorithm in Kingdom, with Minimum Curvature (with a value of 0) and Smoothness set to Midway (with a value of 0.6). Horizon H20 was not gridded in this study as it corresponds to an internal boundary within Unit III (see section 6.2). Extrapolation distance was set to 150 m for the coarsely spaced UHRS lines (250 m) where H30 was picked, 130 m for the SBP lines where H25 was picked, and 50 m for the SBP lines where H05 was picked. The cell size was set to 5 m so that gaps in between lines and the site boundary were filled.

Several parameter variations were tested. Those selected were found to provide the best results once the whole gridding process had taken place – minimising unrealistic artefacts in the data and allowing unit trends that were extrapolated between lines to be more realistic. The cell size enabled high resolution grids to be calculated, retaining almost all horizon undulations, without processes being significantly time intensive. The extrapolation distance needed to be significant to account for line spacing gaps (150 m for the UHRS lines and 130 m or 50 m for the SBP lines depending on the horizon gridded) and gaps between the lines and the site boundary.

- b) The Two-Map calculator in Kingdom was used to calculate the top of each seismic unit that originally had its base picked, and the base for each seismic unit that originally had its top picked such that each unit had grids representing its top and base. Through this process the grids were also trimmed against shallower unit interfaces.
- c) The Depth Conversion Tool ‘Compute Isochron Map’ in Kingdom was then used. This takes the top and base grids for each unit and calculates Isochrons, which represent the thickness of each seismic unit in TWTT.
- d) The Isochron grids were then reviewed. If the Isochron grids revealed unrealistic straight edges with a sudden, impossible, drop in unit thickness, then a copy of the original picked horizons were created and edited such that their subsequent grids

provided consistent isochrons. This is typically done by adding false picks to adjacent lines to prevent abrupt grids truncations in the extrapolated area between lines, hence allowing the grid surface to be smooth. This can take several iterations to ensure consistent Isochrons.

- e) With consistent and realistic isochrons, the Depth Conversion Tool ‘Compute Isochore Map’ in Kingdom was then used. This takes the Isochron (thickness in TWTT), and the Interval Velocity Grid from the velocity modelling of each unit and creates an Isochore (thickness in metres). These were reviewed against the associated Isochrons to ensure processing was as expected. These Isochores were exported for charting unit thicknesses.
- f) The Depth Conversion Tool ‘Depth Map by Isopach Maps’ was then used to calculate grids representing the depth, in mBSF, of each seismic unit base. This required intermediate calculations to ensure that the extent of each successive unit was maintained. These mBSF grids were exported for charting unit depths.
- g) With Depth mBSF grids for the base of each seismic unit calculated, the ‘Depth Map by Isopach Maps’ tool was reused with the interpreted seafloor grids to calculate the Depth mMSL grids for each unit. These mMSL grids were then exported for charting unit depths, relative to datum (MSL).

In Kingdom, updated horizon picks are only present in Time domain. In depth domain, grids can be displayed in depth converted seismic sections (see section 5.5.2). Selection of the time or depth domain constrains the display of data coverage on the Base Map and in seismic sections.

5.5.2 SEG Y DEPTH CONVERSION

The time to depth conversion of the UHRS dataset SEG Ys was performed using the Dynamic Depth Conversion (DDC) tool in Kingdom. Unit tops calculated during the gridding process were used as constraints to setup the velocity model. Velocities used in T-D conversion were the same as the ones used in the T-D conversion of the grids.

Seismic velocities in the water column were assessed based on the T-D conversion of MBES bathymetry data and the tie with the seabed reflector in UHRS data.

In the DDC tool, no particular framework rule was applied as the unit truncations, onlaps, etc. were already accounted for in the unit tops.

Then, the T-D conversion was processed as follows:

1. Using the DDC tool, a constant interval velocity model was implemented and saved as a temporary attribute for each URHS seismic line.
2. Using the T-D conversion tool in Kingdom, the DDC model implemented was applied to the T-D conversion of SEG Ys.
3. Resulting SEG Ys converted to depth are stored as attributes for each line.
4. Seismic sections converted to depth were QC against T-D converted grids and geotechnical markers.

Uncertainties associated with the T-D conversion of the SEGYS includes uncertainties in the bathymetry, which was used as the vertical reference layer. Additionally, because of extrapolation outside the site boundaries, more uncertainties exist for the velocity model used in the T-D conversion of seismic sections extending outside the site boundaries. Uncertainties are summarized in Section 6.3.

In the Kingdom project, SBP and UHRS sections converted to depth domain by GEOxyz and stored in attribute “Amplitudes Depth” (Depth data type) were retained. As part of this study, only the depth converted UHRS sections were updated. The updated UHRS sections in depth domain are stored in attribute “Converted Depth” (Depth data type).

6 DISCUSSION OF SPATIAL INTEGRATED 3D GEOMODEL

6.1 SEAFLOOR INTERPRETATION

6.1.1 MULTIBEAM ECHOSOUNDER BATHYMETRY AND SLOPE

Bathymetry data with a 0.25 m resolution, shown in Figure 6-1 reveals that the seafloor generally deepens gently from north-west to south-east, with elevations ranging from -21.6 m to -34.9 m MSL. The shallowest areas are generally observed along the western part of site, whilst the deepest areas are found in the southeastern corner. Interrupting the generally constant slope of the seafloor in the south and centre of the site are shallow truncated channel features, with maximal localised depths up to 2.5 m deeper than the surrounding seabed. The northwest-southeast orientated channel features which reach up to 1500 m in width separate four raised areas of the seafloor.

Variability in seabed morphology is best observed when a hill shade raster is derived from MBES data and applied as a semi-transparent layer. This allows the identification of more subtle changes in the seabed morphology.

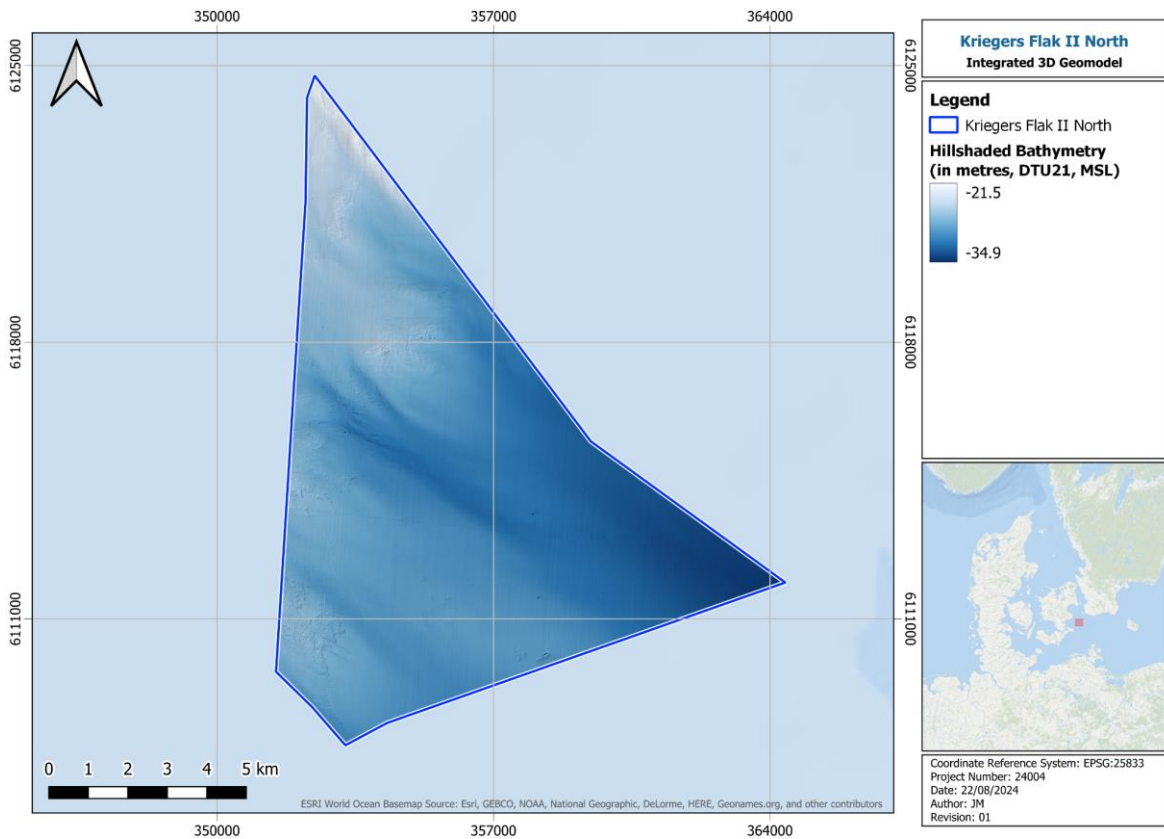


Figure 6-1 - Hillshaded MBES bathymetry

The slope, calculated from the bathymetry data, is presented in Figure 6-2, and reveals that in general the seabed is relatively flat, however in places, the seabed morphology can be complex. The average slope of the site is 0.55°, with the highest values at localised areas reaching up to 32°.

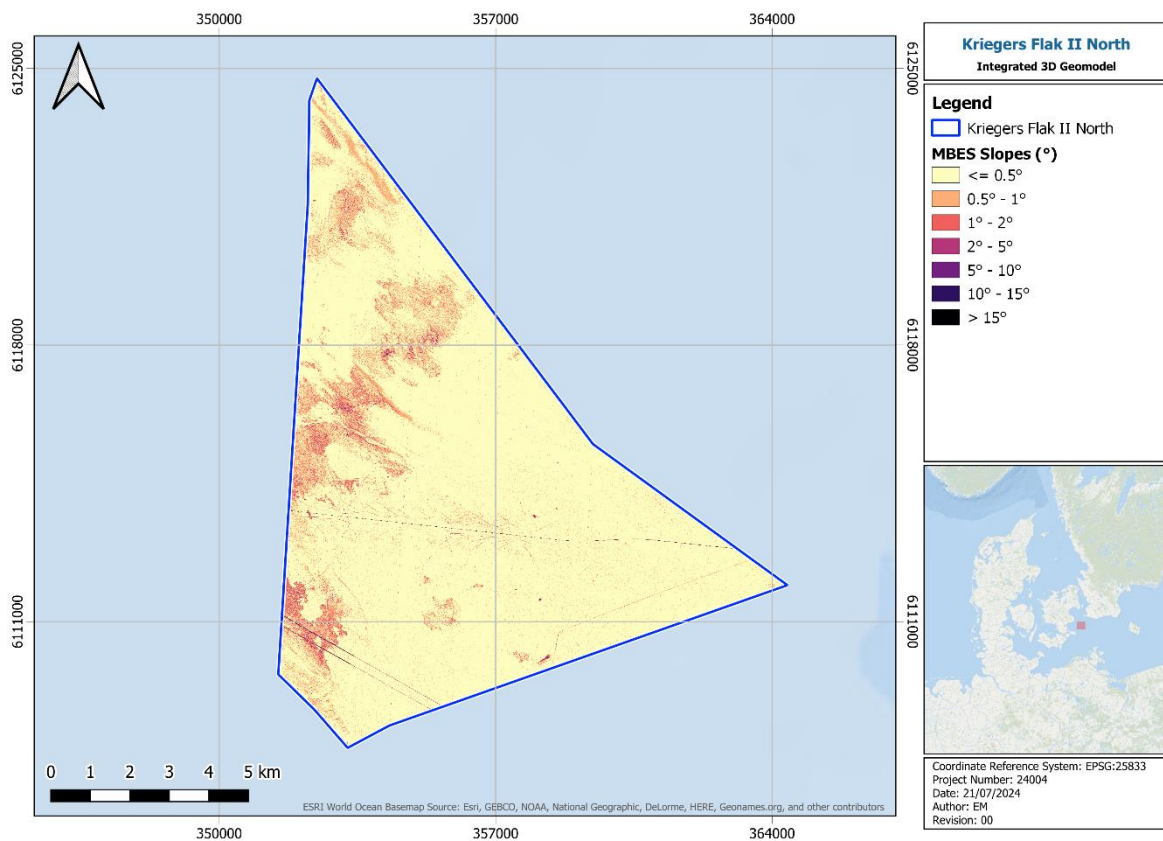


Figure 6-2 - MBES derived slope

The steepest slopes were reported within boulder fields or associated with scouring around seafloor features such as boulders, cable trenches (crossing southern part of the site) and shipwrecks (as presented on Figure 6-3). In the northern and western part of the site, there are areas of higher slope values in comparison to surrounding areas and relatively flat seabed. With increasing distance offshore, the seabed shows low level of slope angle with minimum variation.

Figure 6-3 and Figure 6-4 maps showing the: 1) cable trenches and raised areas consisting of boulder fields; 2) raised areas separated by wide gentle channels and associated slope potentially related to the presence of a wreck; 3) bottom scarring associated with the construction of the Baltic Pipe; 4) associated slope potentially related to the presence of a rock exposure or shipwreck, with parallel cable trenches.

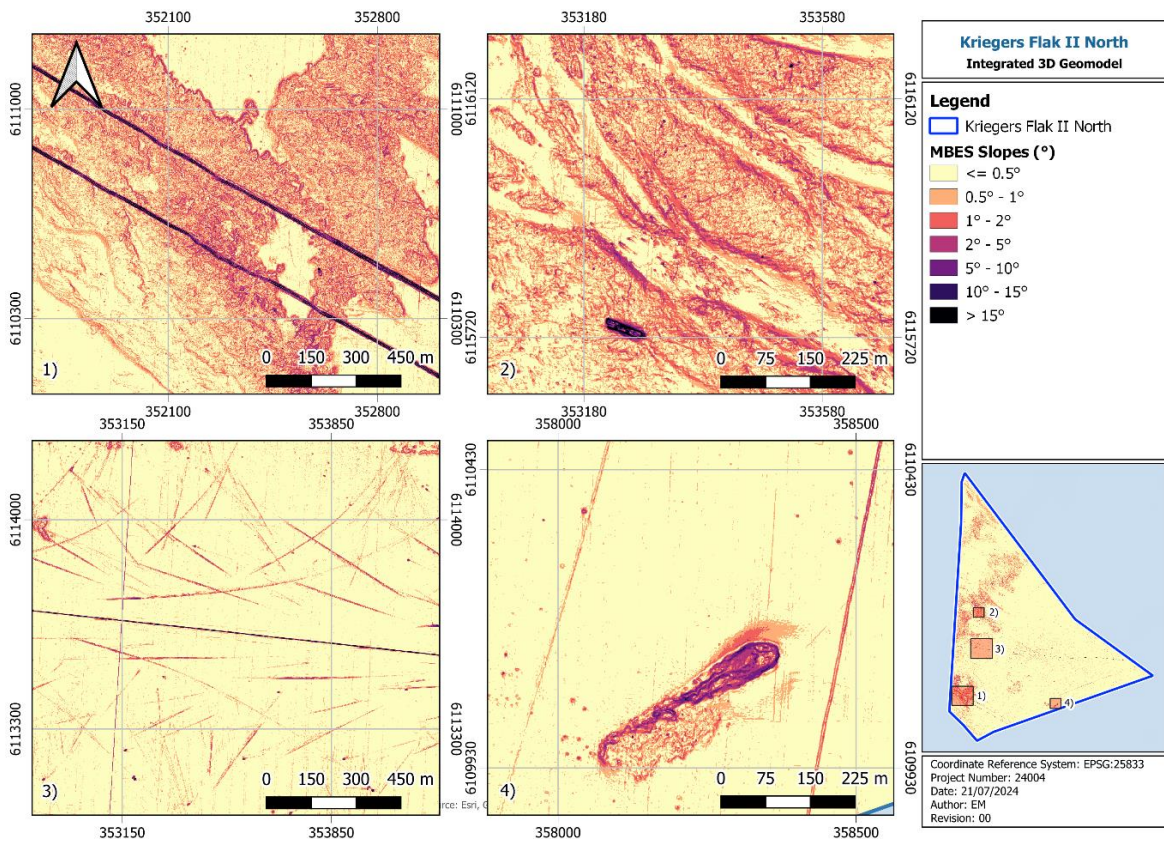


Figure 6-3 - Areas of increased slope angle

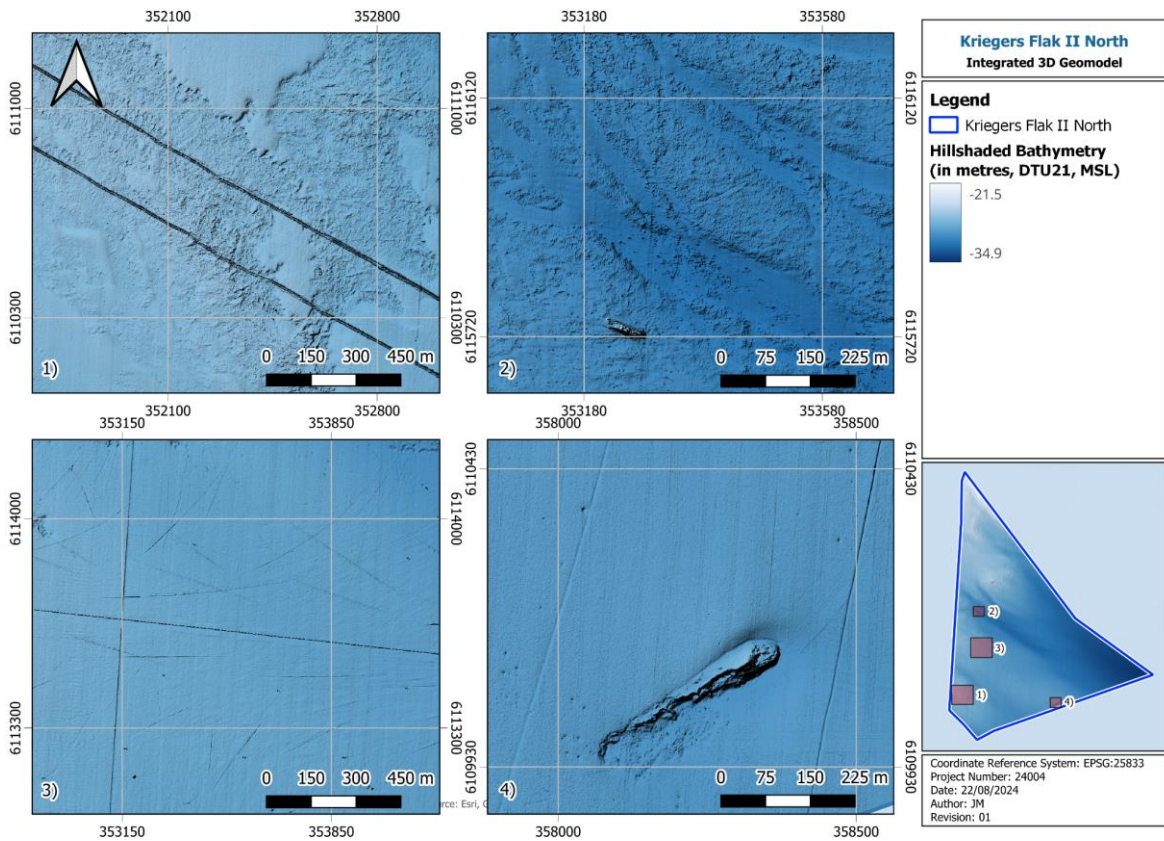


Figure 6-4 - Bathymetry with hillshade

In the northern and western part of the site several elevated seafloors and high gradients were identified (Figure 6-3). The northern and western elevated areas consist of a cluster of features, with a maximum height up to 2 m above the surrounding seafloor. The boulder fields imaged on the MBES data are also depicted in the slope map in areas where the high slope values intensify.

The increase in slope values in the southern part of site was interpreted as seabed scars, which are associated with the construction of the Baltic pipe. Additionally, there are few cable trenches crossing the site in different directions.

There are eight elevated features observed on the MBES and slope imagery (Figure 6-2 and Figure 6-3), which were interpreted as shipwrecks and their associated debris.

6.1.2 SIDE SCAN SONAR

The records of the side scan sonar and bathymetric data have been used by GEOxyz to identify targets laying on the seabed. Based on their findings features identified on the SSS data correlate with the ones interpreted on the MBES grid. The trenching related to the installation of the Baltic Pipe and other infrastructure crossing the site area is noticeable on the SSS data.

The western and northern elevated features identified on the MBES data, are potentially associated with outcropping hard material and boulder fields (Figure 6-5). The highest boulder density is observed in the areas of hard material outcrops (Appendix A).

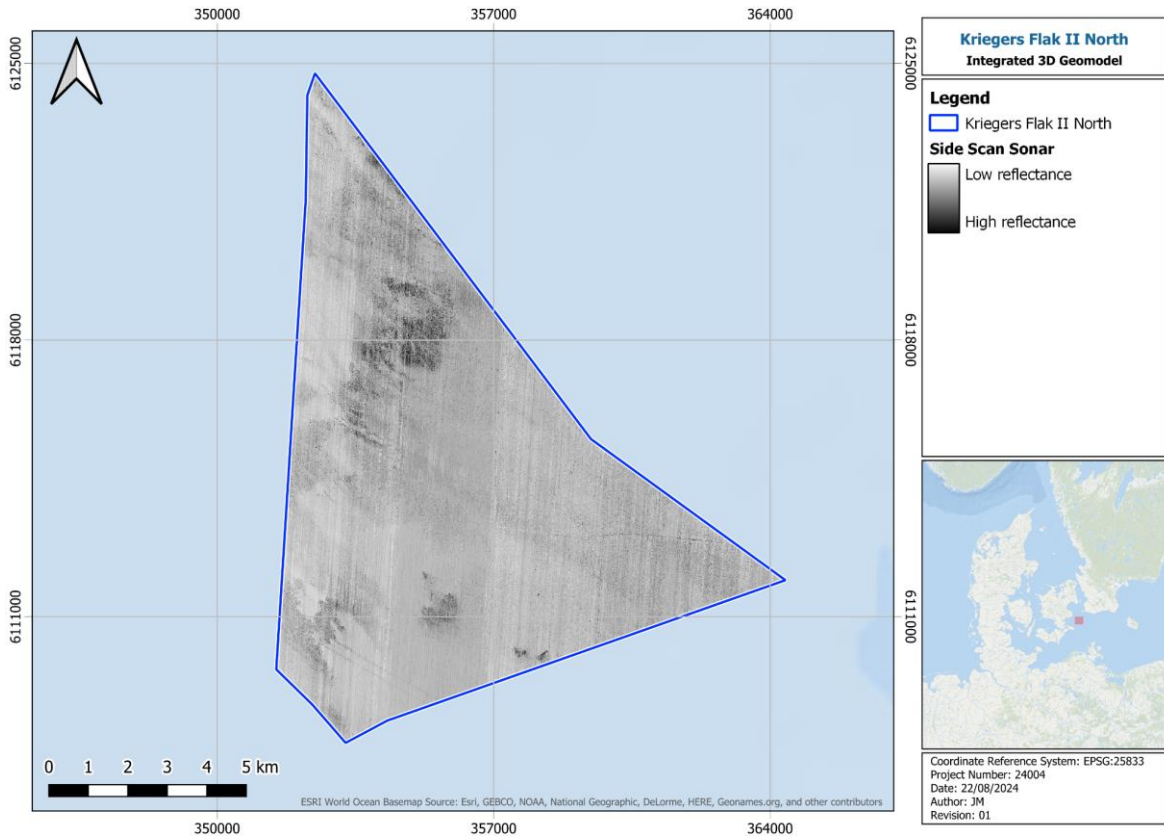


Figure 6-5 - Side scan sonar (GEOxyz, 2024)

The eight MBES features potentially correlated with unknown wrecks and their associated debris, shown on Figure 6-6 can be delineated on the SSS data as well. There are no public records of shipwrecks in this area, therefore further investigation would be needed to confirm their identity and Potential Unexploded Ordnance (pUXO) risk.

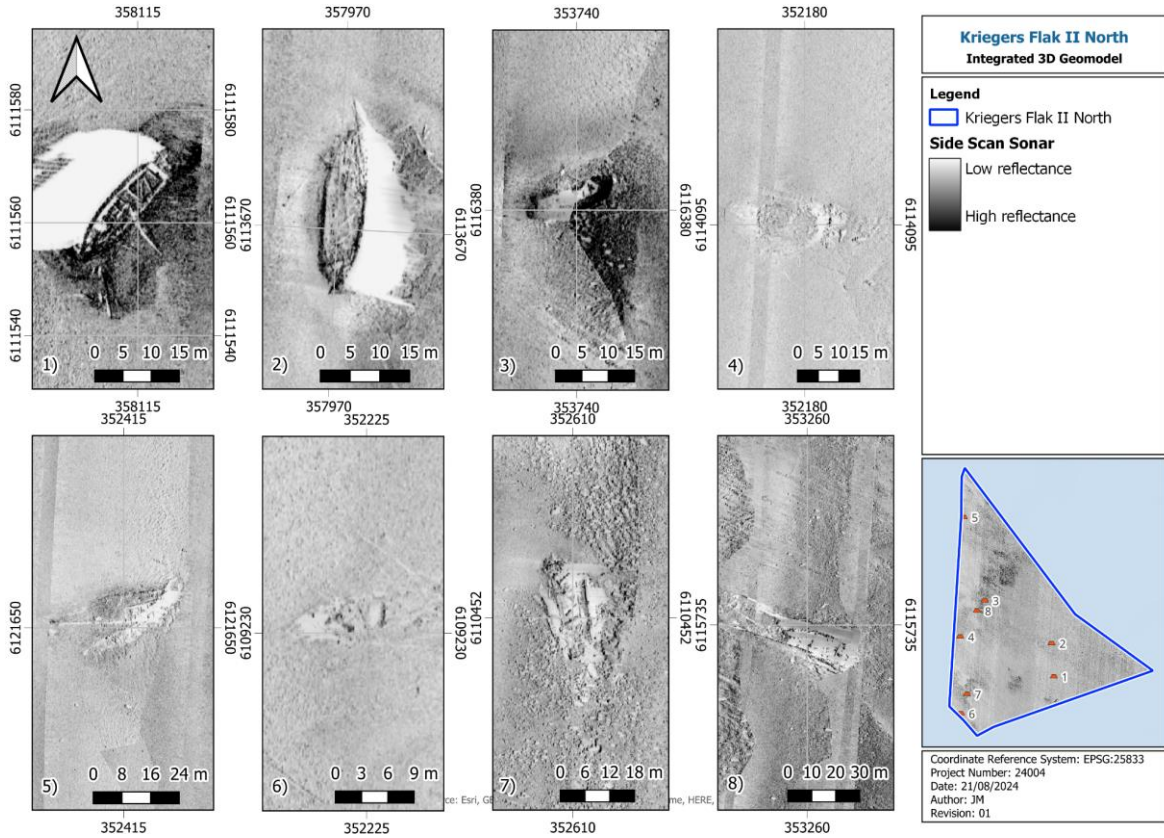


Figure 6-6 - Seafloor features identified as potential wrecks as shown by the SSS data

Eight relatively rounded shaped features (Figure 6-7) have been identified in the southeastern part of the site. Features are aligned along northwest-southeast direction and are located approximately 300 m apart. Change of reflectivity on backscatter and SSS data suggests that the features are covered by coarser sediments than the surrounding material. The size and distribution indicate that the features are likely anthropogenic.

However, further examination based on MBES data revealed that the elevation change associated with the identified features is not substantial (Figure 6-8).

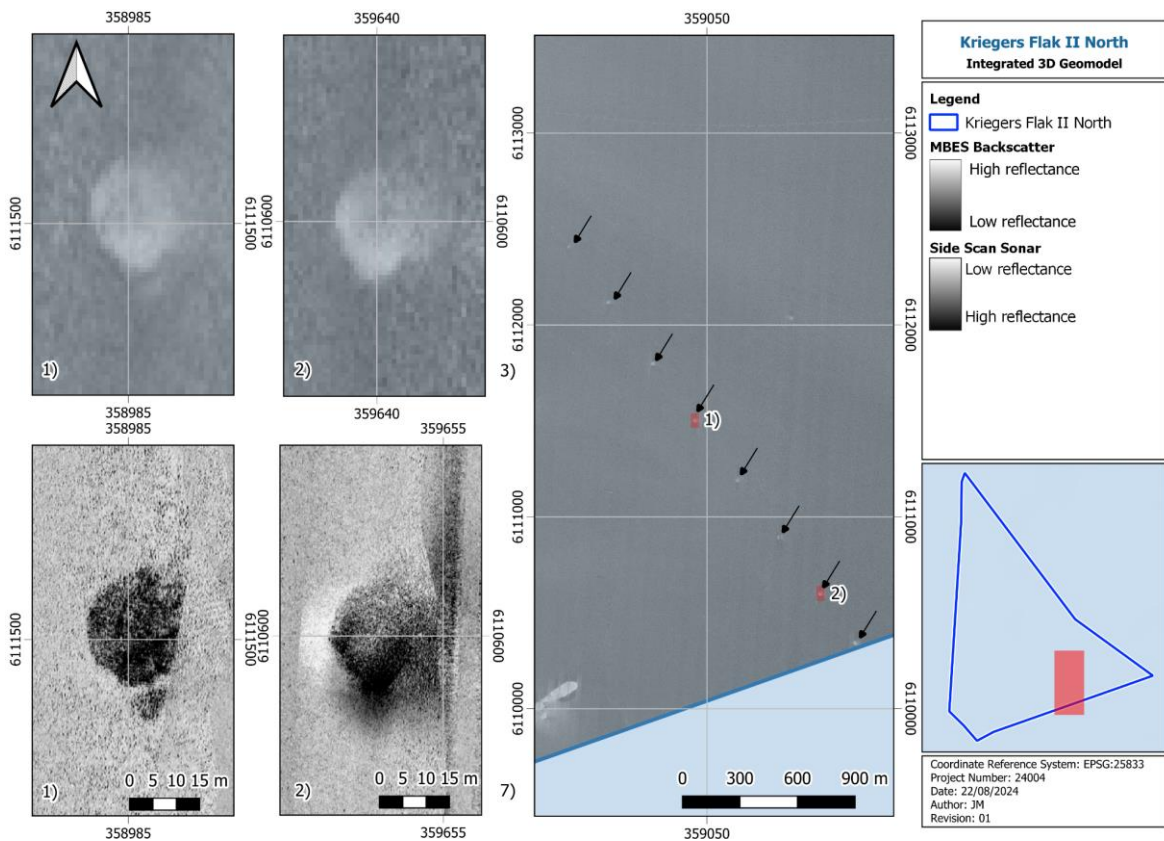


Figure 6-7 - Circular objects identified on SSS and backscatter data

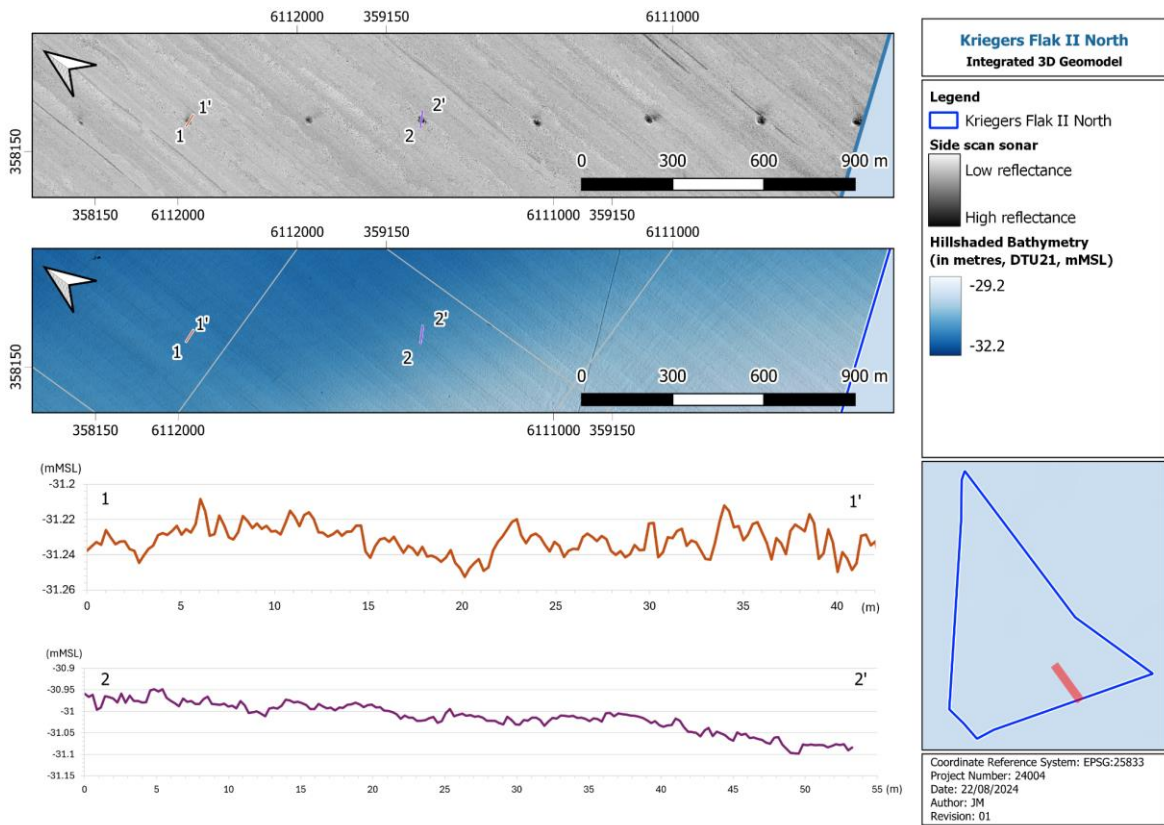


Figure 6-8 - Bathymetry profiles through the observed features

6.1.3 SEAFLOOR LITHOLOGY

The seabed lithology data presented are based on the 2023 GEOxyz geophysical survey and have been refined where deemed necessary. The seabed lithology was assessed based on the available bathymetry (Figure 6-1), backscatter (Figure 6-10), and Low Frequency (LF) and High Frequency (HF) SSS data (Figure 6-5) to determine and define the sediment type and extents. Backscatter measures reflectance and can give indications of seabed texture and sediment grain size, as well as the seafloor relief and overall pattern. This was further constrained using grab samples obtained during the survey.

The seafloor sediment distribution across the site comprises hard substrate observed in the central and northern section of the site. The hard substrate is in places outcropping and sometimes sub-cropping covered by a thin veneer of sediment. These areas have been classed as ‘Till/Diamicton’ as shown in Figure 6-9. The interpreted thin veneer of sediment allows for the undulating elevation changes of the underlying bedrock to be seen with no clear distinction between outcropping hard substrate transitioning to sub-cropping. The hard substrate is usually surrounded by fine grained sediments.

Moving south and east, as the sediment cover is interpreted to increase, the seabed composition is comprised of SAND, muddy SAND and MUD, and sandy MUD, as seen by a change to darker reflectivity of the backscatter. The finest sediments interpreted as MUD to sandy MUD are observed in the southeastern corner of the study area. In the south and centre part of the site, the sediment composition changes to sandy MUD and SAND, as identified by increased MBES reflectivity.

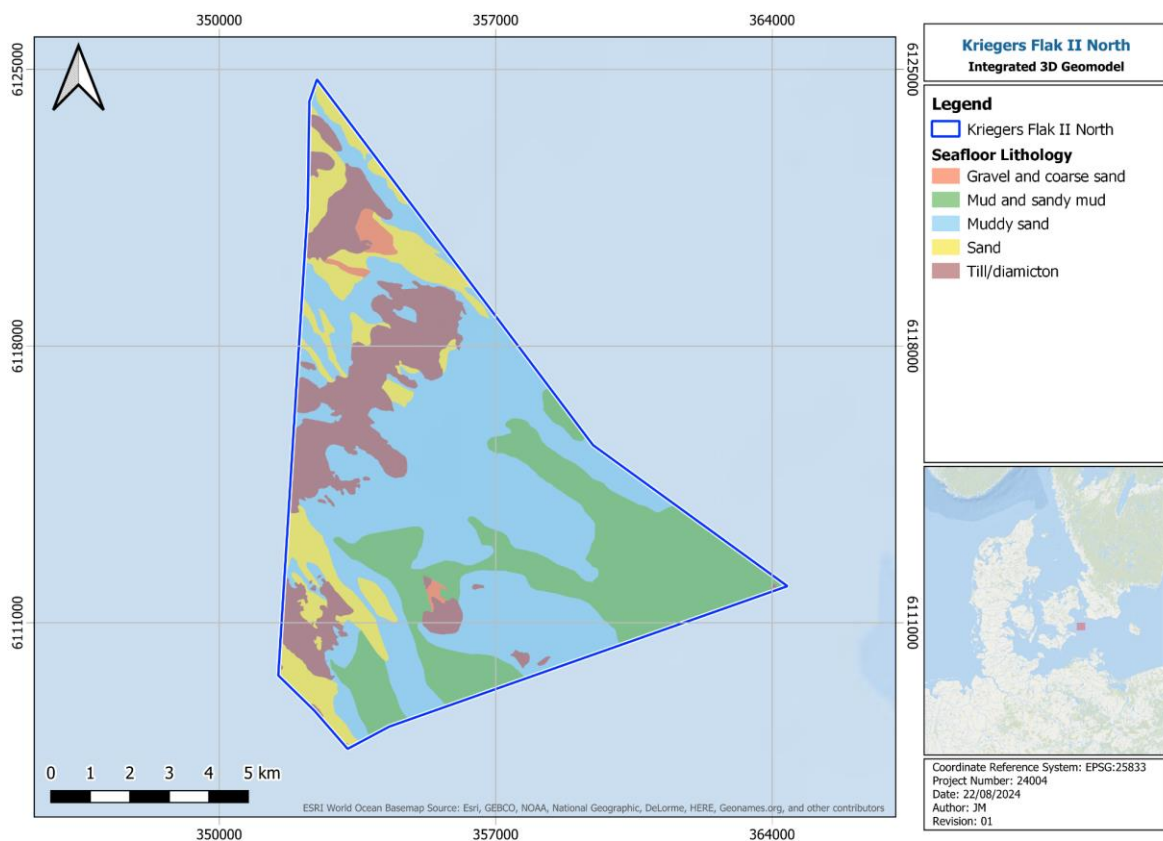


Figure 6-9 - Overview of the seabed lithology classification and extents (GEOxyz, 2024; Gavin and Doherty Geosolutions Ltd., 2024)

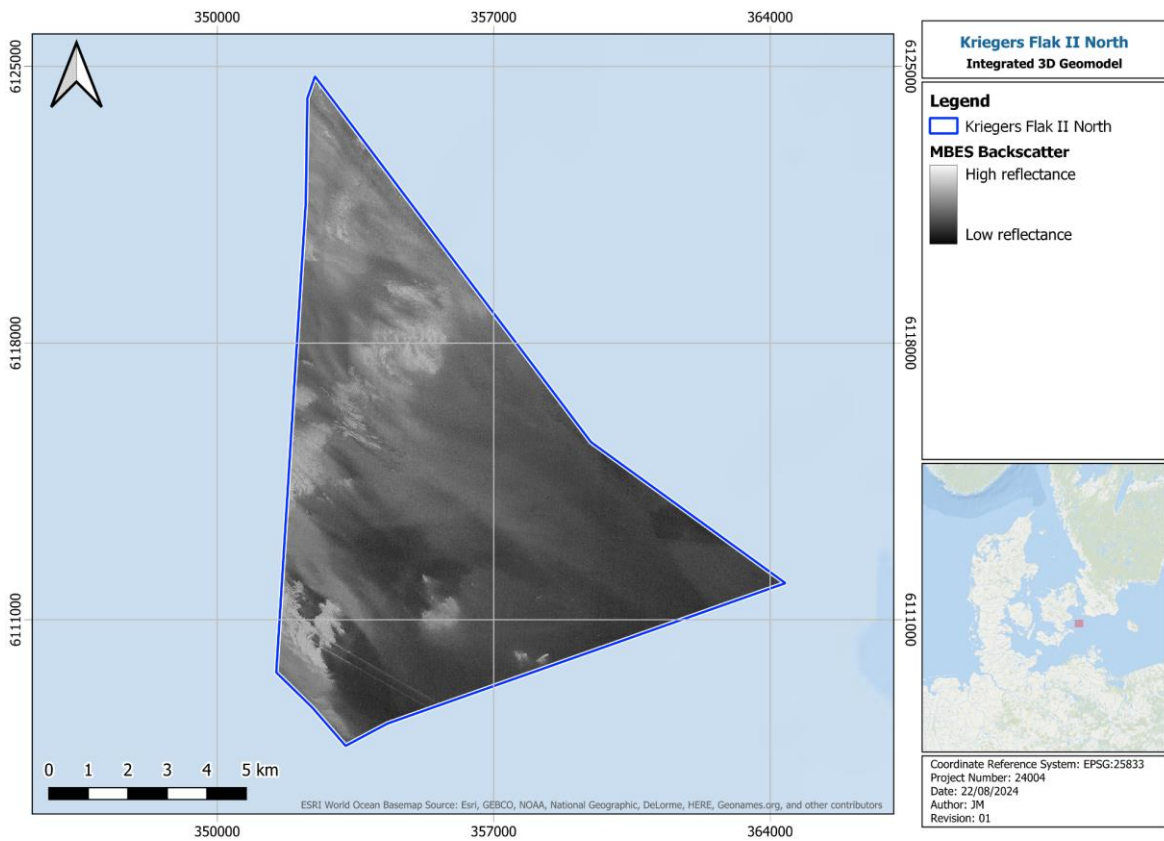


Figure 6-10 - MBES backscatter (GEOxyz, 2024)

Table 6-1 - Sediment classification based on MBES backscatter analysis

Sediment classification based on MBES backscatter analysis		
Data Example	Description	Sediment Classification
	high reflectance; moderately textured	Stony areas and stone reefs with a veneer of sediment
	medium reflectance; smooth texture	SAND
	low reflectance; low/moderate texture	Sandy silty soft bottom

6.1.4 SEAFLOOR MORPHOLOGY

The seabed across the site is generally flat, however, various morphological bedforms have been identified. The main seabed changes are associated with outcropping hard substrate, channels, boulders, sediment waves and scars.

Extensive seabed scarring was found in the southern area of the site (Figure 6-11). These scars were interpreted to be associated with the construction of the Baltic Pipe. There are numerous locations of disturbed seabed and anchor scars. These scars appear to be deeper and more erratic in their shape and positioning, comparing to others found within the site. They are located on both sides of the Baltic Pipe and extend up to 800 m each way. Further south the scars were interpreted to be associated with fishing activity, the trawl marks are more equally spaced and shallower with defined paths across a wider area. This is illustrated in Figure 6-3 and Figure 6-4.

Hard material was interpreted to be outcropping or sub-cropping with a thin veneer of sediment (Section 6.1.2) in central, western, and northern areas, with a few small, isolated locations across the site. Extents for areas of boulder fields usually coincide with the area of hard material. Boulders are difficult to distinguish from the underlying bedrock, in part due to the variable veneer of sediment across the bedrock extents.

Depressions in the seabed were interpreted across the site and are similar in size and distribution. Their distribution varies across the site and are essentially concentrated in the southern part of the site (pitted seabed). These are shallow truncated channel features, with maximal localised depths up to 2.5 m deeper than the surrounding seabed. The northwest-southeast orientated channel features which reach up to 1500 m in width separate four raised areas of the seafloor.

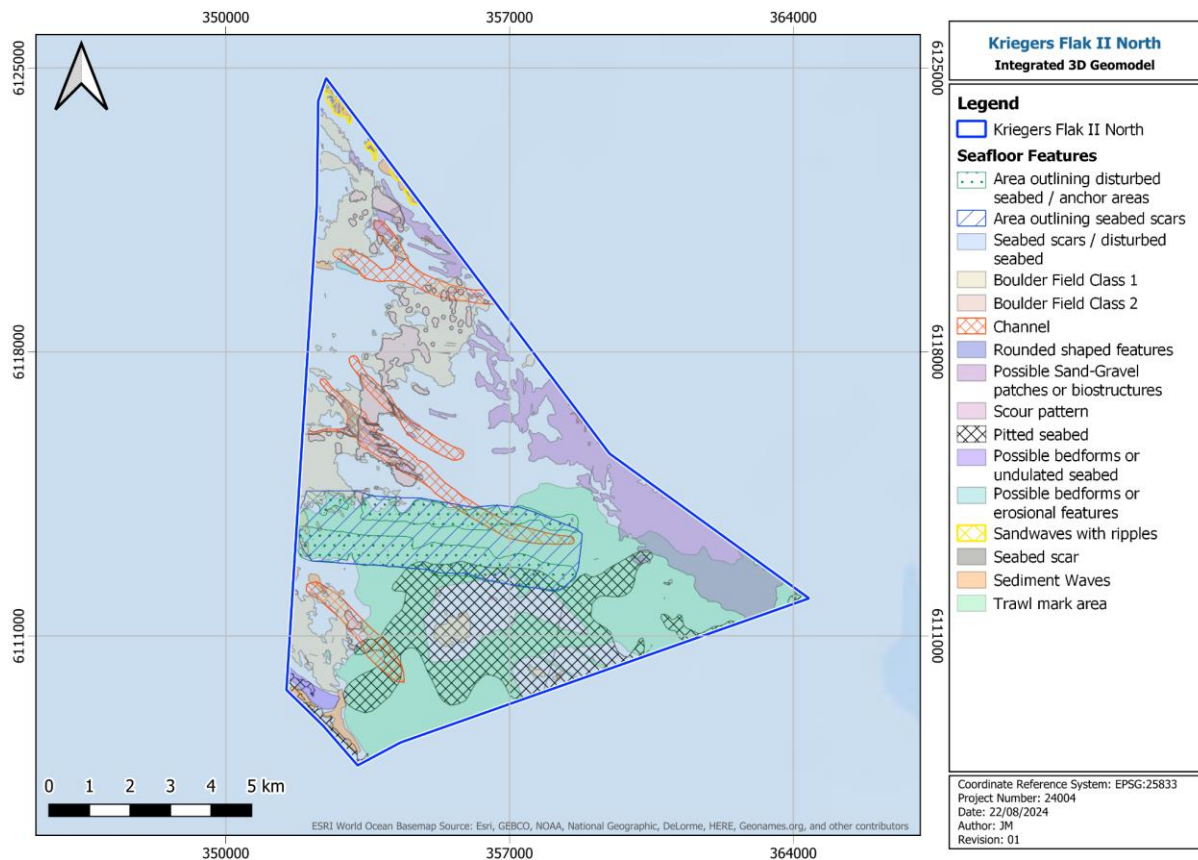


Figure 6-11 - Overview of seabed features (GEOxyz, 2023; refined by Gavin and Doherty Geosolutions Ltd., 2024)

Area of undulated seabed can be observed only in the southwestern part of the site. Those changes in seabed elevation are interpreted to be caused by glacial processes. Figure 6-12 illustrates the location and characteristics of the undulated seabed. In close proximity, boulder fields and sediment waves are also observed.

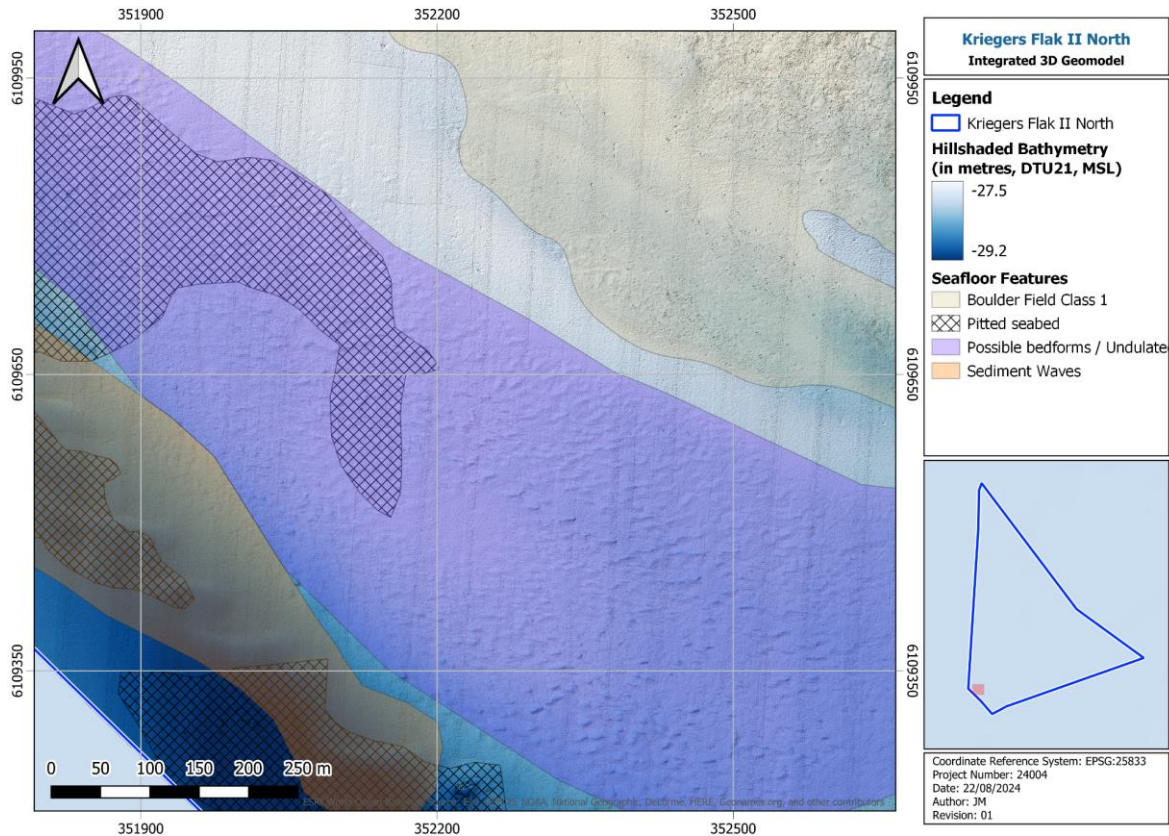


Figure 6-12 - Example of undulated seabed and other seabed features

6.1.5 SEAFLOOR OBJECTS

Seafloor contacts were originally picked by the survey contractor GEOxyz using raw and processed data at a higher resolution within the sensor specific software. The higher resolution enables more precise interpretation, but data are much denser and require sensor specific software to interrogate. Therefore, conventionally data are delivered as mosaics with a reduced resolution.

Venterra reviewed the positioning and correlation of the provided seafloor contacts to other datasets. A total of 13056 seafloor contacts, shown on Figure 6-13, were picked on the SSS (11391) and MBES (1665) data and are classified as either boulder, debris, fishing equipment or unknown, with further comments on contacts potentially associated with known shipwrecks, or rock exposure.

Most of the seafloor contacts, 10842 picked on the SSS and 1635 picked on the MBES are classified as boulders. These targets' locations coincide with the areas of hard material, and areas identified as boulder fields.

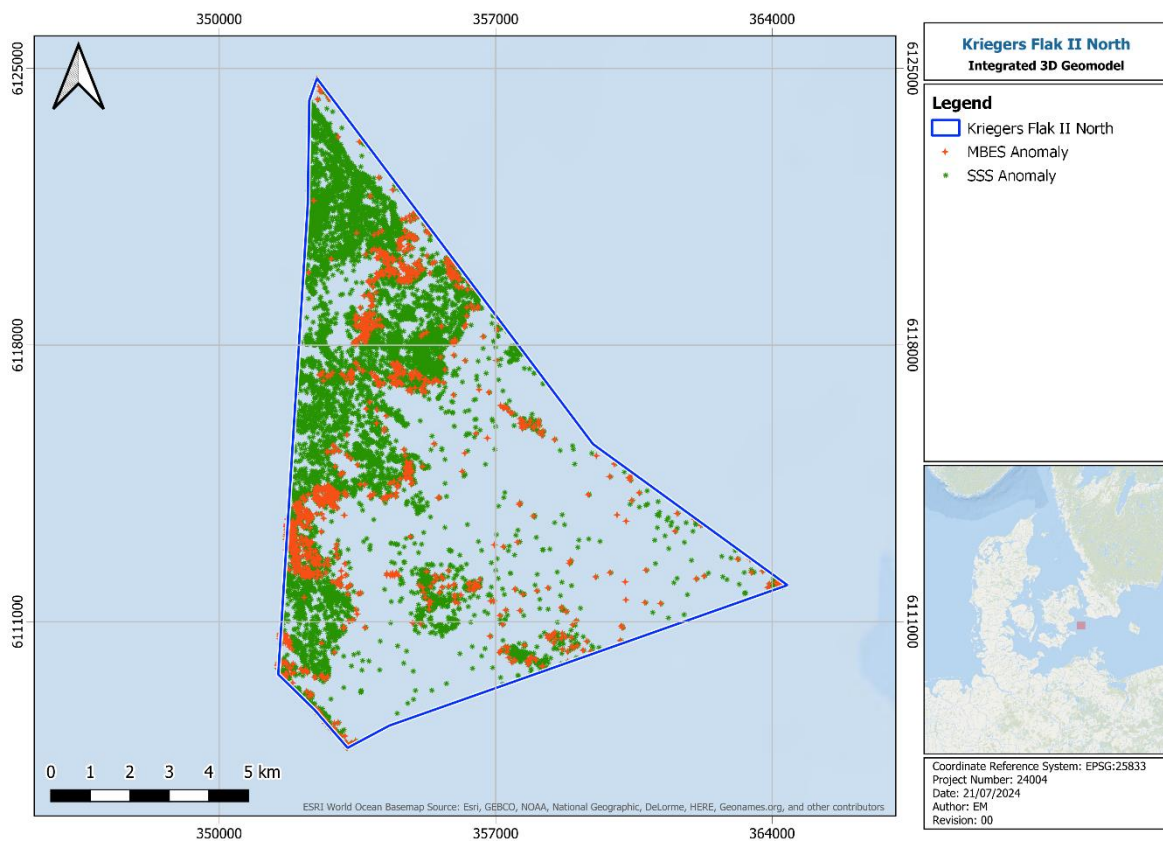


Figure 6-13 - Example of seabed contacts picked on SSS and MBES bathymetry

6.1.6 MAGNETIC ANOMALIES

A total of 541 magnetic anomalies were interpreted within the site area. These were classified as either generated by anthropogenic sources or related to geology. Interpreted magnetic anomalies are shown in Figure 6-14.

Several linear magnetic anomalies were identified in the immediate vicinity of known underwater cables and pipelines across the site. In the south of the site, linear anomalies associated with the Baltic Pipe & HK22008 Kriegers Flak A-Rodvig are observed. Some magnetic anomalies indicate the presence of additional subsea infrastructure, which were not previously identified.

Other linear anomalies were observed, in the northern part of the site following a north-northwest-south-southeast direction, two in the central part of the site following west-northwest-east-southeast direction and southwest-northeast directions. Another linear anomaly was observed in the southern part of the site, parallel to the southern site boundary and following a west-southwest-east-northeast direction. Those anomalies could not be related with any existing of the structures listed.

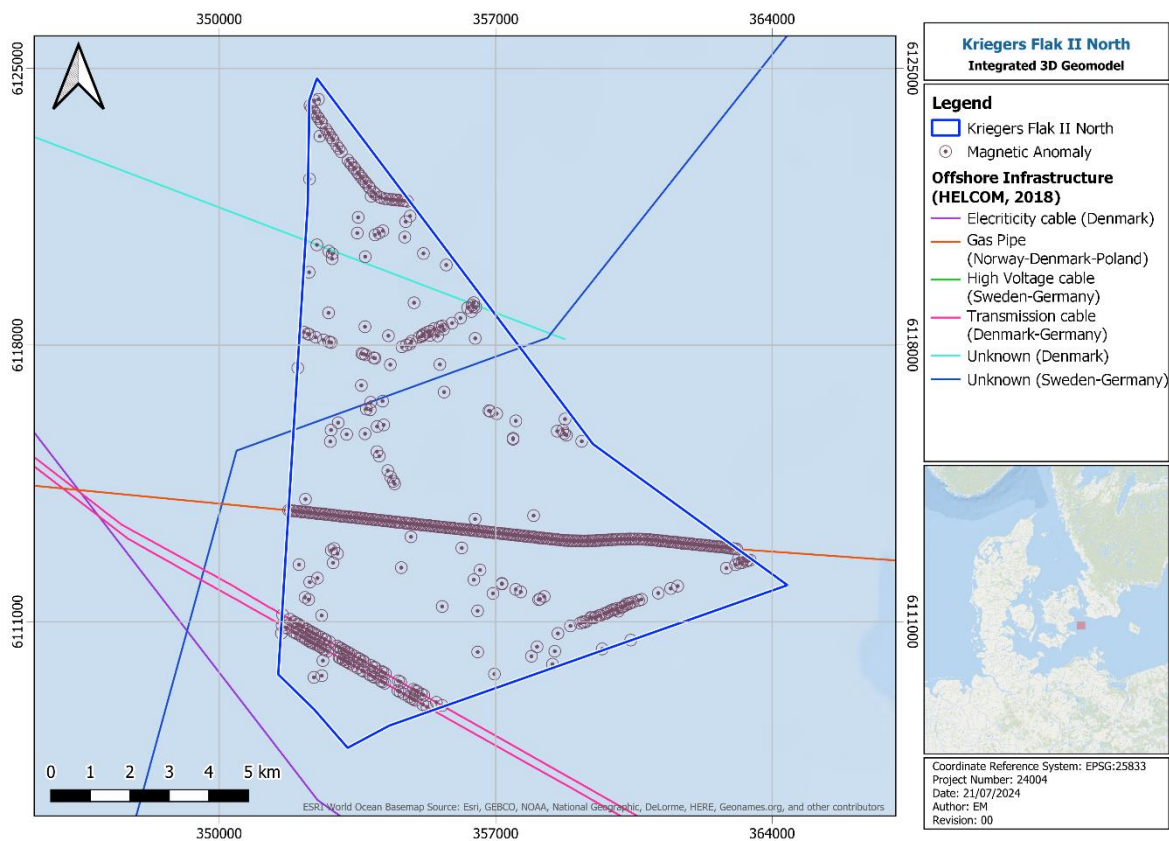


Figure 6-14 - Magnetic contacts and offshore infrastructure (HELCOM, 2018)

6.2 SUB-SEAFLOOR INTERPRETATION

Any mention of “seismic unit” or simply “unit” refers to seismostratigraphic units.

Four horizons were interpreted in the seismic data, differentiating four seismic units, Unit I, Unit III, Unit IV and Unit V. Unit II was identified in seismic data but, at the time of preliminary geotechnical data integration, it was not identifiable in the geotechnical readings. Unit II was then included within Unit III, as agreed with the Client during discussions related with the seismostratigraphic model. Unit III was further subdivided into two subunits based on lithological and/or seismic facies variations (horizon H20) but was gridded as one unit. Table 6-2 shows a summary of the interpreted seismic units and horizons, their acoustic characteristics, age, lithology, and depositional environment (based on newly acquired geotechnical data and literature). A cross-sectional schematic diagram showing the approximate unit distribution across the width of the survey area, south to north, is presented in Figure 6-15. Detailed descriptions of each seismic unit are presented in Sections 6.2.1 to 6.2.4. A summary of maximum and minimum elevations, depths, and thicknesses for each seismic unit can be found in Table 6-3. Description of additional elements identified during the seismic interpretation can be found in Section 8.2.

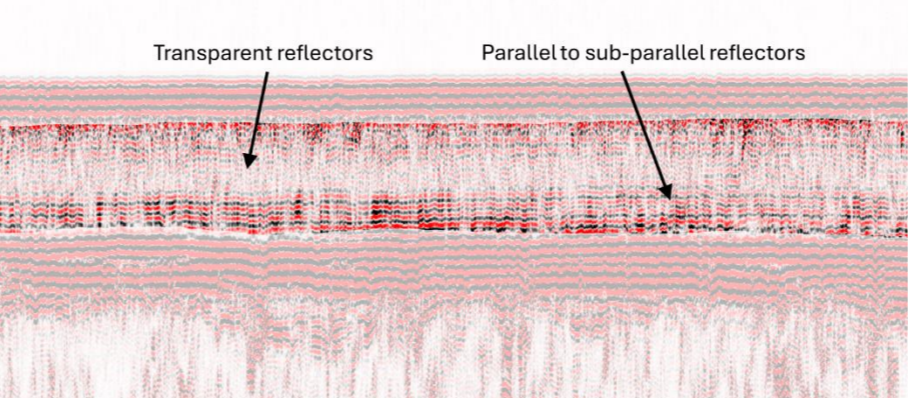
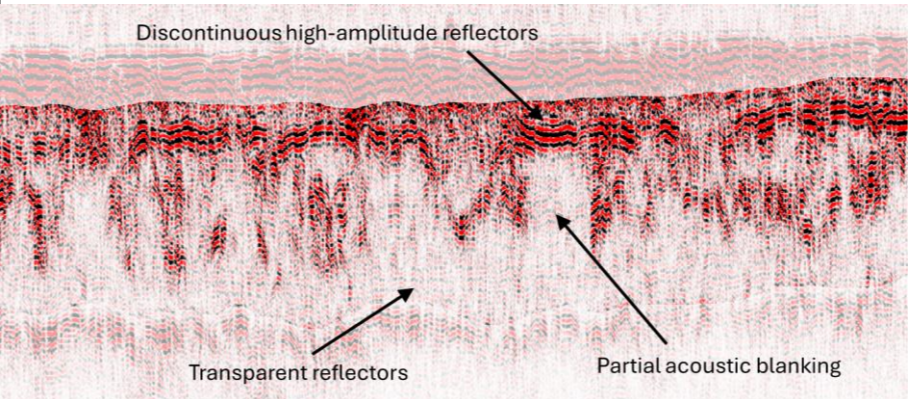
In addition to the figures shown in Section 6.2, counterpart charts are also provided in Appendix A. Charts 24004-MSL-003-01-01 to 24004-MSL-003-04-01 show the elevations (mMSL) of the tops of seismic Units I to V. Charts 24004-BSF-002-01-01 to 24004-BSF-002-04-01 show depths (mBSF) to the top of seismic Units I to V. Charts 24004-ISO-004-01-01 to 24004-ISO-004-03-01 show isochores (vertical thickness in metres) for seismic Units I

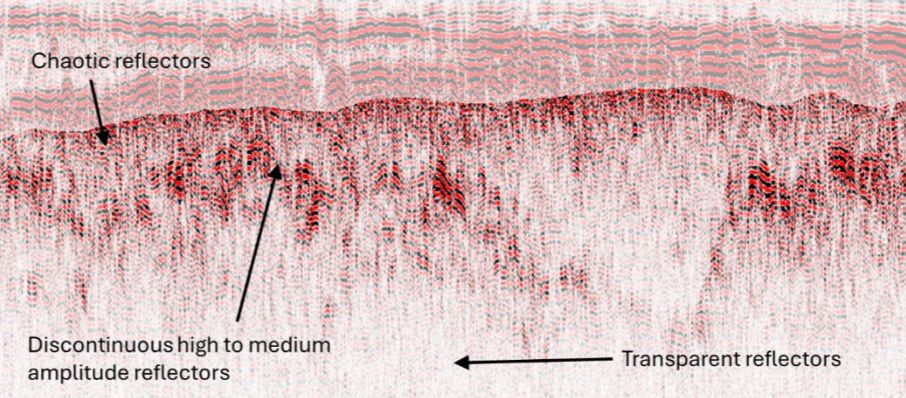
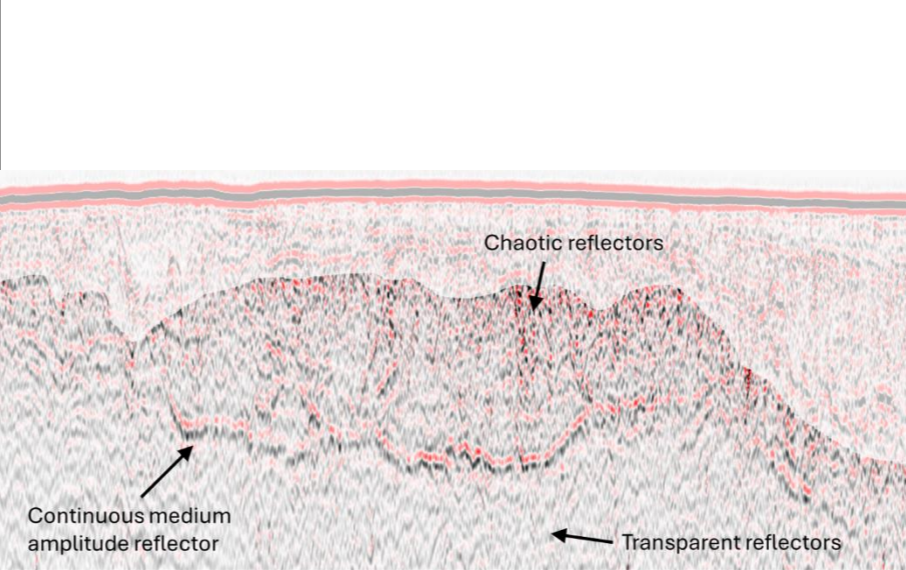
to IV. Charts with interpreted seismic cross sections are shown in Appendix B (Charts 24004-PRO-006-13-00 to 24004-PRO-006-24-00).

The seismic unit numbering takes into account the unit and sub-units that have not been interpreted in the seismic data as it was not part of the remit of this study. These consist of:

- Unit II (post-glacial transition), which was observed across the entire site in seismic data but only evidenced in the geotechnical data at a later stage of the project, when the seismostratigraphic was already finalized and approved by the client. Because this unit represents the transition between Unit I and Unit III, it shares similar geotechnical properties with both GU Ib and GU IIIa1 and does not contrast much with overlying and underlying sediments properties. Therefore, it was considered to have limited impact on design, because its geotechnical properties are captured by the overlying (GU Ib) and underlying (GU IIIa1) sub-units.
- Unit III sub-units separated by H20, which could not be reliably picked because it only corresponds to seismic facies change within Unit III. This horizon was only picked on a SBP subset (WPA) by GEOxyz. Therefore, the refined version of H20 is only available for SBP lines included in the WPA seismic subset in the northern site Kingdom project, and for the time domain only.
- Class-A, Lithified Chalk, which was identified in geotechnical data as GU Vb, but could not be clearly identified in seismic data.

Table 6-2 - Overview of the interpreted units

Overview of the interpreted units									
Seismic Unit	Geotechnical Unit	Seismic Dataset	Top Horizon	Base Horizon	Seismic Facies Description	Seismic Facies Example	Age	Geotechnical Description	Depositional Environment
Unit I (SU I)	GU Ia	SBP	H00 Seafloor	H05	Medium to high amplitude, chaotic and discontinuous reflectors displayed in the upper part, with transparent or low amplitude, sub-parallel and semi-continuous reflectors seen in the mid-section. The lower part displays higher amplitude, continuous, parallel reflections in discrete areas.		Holocene	Loose to medium dense SAND	Marine
	GU Ib							Very low to low strength CLAY	
Unit III (SU III)	GU II	SBP	H00 H05	H25 H30	High amplitude, sub-parallel, semi-continuous reflectors displayed in the upper part (Unit II), with medium amplitude, chaotic, discontinuous reflectors which show partial acoustic blanking seen in the mid-section. The lower part, located below internal reflection H20, displays low amplitude and occasionally transparent reflections.		Pleistocene (Weichselian)	GU II was not picked as part of the seismostratigraphic unitisation but can be observed from both the geophysical and geotechnical data. This unit consists of very silty, sandy to very sandy, low to medium plasticity, very low to medium strength CLAY/SILT	Post Glacial/ Glaciolacustrine
	GU IIIa1							Silty to very silty, slightly sandy, medium to high plasticity, very low to low strength CLAY	
	GU IIIa2							Dense to very dense well sorted silty SAND	
	GU IIIb1							Medium dense to dense silty SAND with closely to widely spaced thin beds of clay	
	GU IIIb2							Sandy, slightly gravelly, medium to extremely high strength Clay	
	GU IIIb2								

Overview of the interpreted units									
Seismic Unit	Geotechnical Unit	Seismic Dataset	Top Horizon	Base Horizon	Seismic Facies Description	Seismic Facies Example	Age	Geotechnical Description	Depositional Environment
Unit IV (SU IV)	GU IVa	SBP	H00 H05 H25	H30	On the SBP dataset, the upper part of the unit shows low-medium amplitude, chaotic and semi-continuous reflectors. The signal is then lost. Occasionally, features such as incisions and infilled channels are visible. On the UHRS dataset, the unit shows high amplitude, chaotic and semi-continuous reflectors, depicting complex geological/glacial structures.		Pleistocene (Weichselian)	CLAY TILL, very silty, very sandy, slightly gravelly, low plasticity, calcareous, micaceous, sand is fine to coarse, gravel is fine to coarse, subangular to subrounded, of mixed lithology (Extremely high strength)	Glacial
	GU IVb							SAND TILL, fine to coarse, poorly sorted, clayey, very silty, very gravelly, calcareous (Dense to very dense), with fine to coarse gravel size chalk nodules, highly calcareous	
Unit V (SU V)	GU Va	UHRS	H30	N/A	Seismic transparency along with low-medium amplitude, chaotic reflections describe a significant part of this unit. In addition, occasional low amplitude sub-parallel, undulating, and semi-continuous reflections were seen.		Upper Cretaceous	CHALK (Dm/Dc), unlithified (H1), white (N9), highly calcareous (Very high to extremely high strength) with rare fine to coarse gravel and stone sized fragments of chert, very strongly indurated (H5), non-calcareous (Very strong to extremely strong)	Marine (sedimentary bedrock)
	GU Vb							CHALK (A1-B2), slightly indurated (H2), unfractured to slightly fractured (S1-S2), highly calcareous (Extremely weak to very weak), with rare fine to coarse gravel sized pockets and extremely closely to closely spaced thin to thick laminae of marl, highly calcareous, and rare fine gravel to stone size fragments of chert, very strongly indurated (H5), dark grey to black (N3-N1), non-calcareous (Very strong to extremely strong)	

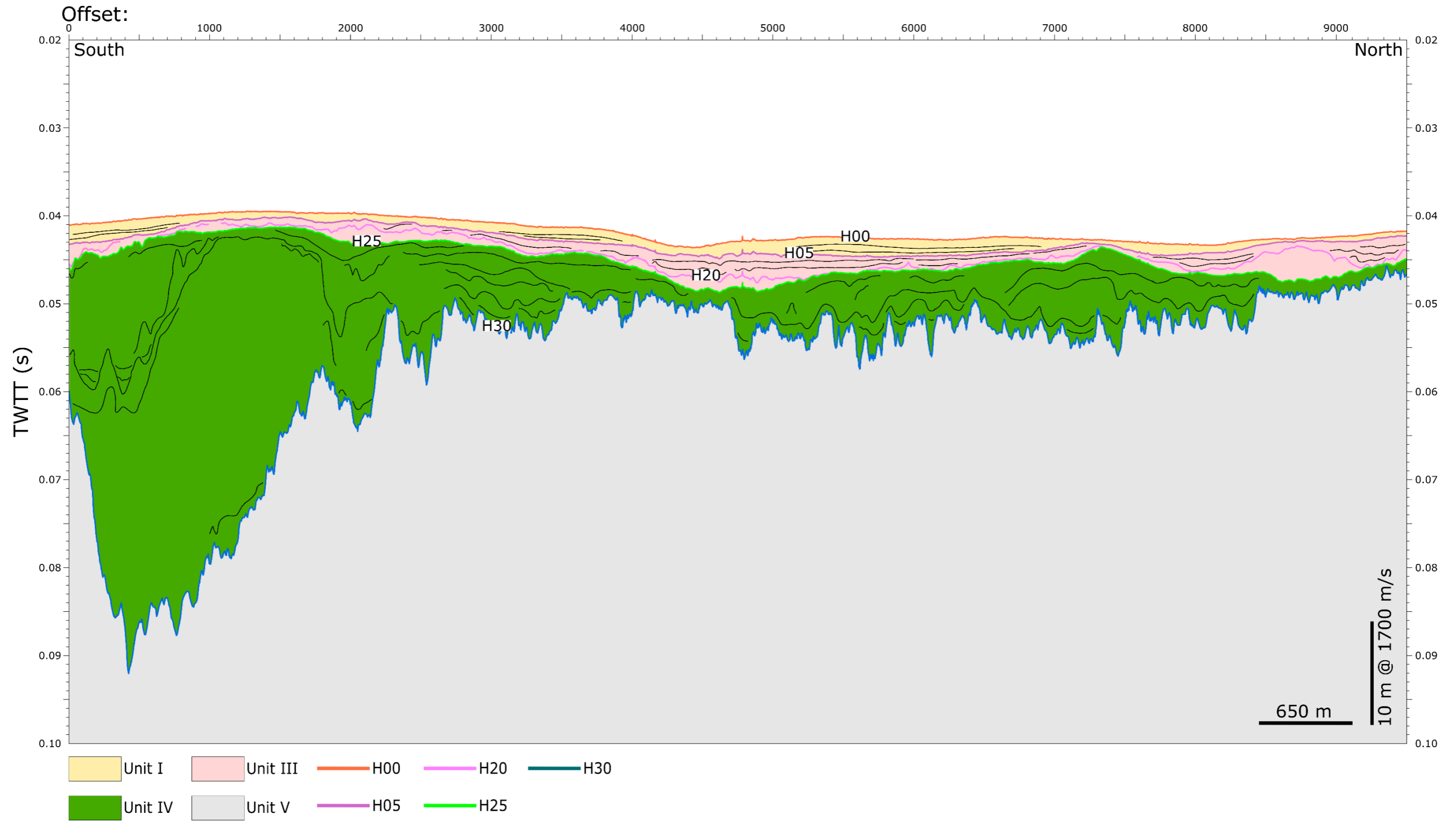


Figure 6-15 - Schematic diagram showing seismic unit distribution west to east in the survey area

6.2.1 SEISMIC UNIT I (SU I) - MARINE SEDIMENTS

6.2.1.1 GEOPHYSICAL DESCRIPTION

The top of Unit I corresponds to the seafloor, which is represented by a high amplitude reflection across the entirety of the site. The upper section of the unit displays medium to high amplitude, chaotic and discontinuous reflectors. The mid-section shows transparent or low amplitude, sub-parallel and semi-continuous reflectors. The lower section of the unit often shows higher amplitude, continuous, parallel reflections in discrete areas. Overall, the unit is mainly represented as lower amplitude, and transparent seismic facies. The horizon H05 is a high amplitude reflection which corresponds to the base of Unit I. H05 represents the interface between seismic Units I (marine sediments) and III (glaciolacustrine), though in some areas, where H05 becomes shallower and truncates against the seabed, there is some evidence of an underlying unit. The visibility and occurrence of these reflectors are not consistent such that a corresponding unit/reflector was not picked. It is believed this may correspond to Unit II, post-glacial transition. H05 was solely mapped on the SBP dataset, with minimal reflectors seen within the depth range of the unit within the UHRS dataset.

6.2.1.2 SPATIAL DISTRIBUTION

Unit I was interpreted across most of the site, with the exception of areas in which the unit is truncated against the seabed or is not seen within the seismic data. This corresponds to north-south trending gaps that span the length of the site along the western side of the site. In these areas, Units III and IV are outcropping. The top of Unit I corresponds to the seabed and its elevation varies between -21.6 mMSL to -34.8 mMSL (Figure 6-16).

The unit is present as a relatively thin layer of up to 2.2 m thick, as shown in the isochore map (Figure 6-17), with the highest thicknesses observed in the central and south-eastern parts of the site. The unit is at its thinnest in the north of the site and along the western boundary.

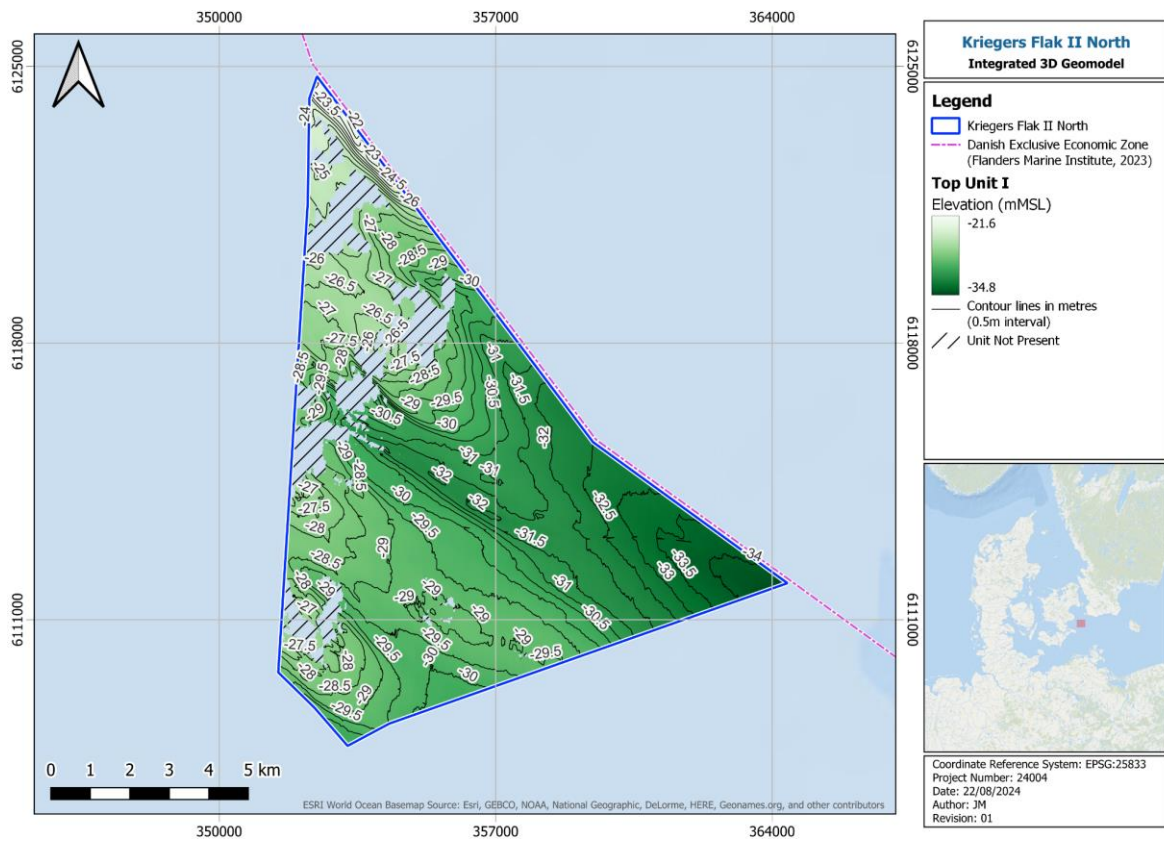


Figure 6-16 - Top of Unit I elevation (mMSL)

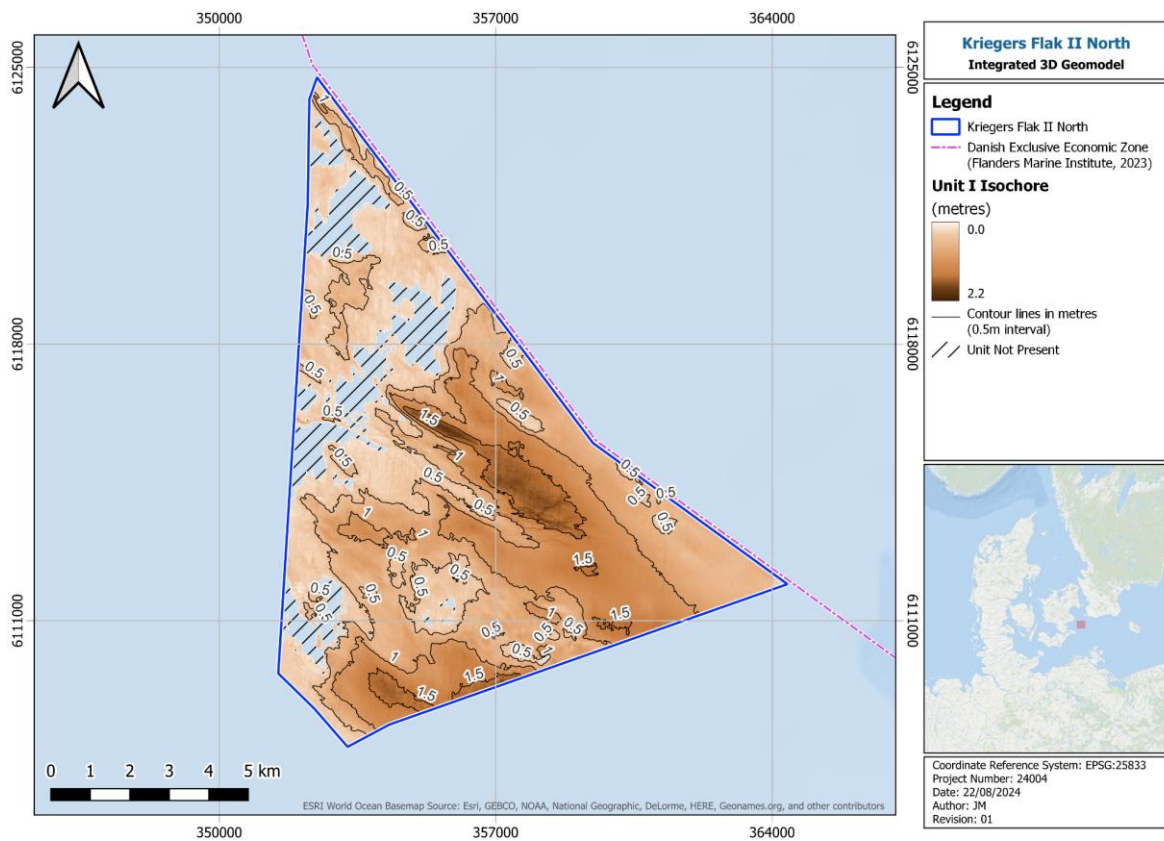


Figure 6-17 - Unit I vertical thickness isochore

6.2.1.3 GEOTECHNICAL DESCRIPTION

Unit I is described based on seismic as medium to high amplitude, chaotic and discontinuous reflectors displayed in the upper part, with transparent or low amplitude, sub-parallel and semi-continuous reflectors seen in the mid-section. The lower part displays higher amplitude, continuous, parallel reflections in discrete areas.

The geotechnical properties for this unit were described from CPT data to determine the appropriate geotechnical unitisation. Unit I was split into two geotechnical units (Table 6-2):

- GU Ia described as loose to medium dense SAND
- GU Ib described as very low to low strength CLAY

6.2.1.4 INTERPRETATION

Seismic horizon H05 is a continuous reflector, corresponding to a minor unconformity at the base of Unit I (Figure 6-18 and Figure 6-19). Based on the interpretation of seismic facies and expected soil units, Unit I corresponds to post-glacial marine deposits. Locally this represents the top of Unit III where it is underlying Unit I. This reflector marks the transition from the mostly transparent lower facies of Unit I (marine sediments) and the reflectors of increased amplitude of Unit III (glaciolacustrine). Where the unit is truncated against the seabed (Figure 6-16 and Figure 6-17) it is not possible to fully trace H05 up to the H00 (seabed) reflector due to the width of the ringing signal of the seabed reflection (Figure 6-18). Due to this, pseudo picks were applied to force the horizon up to and above the seabed for gridding purposes. The effect of the pseudo pick is visible within the final grids, though this is the current limitation of the methodology.

During this interpretation, the Unit I extents have been refined and revised based on the original extents provided by GEOxyz (GEOxyz, 2024). The original H05 interpretation (GEOxyz, 2024) had a slightly more extensive coverage of the site, with the main difference being the coverage in the northern part of the site. Some of GEOxyz's original H05 picks were reinterpreted as H25, a horizon which corresponds to the top of Glacial, a unit that GEOxyz did not interpret.

The SBP dataset had an inconsistent tidal reduction applied during the original data processing stage (GEOxyz, 2024). This adds difficulty to establishing a consistent H05 pick and tie-in across a large dataset when working in TWTT. Every effort has been made to reduce offsets between lines using mistie analysis, though there may be some remnant evidence of this in the final grids.

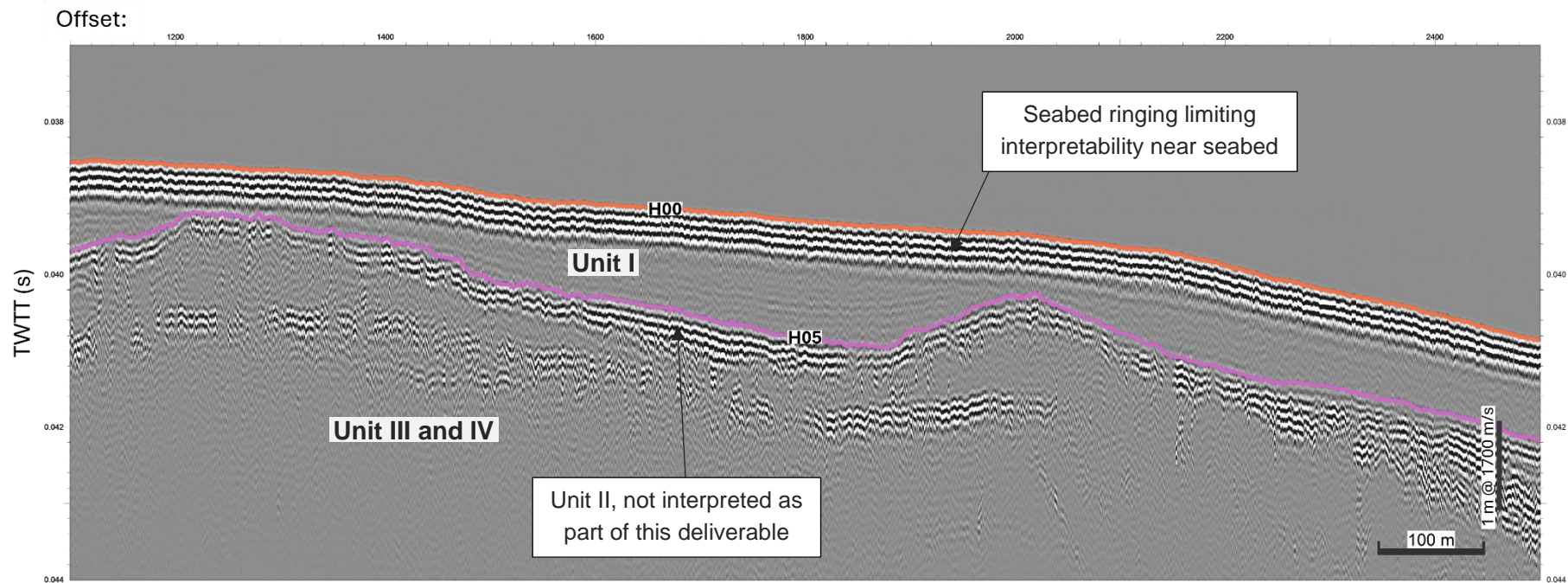


Figure 6-18 - Interpretation of SBP line '0003_A_KN_GO5_L052'

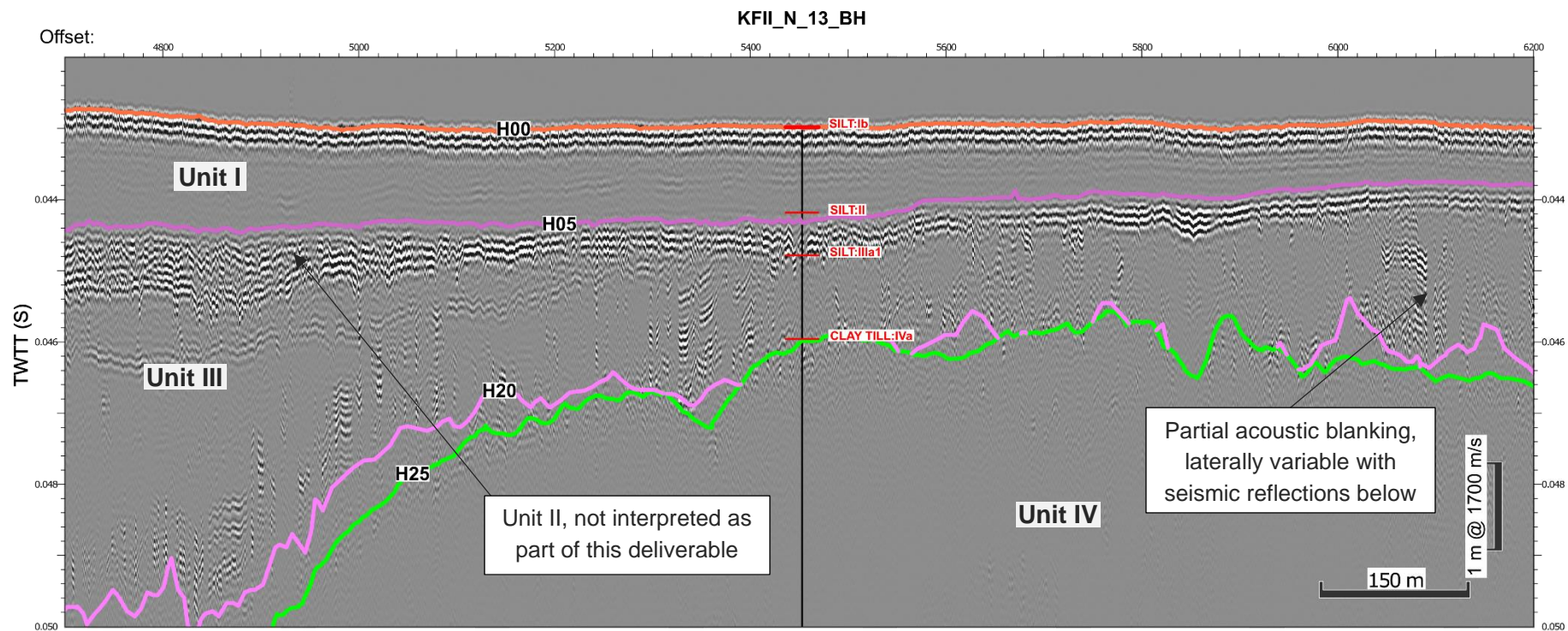


Figure 6-19 – Interpretation of SBP line '0048_A_KN_GO5_L030' with GI location KFII_N_13_BH

6.2.2 SEISMIC UNIT III (SU III) – GLACIOLACUSTRINE

6.2.2.1 GEOPHYSICAL DESCRIPTION

Unit III is bounded by the high amplitude reflections of H05 and H00 at the top, and by the low-medium amplitude, discontinuous reflections of H25 at the base. The internal seismic facies of this unit varies laterally across the site, due to the change in unit composition from the varied historic depositional environments that the proposed site extents cover.

Right below H05, parallel to sub-parallel medium to high amplitude reflections can be observed. Locally, contorted reflections have been interpreted as small channels. Those seismic reflections have been interpreted as a transitional unit between Unit I and Unit III, and labelled Unit II. This transitional unit was not picked as part of this study (see Section 6.2) and was included within Unit III.

In the east of the site, the seismic facies show high amplitude, sub-parallel, semi-continuous reflectors in the upper section of the unit. The mid-section shows medium amplitude, chaotic, discontinuous reflectors which show partial acoustic blanking. The lower section of the unit is low amplitude and occasionally transparent. In the centre of the site, the upper section of Unit III becomes thicker and more chaotic and the mid-section where the partial acoustic blanking is seen becomes less extensive. Towards the west, Unit III thins out and only the upper and lower sections are present.

Horizon H25 corresponds to the top of Unit IV and the base of Unit III. H25 represents the interface between seismic Units III (glaciolacustrine) and IV (glacial). Unit III's bounding horizons (H00, H05 and H25) were mapped on the SBP data exclusively. H20 which represents an internal reflector within Unit III, marks the base of the mid-section where the partial acoustic blanking was observed.

6.2.2.2 SPATIAL DISTRIBUTION

Unit III was interpreted across most of the site, except for areas in which the unit is truncated against the seabed. This corresponds to north-south trending gaps that span the length of the site along the western side of the site. In these areas, Unit IV is outcropping. The top of Unit III corresponds to the base of Unit I or the seabed and its elevation varies between -21.9 mMSL to -35.1 mMSL (Figure 6-20).

The unit is up to 7.0 m thick, as shown in the isochore map (Figure 6-21), with the highest thicknesses observed in the central and eastern parts of the site. The unit is at its thinnest in the north and west of the site.

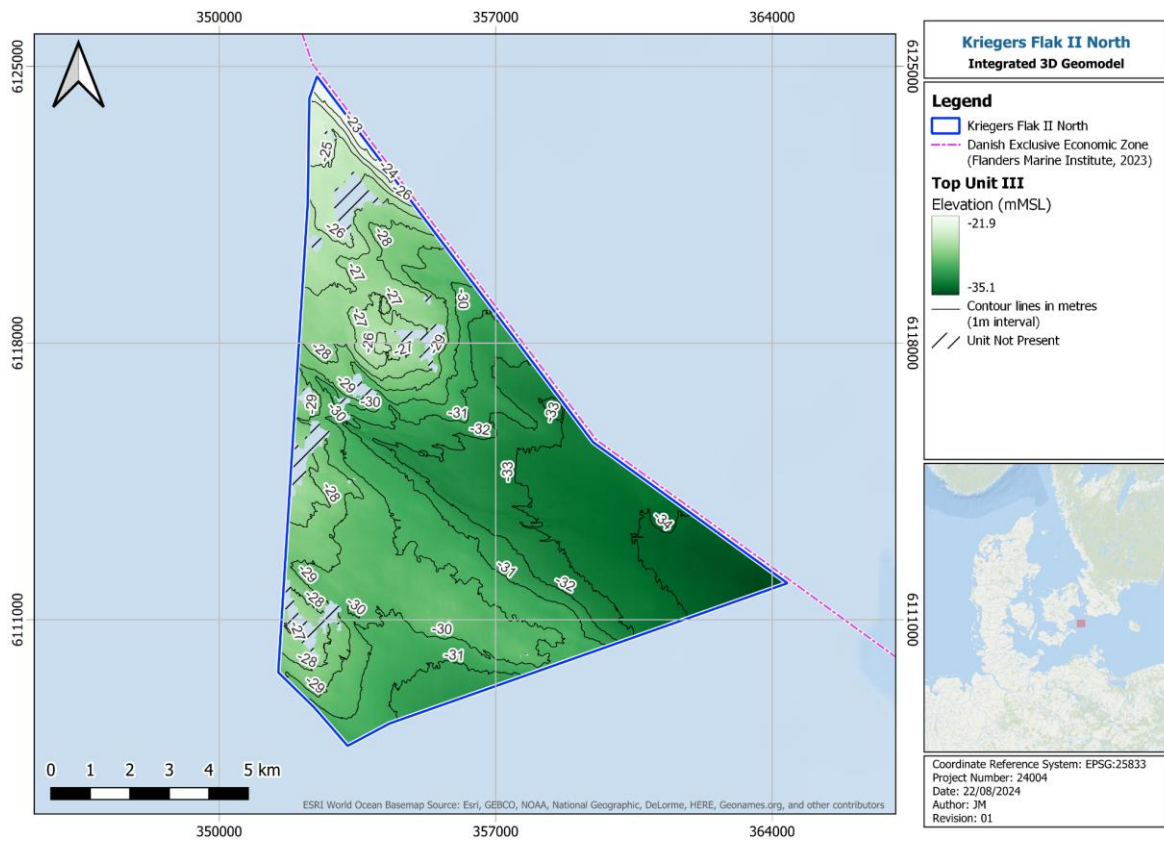


Figure 6-20 - Top of Unit III elevation (mMSL)

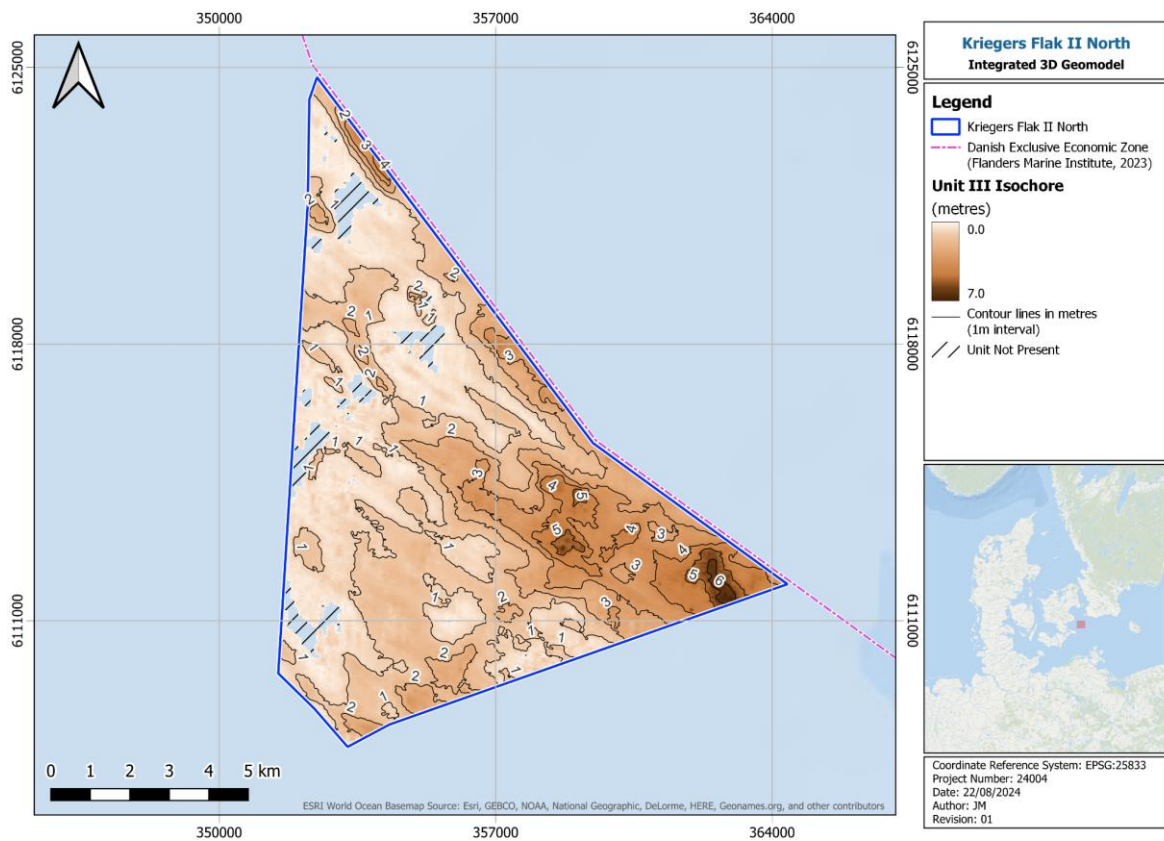


Figure 6-21 - Unit III vertical thickness isochore

6.2.2.3 GEOTECHNICAL DESCRIPTION

Unit III is described based on seismic as high amplitude, sub-parallel, semi-continuous reflectors displayed in the upper part (Unit II), with medium amplitude, chaotic, discontinuous reflectors which show partial acoustic blanking seen in the mid-section. The lower part displays low amplitude and occasionally transparent reflections.

The geotechnical properties for this unit were described from CPT data, PSD and Atterberg limit test data to determine the appropriate geotechnical unitisation. Unit III was split into five geotechnical units (Table 6-2):

- GU II was not picked but is included as Unit III. This unit is described as very silty, sandy to very sandy, low to medium plasticity, very low to medium strength Clay/Silt
- GU IIIa1 is described as silty to very silty, slightly sandy, medium to high plasticity, very low to low strength Clay
- GU IIIa2 is described as dense to very dense well sorted silty Sand
- GU IIIb1 is described as medium dense to dense silty Sand with closely to widely spaced thin beds of clay
- GU IIIb2 is described as sandy, slightly gravelly, medium to extremely high strength Clay

6.2.2.4 INTERPRETATION

Seismic horizon H05 is a continuous reflector, corresponding to a minor unconformity at the base of Unit I. Locally this represents the top of Unit III where it is underlying Unit I (Figure 6-22 and Figure 6-23). This reflector marks the transition from the mostly transparent lower facies of Unit I (marine sediments) and the reflectors of increased amplitude of Unit III (glaciolacustrine). Locally, at the top of Unit III, parallel reflections can be associated with the post-glacial transition unit, Unit II (Figure 6-22) and are associated with the geotechnical unit GU II. Unit II is interpreted as a transitional unit between a marine environment (Unit I) and glaciolacustrine environment (Unit III). This interpretation is supported by the occurrence of different types of sediment encountered, varying from clays to sands interpreted as change in depositional environment. This interpretation is also supported by the geotechnical data interpretation which indicates that GU II shares geotechnical properties with both GU Ib (marine) and GU IIIa1 (glaciolacustrine) sub-units.

Seismic horizon H25 is a discontinuous reflector, corresponding to the base of Unit III and the top of Unit IV. This reflector marks the transition from the mostly transparent lower facies of Unit III (glaciolacustrine) and the reflectors of increased amplitude of Unit IV (glacial).

Unit III was not directly interpreted but mapped using the base of the overlying unit and the top of underlying unit. The base of Unit I (H05) was picked, and the top of Unit IV (H25) was picked. Unit III is composed of variable seismic facies present between the base of Unit I and the top of Unit IV, which corresponds to glacio-lacustrine deposits.

The horizon H20 is based on GEOxyzs H20 horizon but has been reinterpreted as an internal boundary within Unit III (Figure 6-22). This boundary marks the base of the mid-section of the unit where the partial acoustic blanking was observed (Figure 6-23). Based on expected soil units this boundary is likely to correspond to the limit between the upper and lower glacio-

lacustrine units. Considering the geotechnical behaviour of sediments at the base of Unit III (Figure 6-23), it is possible that those sediments locally correspond to post-glacial deposits with a geotechnical behaviour similar to the glacial deposits.

The client requested to preserve this internal reflector, previously interpreted by GEOxyz (GEOxyz, 2024). Because this internal boundary is based on the interpretation of seismic facies and do not correspond to a surface associated with a seismic reflection, it could not be picked with high accuracy. During this reinterpretation, the H20 extents have been refined and revised based on the original extents provided by GEOxyz (GEOxyz, 2024). The original H20 interpretation (GEOxyz, 2024) had a less extensive coverage across the site. The reinterpreted H20 extends further to the west and north. H20 was interpreted on the 67 of the total 325 SBP tracklines (the WPA subset).

The SBP dataset had an inconsistent tidal reduction applied during the original data processing stage (GEOxyz, 2024). This adds difficulty to establishing a consistent pick for H05, H20 (not gridded) and H25 that tie-in across a large dataset when working in TWTT. Every effort has been made to reduce offsets between lines using mistie analysis, though there may be some remnant evidence of this in the final grids.

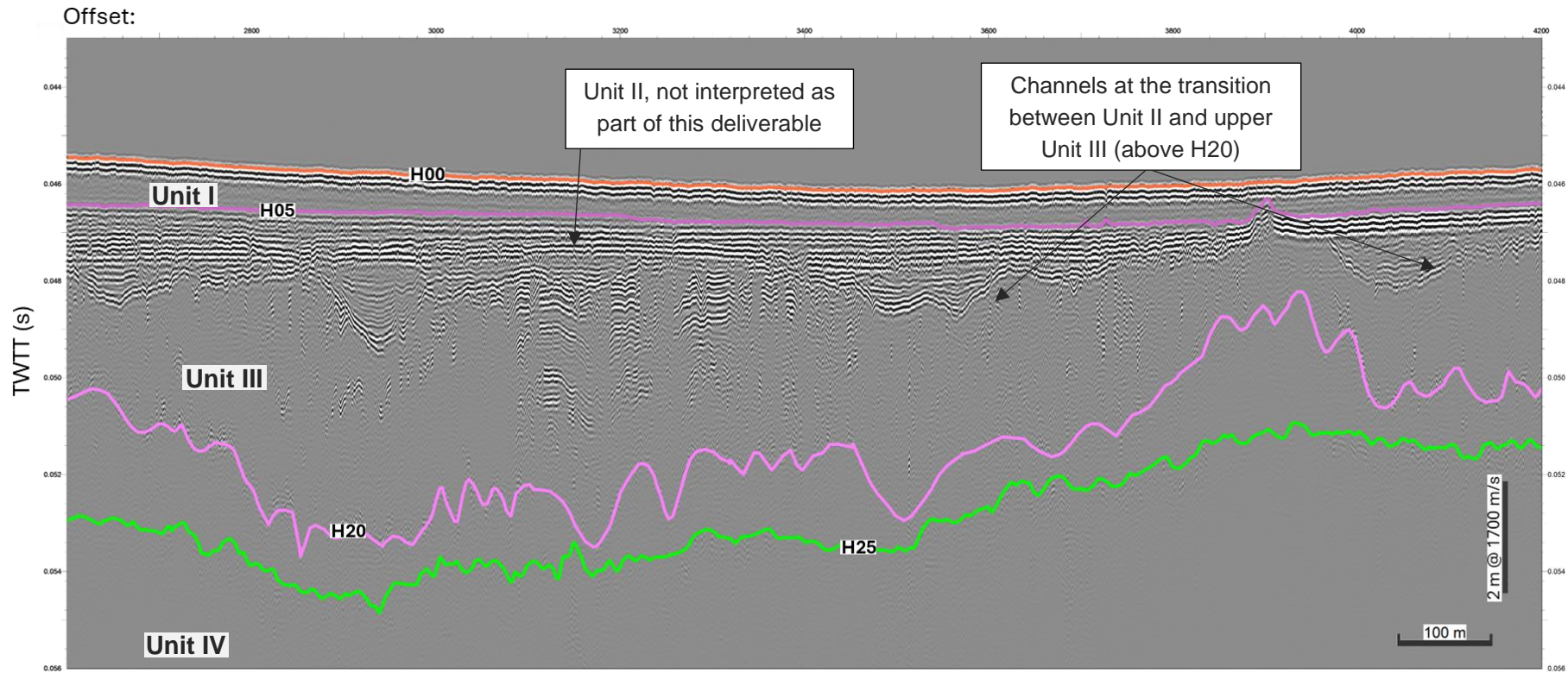


Figure 6-22 - Interpretation of SBP line '0097_A_KN_GO5_L046A'

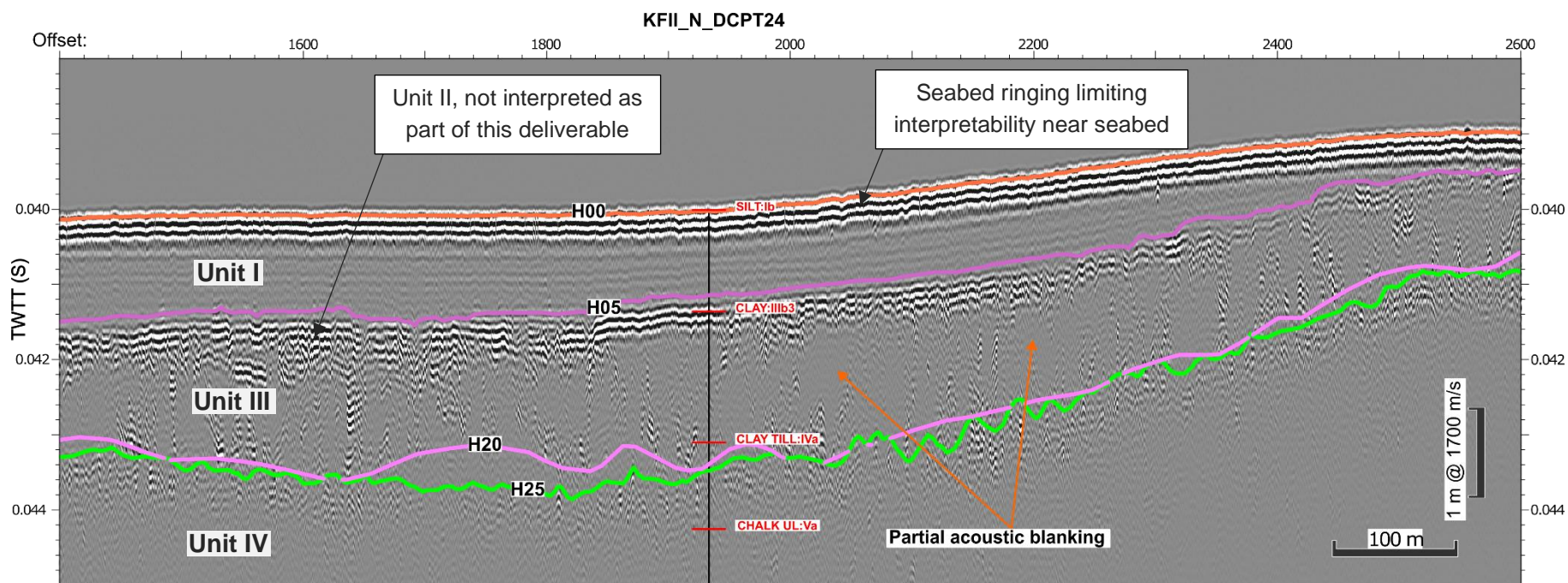


Figure 6-23 – Interpretation of SBP line '0057_A_KN_GO5_L016' with GI location KFII_N_DCPT24

6.2.3 SEISMIC UNIT IV (SU IV) – GLACIAL

6.2.3.1 GEOPHYSICAL DESCRIPTION

Unit IV is bounded by H25 at the top, a low-medium amplitude, discontinuous reflection. H25 is the deepest horizon interpreted on the SBP dataset and it represents the interface between seismic Units III (glaciolacustrine) and IV (glacial). Unit IV is bounded by H30 at the base, a continuous, undulating, medium to high amplitude reflector. H30 represents the top of bedrock which was interpreted on the UHRS dataset only.

On the SBP dataset, the seismic facies show low-medium amplitude, chaotic and semi-continuous reflectors in the upper section of the unit. Due to loss of signal on the SBP dataset, the unit becomes transparent just below the H25 horizon. In areas where H25 is shallower, more of the unit is visible on the SBP dataset. Occasionally features such as incisions and filled channels are visible within Unit IV.

H25 was transposed across to the UHRS dataset where more of the unit would be visible due to the deeper penetration of the signal. On the UHRS lines, the transposed H25 horizon can be seen along with the H30 horizon, bounding the full unit. The H25 reflector seen on the UHRS dataset is high amplitude, and mostly continuous. Complex structures are seen within Unit IV on the UHRS dataset. Series of Incisions and infilled channels are seen within the unit across the whole site.

6.2.3.2 SPATIAL DISTRIBUTION

Unit IV was interpreted across the whole site and is outcropping in north-south trending gaps that span the length of the site, along the western side of the site. The top of Unit IV corresponds to the base of Unit I, Unit III or the seabed and its elevation varies between -23.5 mMSL to -41.6 mMSL (Figure 6-24).

The unit is up to 45.2 m thick, as shown in the isochore map (Figure 6-25), with the highest thicknesses observed within the northeast-southwest trending channel feature in the central-southern part of the site. The unit is at its thinnest along the eastern boundary of the site.

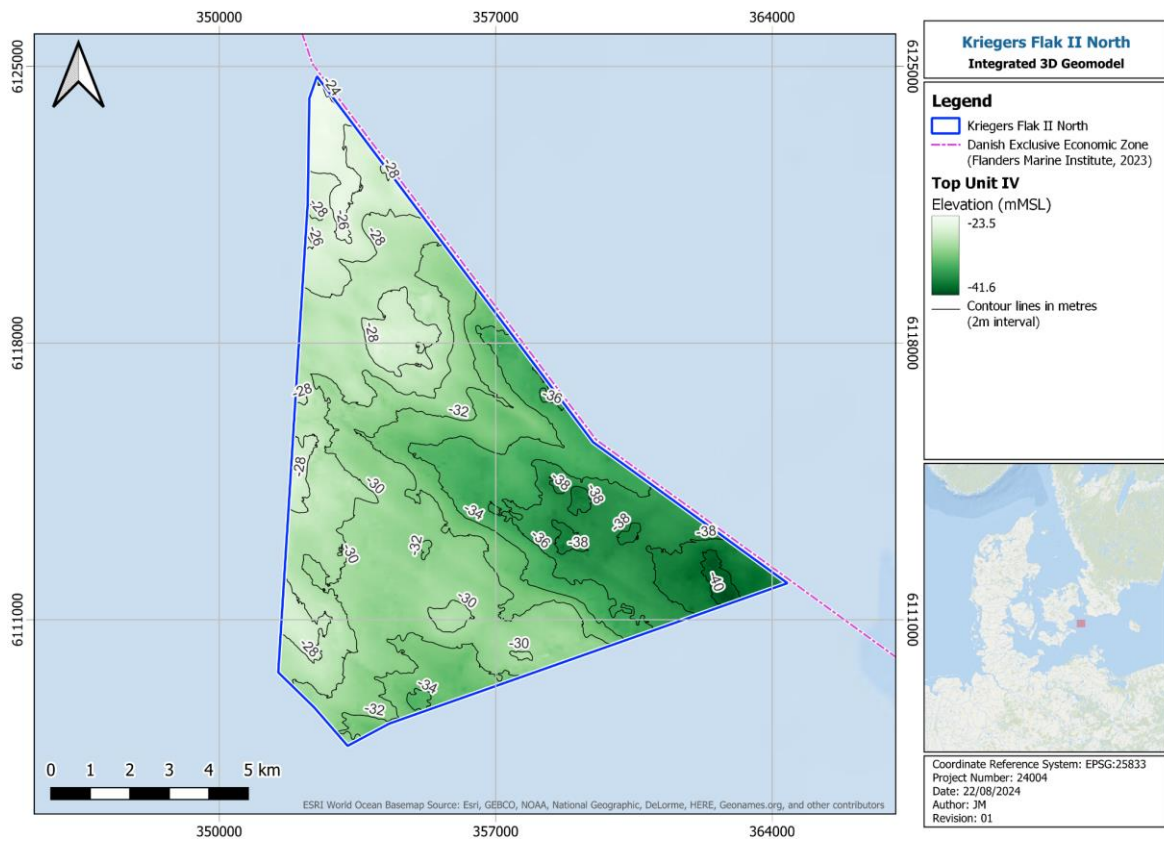


Figure 6-24 - Top of Unit IV elevation (mMSL)

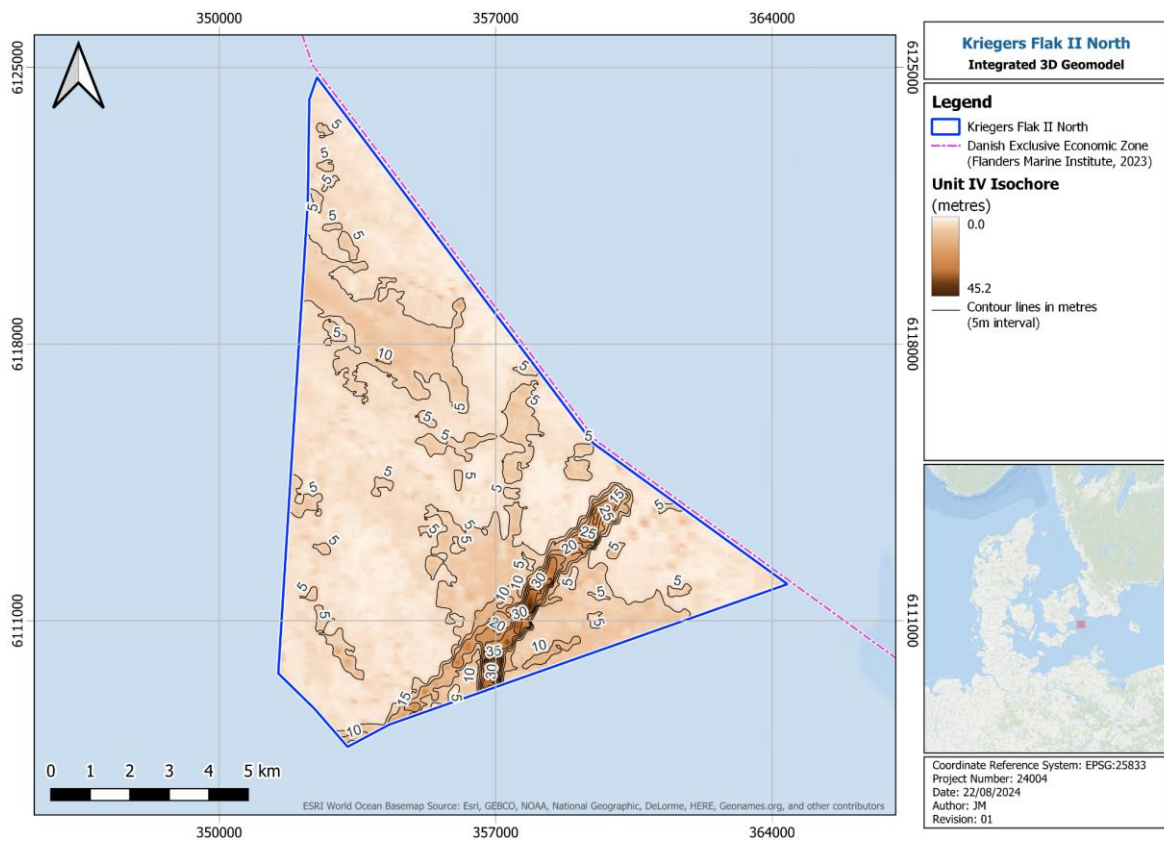


Figure 6-25 - Unit IV vertical thickness isochore

6.2.3.3 GEOTECHNICAL DESCRIPTION

Unit IV is described based on seismic as low-medium amplitude, chaotic and semi-continuous reflectors at the upper part of the SBH dataset. The signal is then lost. Occasionally, features such as incisions and infilled channels are visible. On the UHRS dataset, the unit shows high amplitude, chaotic and semi-continuous reflectors, depicting complex geological/glacial structures.

The geotechnical properties for this unit were described from CPT data, PSD and Atterberg limit test data to determine the appropriate geotechnical unitisation. Unit IV was split into two geotechnical units (Table 6-2):

- GU IVa described as Clay Till, very silty, very sandy, slightly gravelly, low plasticity, calcareous, micaceous, sand is fine to coarse, gravel is fine to coarse, subangular to subrounded, of mixed lithology (Extremely high strength)
- GU IVb is described as Sand Till, fine to coarse, poorly sorted, clayey, very silty, very gravelly, calcareous (Dense to very dense), with fine to coarse gravel size chalk nodules, highly calcareous.

6.2.3.4 INTERPRETATION

Seismic horizon H25 is a discontinuous reflector, corresponding to the top of Unit IV. This reflector marks the transition from the mostly transparent lower facies of Unit III (Glaciolacustrine) and the reflectors of increased amplitude of Unit IV (Glacial) (Figure 6-26 and Figure 6-27). This boundary has been interpreted as the possible last ice-contact in the area.

H25 and Unit IV was not previously interpreted by GEOxyz. H25 was interpreted to align with the geotechnical interpretation. Top of Glacial was interpreted as opposed to top of Till (Figure 6-27), as the top of Glacial was a regionally continuous surface which could be tracked across the whole site extent. Top of till was only visible in the SBP datasets only in discrete and widely dispersed areas, as such, consistently picking this reflector would not have been possible. H25 was interpreted on the 118 of the total 325 SBP tracklines. In UHRS data, several possible till members separated by sand deposits and often associated with channels, are observed across the site, where the glacial unit is the thickest (Figure 6-27). In areas where the glacial unit is thinner, it is likely that those possible different till member have been partially eroded by the last ice-contact surface.

The SBP dataset had an inconsistent tidal reduction applied during the original data processing stage (GEOxyz, 2024). This adds difficulty to establishing a consistent H25 pick and tie-in across a large dataset when working in TWTT. Every effort has been made to reduce offsets between lines using mistie analysis, though there may be some remnant evidence of this in the final grids.

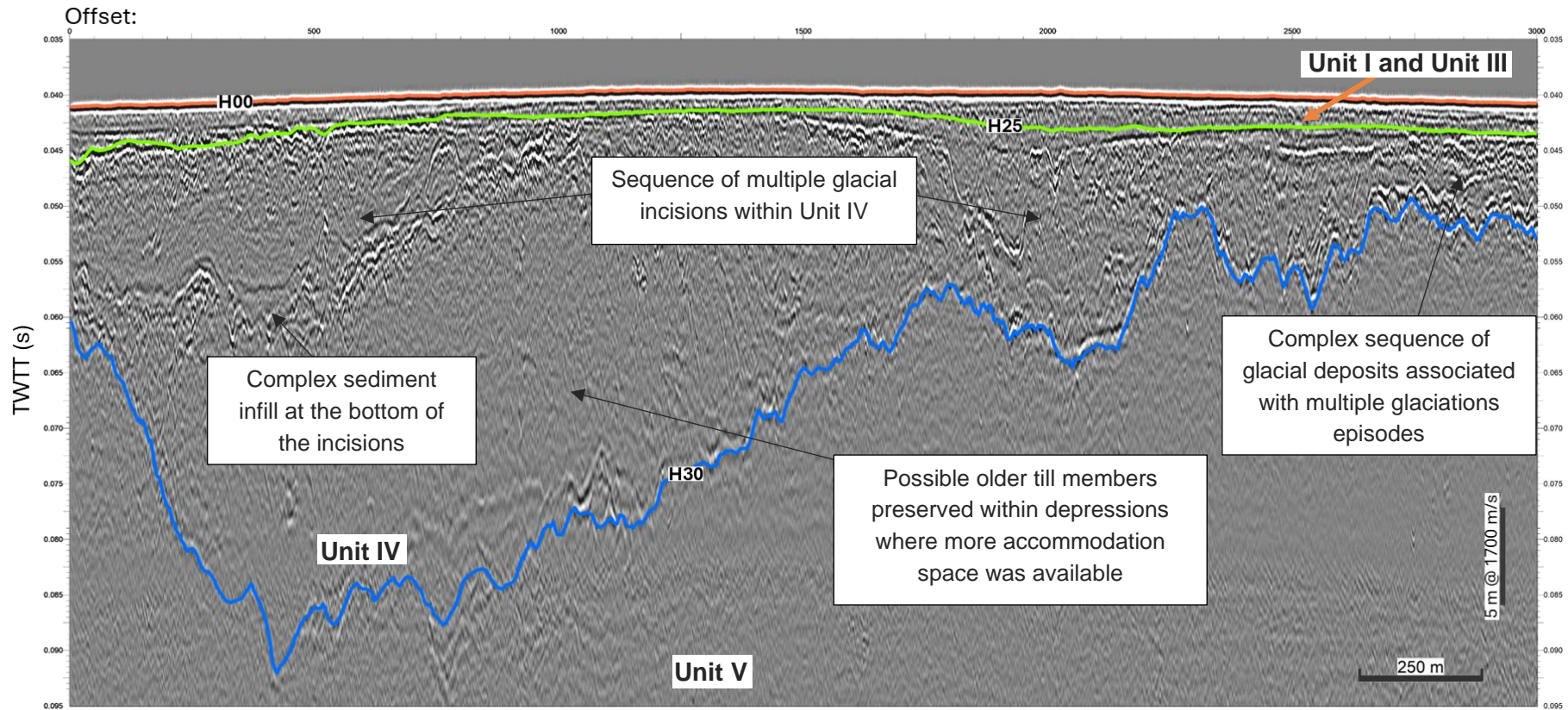


Figure 6-26 - Interpretation of SBP line 'A_KN_L023_UHR_T_MIG_STK'

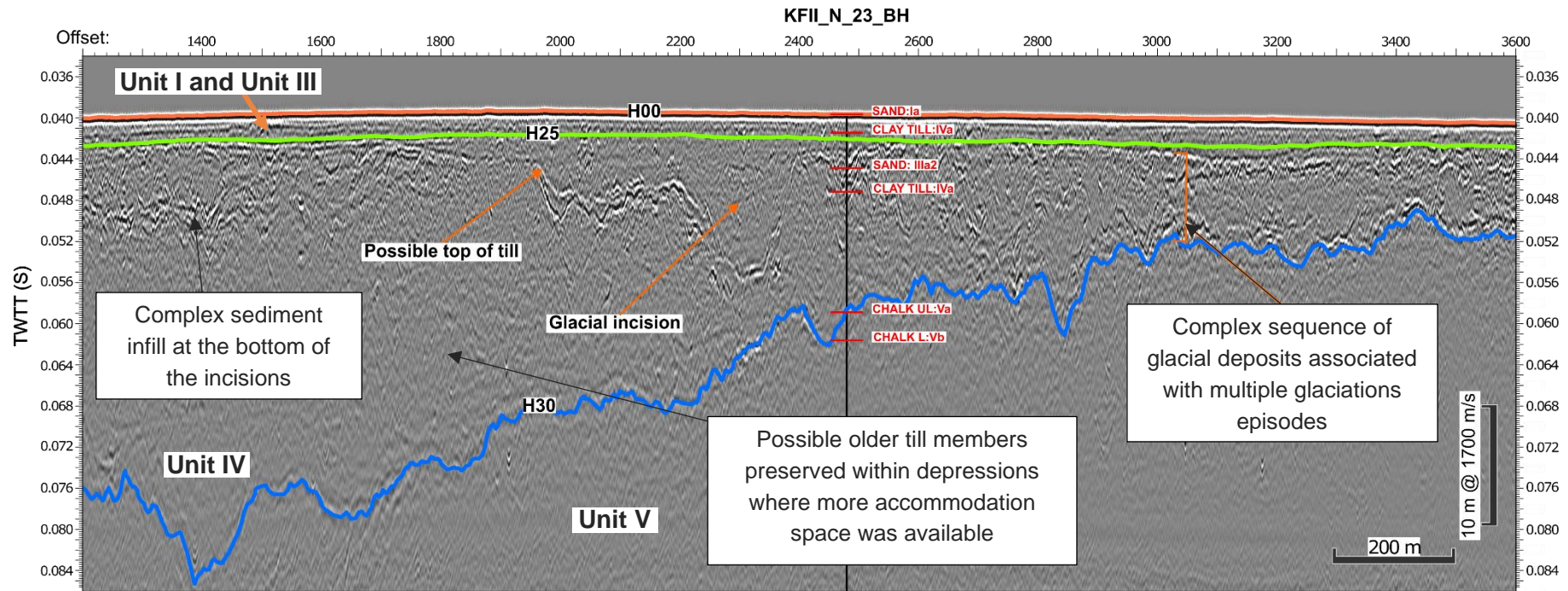


Figure 6-27 - Interpretation of UHRs line 'A_KN_L022_UHR_T_MIG_STK' with GI location KFI_N_23_BH

6.2.4 SEISMIC UNIT V (SU V) – CHALK

6.2.4.1 GEOPHYSICAL DESCRIPTION

H30, the top of Bedrock (Chalk) was interpreted on the UHRS dataset. This was the only horizon interpreted on the UHRS dataset other than the seabed (H00). H30 is a continuous, undulating reflector which varies from medium to high amplitude depending on depth and overlying lithology. Internally, the unit displays seismic transparency with areas of low-medium amplitude, chaotic reflections. Occasionally, low-medium amplitude sub-parallel, undulating and continuous/semi-continuous reflections were visible. H30 represents the interface between seismic Units IV (Glacial) and V (Bedrock).

6.2.4.2 SPATIAL DISTRIBUTION

Unit V was interpreted across the whole site. The top of Unit V corresponds to the base of Unit IV and its elevation varies between -25.8 mMSL to -77.4 mMSL (Figure 6-28).

The thickness of this unit cannot be measured as there is no base of bedrock or horizon bounding the base.

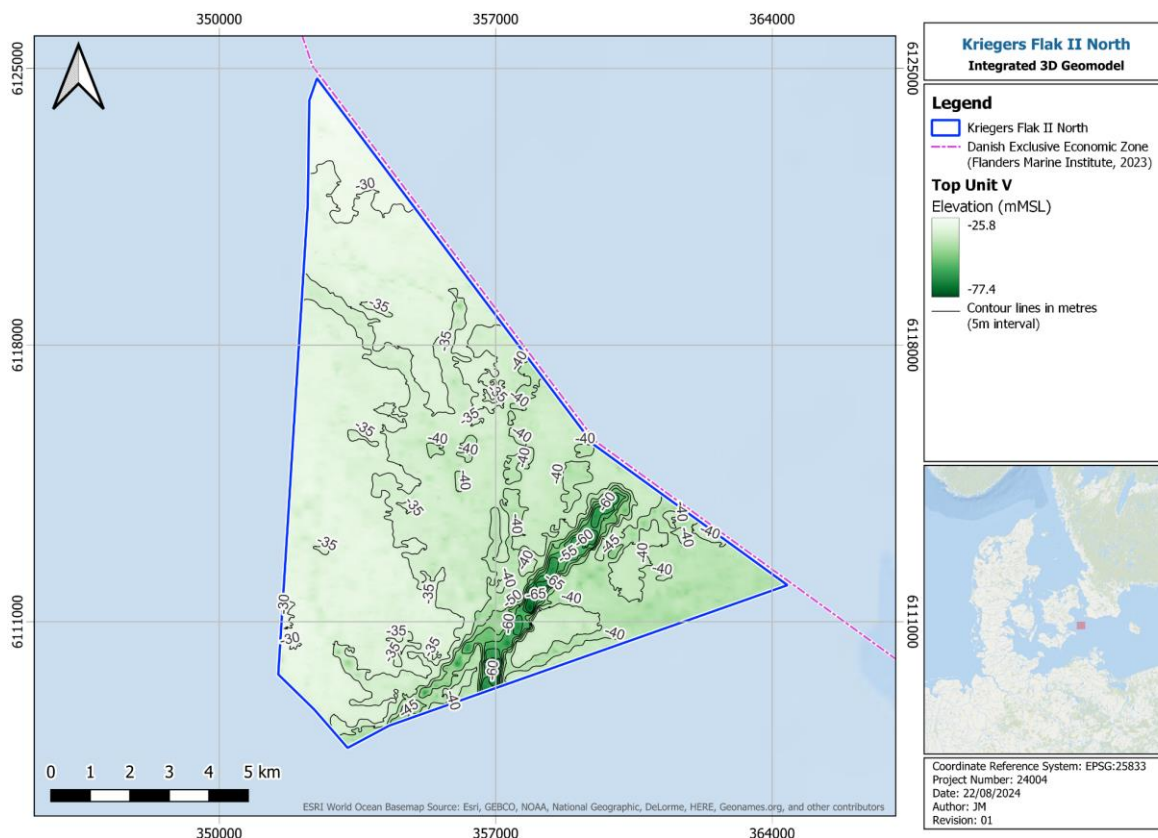


Figure 6-28 - Top of Unit V elevation (mMSL)

6.2.4.3 GEOTECHNICAL DESCRIPTION

Unit V facies are as seismically transparent along with low-medium amplitude, chaotic reflections describe a significant part of this unit. In addition, occasional low amplitude sub-parallel, undulating, and semi-continuous reflections were seen.

Geotechnical unitisation within this unit was identified from CPT data, sampling and borehole descriptions. It should be noted that where CPT data only was performed, top of the unlithified chalk was not always picked with certainty. This led to review and reprocessing of some of the top of the unlithified chalk with geophysical seismic points.

The geotechnical properties for this unit were described from CPT data and BH descriptions to determine the appropriate geotechnical unitisation. Unit V was split into two geotechnical units (Table 6-2):

- GU Va described as Chalk (Dm/Dc), unlithified (H1), white (N9), highly calcareous (Very high to extremely high strength) with rare fine to coarse gravel and stone sized fragments of chert, very strongly indurated (H5), non-calcareous (Very strong to extremely strong)
- GU Vb described as Chalk (A1-B2), slightly indurated (H2), unfractured to slightly fractured (S1-S2), highly calcareous (Extremely weak to very weak), with rare fine to coarse gravel sized pockets and extremely closely to closely spaced thin to thick laminae of marl, highly calcareous, and rare fine gravel to stone size fragments of chert, very strongly indurated (H5), dark grey to black (N3-N1), non-calcareous (Very strong to extremely strong)

6.2.4.4 INTERPRETATION

Seismic horizon H30 is a continuous reflector, corresponding to the top of Unit V. This reflector marks the transition from the lower facies of Unit IV (Glacial) and the reflectors of Unit V (Bedrock) (Figure 6-29 and Figure 6-30). Within the site, the bedrock was interpreted as Upper Cretaceous chalk. Locally, incisions at the top of the bedrock have been interpreted as associated with glacial processes (Figure 6-30). Internal reflections within the bedrock were observed and interpreted as structural elements (Figure 6-30).

During this interpretation, the extents of Unit V have remained the same, as this unit is seen across the entirety of the site. The H30 pick has been refined and revised based on the original interpretation provided by GEOxyz (GEOxyz, 2024). The original H30 interpretation (GEOxyz, 2024) was shallower within the channel features at the south of the site.

The UHRS dataset had a more consistent tidal reduction applied during the original data processing stage (GEOxyz, 2024) than the SBP dataset. This meant that H30 could be picked more consistently than the horizons interpreted on the SBP dataset. Though the larger line spacing of the UHRS dataset resulted in artefacts visible within the final grids, which is a current limitation of the methodology.

Unit V has been interpreted to be comprised of both Class-D, Unlithified Chalk and Class-A, Lithified Chalk (of Upper Cretaceous age), both of which were identified on the recovered boreholes (Gardline, 2024) across the site. The Class-D, Unlithified Chalk was the most continuous surface which could be consistently picked and tied-in across the wide line spacing of the dataset. The Class-A, Lithified Chalk was visible only in discrete and widely dispersed areas, as such, consistently picking this reflector would not have been possible. Overall, H30 corresponds to the top of Class-D, Unlithified Chalk, but in discrete areas, the Class-D, Unlithified Chalk is not present, and H30 represents the interface between Unit IV (Glacial) and Class-A, Lithified Chalk.

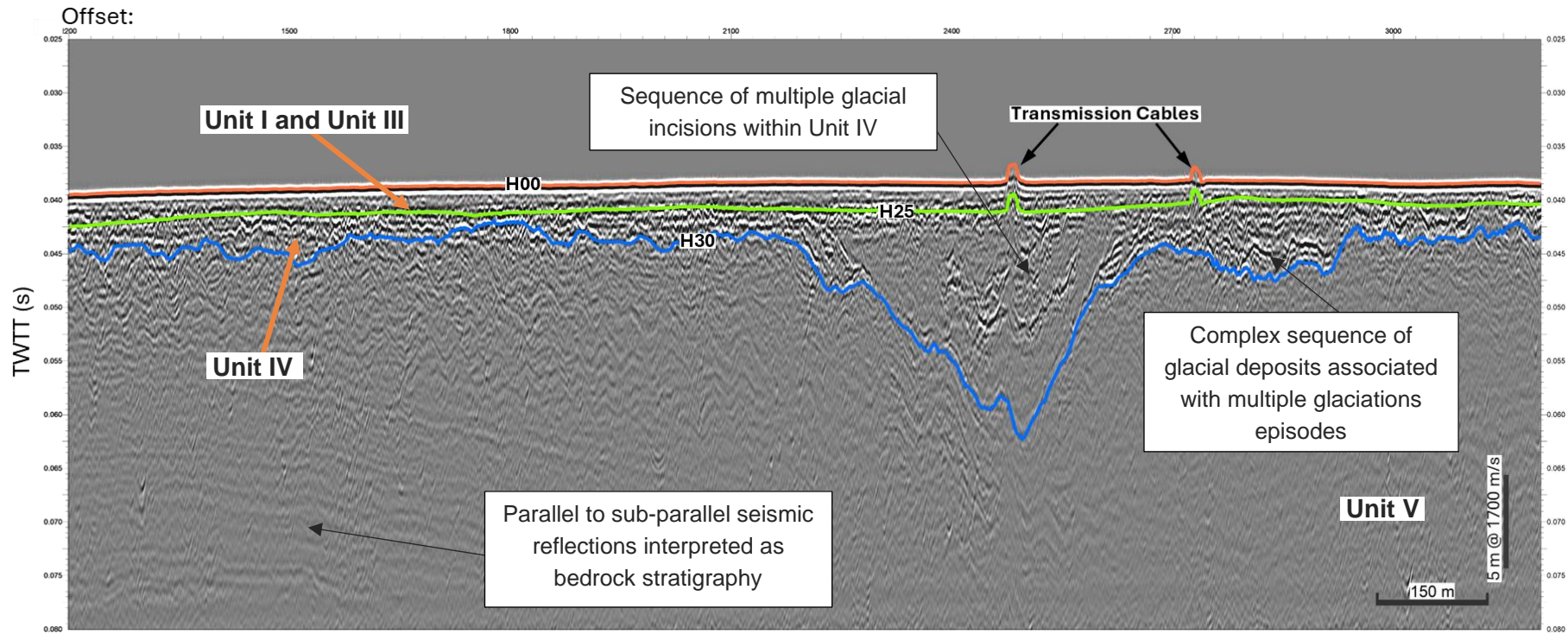


Figure 6-29 - Interpretation of SBP line 'A_KN_L008_UHR_T_MIG_STK'

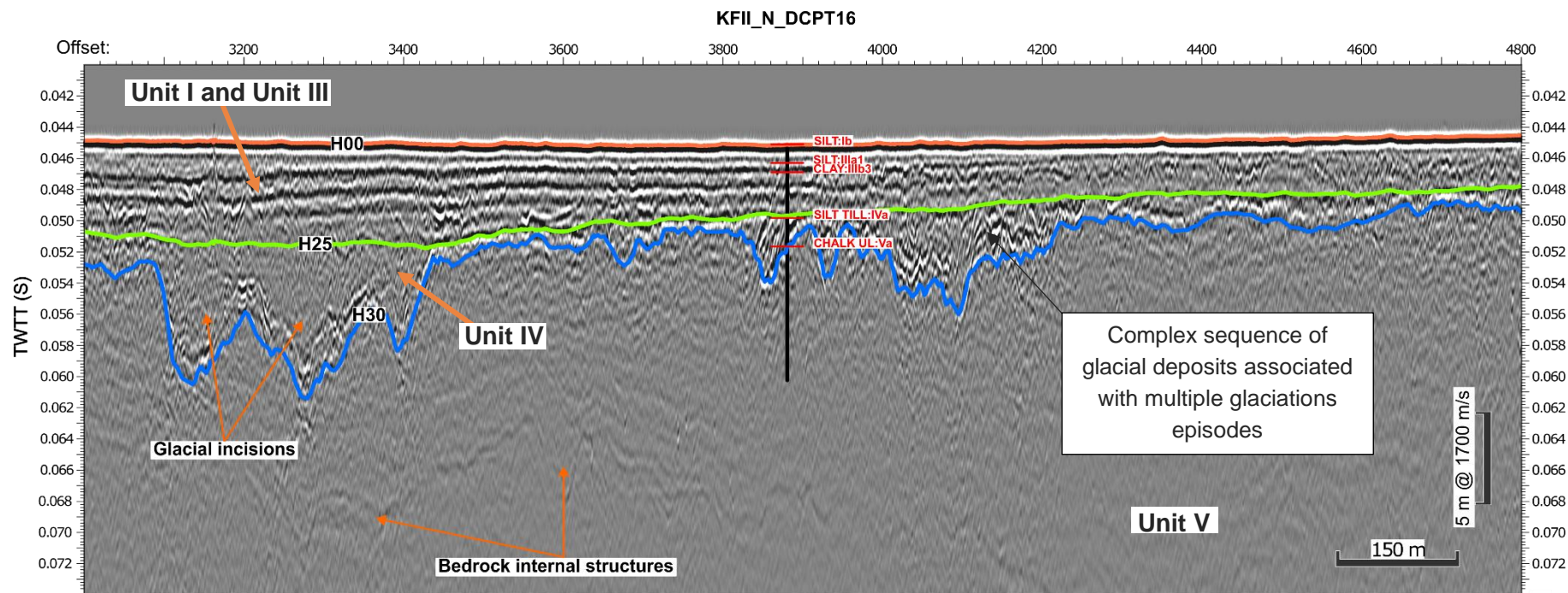


Figure 6-30 - Interpretation of UHRS line 'A_KN_L036_UHR_T_MIG_STK' with GI location KFII_N_DCPT16

6.2.5 GEOLOGICAL UNITS SUMMARY

A summary of the interpreted geological units, their minimum and maximum elevations in mMSL and depths in mBSF, and their thicknesses is presented in Table 6-3.

Table 6-3 - Geological units summary

Geological units summary									
Seismic Unit	Top	Base	Distribution	Top Min. Elevation (mMSL)	Top Max. Elevation (mMSL)	Top Min. Depth (mBSF)	Top Max. Depth (mBSF)	Thickness (m)	Geotechnical Unit
I	H00	H05	Present across most of the site, except in areas where the unit is truncated against the seabed or is not seen within the seismic data; the north-south trending gaps that span the length of the site along the western side of the site. In these areas, Units III and IV are outcropping. The unit is thickest in the central and south-eastern parts of the site and thinnest in in the north of the site and along the western boundary.	-21.6	-34.8	0.0	0.0	0 – 2.2	GU Ia/ Ib
III	H00 H05	H25	Present across most of the site, except in areas where the unit is truncated against the seabed; the north-south trending gaps that span the length of the site along the western side of the site. In these areas, Unit IV is outcropping. The unit is thickest in the central and eastern parts of the site and thinnest in the north and west of the site.	-21.9	-35.1	0.0	2.2	0 – 7.0	GU II, IIIa1, IIIa2, IIIb1, IIIb2
IV	H00 H05 H25	H30	Present across the whole site and is outcropping in north-south trending gaps that span the length of the site, along the western side of the site. The unit is thickest within the northeast-southwest trending channel feature in the central-southern part of the site and thinnest along the eastern boundary of the site.	-23.5	-41.6	0.0	7.9	0 – 45.2	GU Iva, IVb
V	H30	N/A	Present across the whole site and is fully subsurface. The maximum depths occur in the northeast-southwest trending channel feature in the central-southern part of the site.	-25.8	-77.4	1.4	47.8	N/A	GU Va, Vb

6.3 SOIL ZONATION

Soil zonation (provinces) across the site highlights the horizontal and vertical variability in ground conditions. Soil provinces were defined following the subseafloor interpretation, seismic unitisation, geotechnical unitisation, integration of the available geophysical and geotechnical data.

Soil provinces were initially defined based on the geophysical seismostratigraphic units across the site based on the IGM. The soil zonation was further refined based on the geotechnical unitisation considering the available geotechnical data as well as the engineering drivers influenced by the zone of interest for structures/ foundations being considered such as depth to top of rockhead, channels across the site where geotechnical features may vary both laterally and axially etc.

Five main provinces were defined across the site. Table 6-4 summarises the 5 geotechnical provinces defined.

Table 6-4 - Defined provinces

Defined provinces	
Province	Definition
1	Depth to top of Chalk, 0 – 5 m
2	Depth to top of Chalk, 5 – 10 m
3	Depth to top of Chalk, 10 – 20 m
4	Depth to top of Chalk, 20 – 30 m
5	Depth to top of Chalk, greater than 30 m

Figure 6-31 illustrates the soil provinces at the north site.

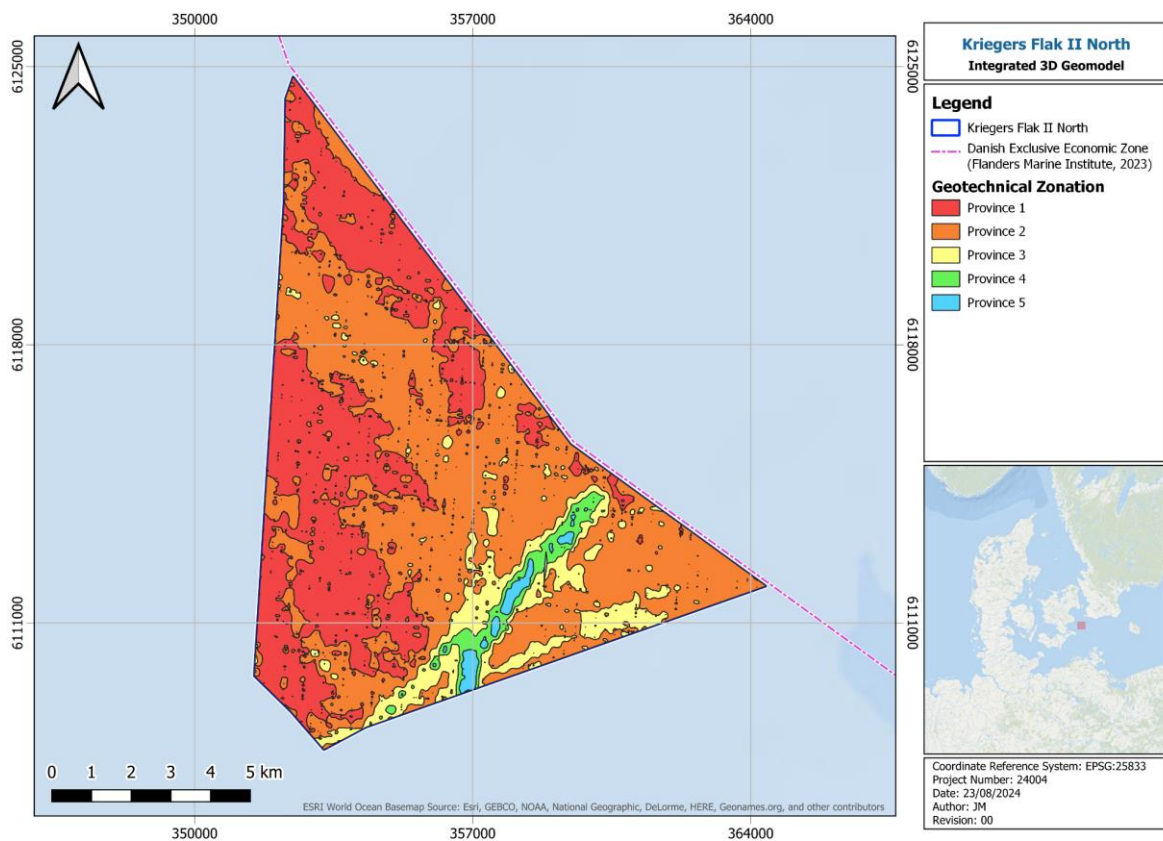


Figure 6-31 Geotechnical zonation provinces

The site is characterised by shallow bedrock consisting of Chalk. The provinces were defined based on the depth to the top of bedrock which is the main engineering driver. Table 6-5 further describes the soil provinces delineated. The following points should be considered when designing and installing foundations in Chalk:

- Uncertainty in chalk properties can lead to excessively long monopiles which can increase the overall weight of the monopiles.
- The chalk is observed to be within the foundation depth across most of the site. Hence, there may be potential damage of the piles during installation or specialised installation methods maybe required such as drive-drill-drive or drill and grouting. These can have cost impact to foundation installation.
- Competent (strong) Chalk layers are present within the structureless and structured Chalk which may lead to premature refusal during foundation installation or foundation damage.
- Flint beds or layers maybe present within the structureless and structured Chalk which may lead to premature refusal during foundation installation or foundation damage.
- The behaviour of Chalk can be affected based on different installation methods and loading conditions. Therefore, design of foundation (monopiles) in chalk need to consider latest findings such as ALPACA JIP (Jardine et al 2022).

It should be noted that the soil province map represents incorporation of a wide distribution of similar geotechnical units to aid in the understanding of the formations that may influence geotechnical foundation design. However, the soil province map should be viewed with caution

as it does not incorporate the substrata data and only considers a wide spread of geotechnical data. Hence, the geotechnical unitisation which represents the vertical and lateral variability of the substrata should be reviewed alongside the soil province map.

Appendix E presents the zonation map for the site and various cross-sections across the site. It should be noted that the soil profiles presented with the zonation map are representative of the seismic and geotechnical data, combined. The cross sections are presented to understand the geological and geotechnical profiles across the site. It should be noted that some boreholes were offset from some cross sections and there may be an apparent misfit of the boreholes with the cross sections. However, the boreholes are representative of the location data. Table 6-5 summarises the ground conditions within each province and probable foundation design and installation challenges in general.

Table 6-5 - Ground conditions and design challenges at each Province

Ground conditions and design challenges at each Province		
Province	Ground Conditions	Foundation Design and Installation Challenges
1	<p>Chalk is encountered less than 5 m BSF</p> <p>Soil province 1 covers approximately 40% of the site.</p> <p>Low strength sediments overlying the Chalk bedrock. However, in few locations very dense sand overlies the Chalk bedrock</p>	<ul style="list-style-type: none"> • Low strength sediments may result in jack-up installation challenges such deep leg penetration, rapid leg penetration etc • The shallow Chalk depth should be reviewed in regards to cable burial and installation. • Most foundation types are likely to encounter Chalk • Design of piles in Chalk may lead to excessively long piles or piles with larger wall thicknesses • Installation of piles in Chalk may result in premature refusal, damage to pile tip due to hard competent layers of Chalk or layers of flint
2	<p>Chalk is encountered between 5 m and 10 m BSF</p> <p>Sediments consist Sand and Clay Till, overlain by low to medium strength clays and very loose top dense sands</p>	<ul style="list-style-type: none"> • Most foundation types are likely to encounter Chalk • Design of piles in Chalk may lead to excessively long piles or piles with larger wall thicknesses • Installation of piles in Chalk may result in premature refusal, damage to pile tip due to hard competent layers of Chalk or layers of flint
3	<p>Chalk is encountered between 10 m and 20 m BSF</p> <p>Sediments consist of loose to very dense Sand becoming medium dense to dense overlying Silt, Sand Till and Clay Till</p>	<ul style="list-style-type: none"> • The very dense Sands at shallow depths may result in shallow design penetrations of foundations and installation challenges for foundations. • The Silts, Sand and Clay Till is observed overlying the bedrock. These tills should be considered with caution as they may behave like a transitional soil. • Transitional soils may behave as either cohesive and cohesionless dependent on the design condition; hence, should be considered with caution by the designer. • The Till is observed to consist of very high to extremely high strength gravelly clay and dense

Ground conditions and design challenges at each Province		
Province	Ground Conditions	Foundation Design and Installation Challenges
		to very dense gravelly sand. Hence, installation of foundations within this soil may be challenging and lead to premature refusals.
4	<p>Chalk is encountered between 20 m and 30 m BSF</p> <p>Sediments consist of predominantly medium dense to very dense Sand overlying transitional soil consisting of Silt, Clay Till or Sand Till</p> <p>Very dense Sand is observed at shallow depths close to seafloor.</p>	<ul style="list-style-type: none"> • Dependent on depth of the foundation type, Chalk may not be encountered. • The Silts, Sand and Clay Till is observed overlying the bedrock. These tills should be considered with caution as they may behave like a transitional soil. • Transitional soils may behave as either cohesive and cohesionless dependent on the design condition; hence, should be considered with caution by the designer. • The Till is observed to consist of very high to extremely high strength gravelly clay and dense to very dense gravelly sand. Hence, installation of foundations within this soil maybe challenging and lead to premature refusals.
5	<p>Chalk is encountered greater than 30 m BSF</p> <p>This province represents the channel observed across the south of the site. No geotechnical sampling and testing was performed within this unit.</p> <p>The interpretation from the IGM was used to infer the geotechnical parameters.</p>	<ul style="list-style-type: none"> • Dependent on depth of the foundation type, Chalk may not be encountered. • The Silts, Sand and Clay Till is observed overlying the bedrock. These tills should be considered with caution as they may behave like a transitional soil. • Transitional soils may behave as either cohesive and cohesionless dependent on the design condition; hence, should be considered with caution by the designer. • The Till is observed to consist of very high to extremely high strength gravelly clay and dense to very dense gravelly sand. Hence, installation of foundations within this soil maybe challenging and lead to premature refusals.

6.4 GEOTECHNICAL UNITISATION

Geotechnical soil unitisation was performed based on the factual geotechnical data and considering the seismostratigraphic unitisation presented in the IGM and understanding of the geotechnical and geological conditions across the site.

The geotechnical units identify ground conditions with similar geotechnical properties. Therefore, a single seismic unit could be broken down into different geotechnical units e.g. SU III is defined as GU IIIa1, IIIa2, IIIb1, IIIb2, to define different geotechnical properties. Table 6-2 summarises the different geotechnical units identified at the site.

6.5 INTEGRATED 3D GEOMODEL UNCERTAINTY

The remaining uncertainties for the site for this iteration of the IGM are presented in Table 6-6.

Table 6-6 - Geomodel uncertainties

Geomodel uncertainties						
Item	Associated Uncertainty	Data Type	Horizon	Seismic Unit	Geotechnical Unit (s)	Extents
Seabed ringing	The SBP data supplied from the survey contractor have a component of seabed ringing at the seabed interface for the entire dataset. This influences the capability of identifying the true extent of the shallowest unit (Unit I), where it's corresponding reflector (H05) pinches out against the seabed. Pseudo picks were generated for the H05 reflector to allow for a correct gridding process, though there remains some uncertainty because of this.	SBP	H05	I	N/A	Site-wide
Tide reduction	The tidal reduction applied to the SBP dataset is inconsistent between lines and across the site. When observing the cross lines, there is a significant variability in elevation between the crossing in-lines. This means that all SBP are not accurately reduced to a correct MBES level and therefore any result in time relative to MSL, are not reliable.	SBP	H00, H05	I	N/A	Site-wide
Processing artefact	The processing techniques applied to the UHRS data for the removal of the seabed multiple have left a remnant area of blanking within the data, which follows the path of the seabed multiple, at depth. Unfortunately, this blanking cuts through the H30 reflector and breaks its continuity in discrete areas. As a result, there are small areas of the site where there is uncertainty in the H30 pick. This mainly occurs in the northeast-southwest trending channel feature in the central-southern part of the site.	UHRS	H30	V	N/A	Central-southern part of the site
Geotech and seismic correlation	The geotechnical layering at some of the BH or CPT locations does not match the seismic layering. Hence, some of the geotechnical location layering was reviewed and revised to ensure a consistent tie in with the seismic data.	UHRS	N/A	III	II, IIIa1, IIIa2, IIIb1, IIIb2	Site Wide
Geotech and seismic correlation	Geotechnical Unit II was identified at various locations. However, in the seismostratigraphic units, this was not considered and is incorporated into Unit III top (Section 6.2). This has resulted in discrepancy between the seismic and geotechnical unitisation.	UHRS	H05	III	II	Site Wide
Geotech and seismic correlation	Geotechnical Unit Va and Vb have been described and corresponds to unlithified and lithified chalk, respectively. However, in the seismic unitisation the lateral extents of the boundary between lithified and unlithified chalk cannot be reliably picked. As a result, where CPTs were terminated at shallow depths or at top of bedrock there is uncertainty on the depth and extent of the unlithified chalk which will have a significant impact on engineering design.	UHRS	N/A	V	Va, Vb	Site-wide
Geotech	Transitional soil units: Silt, very sandy Clay, very clayey Sand. The geotechnical behaviour of this soils needs to be reviewed with caution dependent on the foundation type, loading conditions etc.	GEO		III, IV	II, Iva, IVb	Site Wide
Geotech	Chalk: Chalk was encountered at the site. Unlithified (structureless) Chalk was observed overlying Lithified (structured) Chalk. The behaviour of chalk needs to be considered with caution by the foundation designer.	GEO		V	Va, Vb	Site wide
Unit II interpretation	Unit II corresponds to a transitional unit between Unit I (marine) and Unit III (glaciolacustrine). This unit was evidenced in seismic data at the beginning of the project but could not be evidenced in geotechnical data until a later stage of the project, once the seismostratigraphic model was finalized and agreed with the client. Unit II can be observed across the whole site and represents a transition of depositional environment from glaciolacustrine (Unit III) to marine (Unit I). This interpretation is supported by the variability of the sediment composition and by the fact that geotechnical GU II associated with Unit II shares geotechnical properties with both overlying (GU Ib) and underlying (GU IIIa1) sub-units. While this unit can be reliably identified in geotechnical data, its properties are captured by the overlying and underlying units. Therefore, it was considered that this unit has limited impact on design.	SBP, UHRS, GEO	N/A	II	GU II	Site wide
H20 internal boundary in Unit III (glaciolacustrine)	Horizon H20 corresponds to an internal boundary within Unit III (glaciolacustrine). This horizon was initially identified and picked by GEOxyz (GEOxyz, 2024). The client requested to preserve and revise H20 horizon. Interpretation of H20 horizon is based on seismic facies change within Unit III and do not correspond to a surface associated with seismic reflections. Horizon H20 picks were revised, as well as its extent, but could be not accurately picked because of the intrinsic nature of this horizon. Uncertainties associated with the position of H20 in the stratigraphy remains in the current model and will require direct efforts to reduce in future studies.	SBP	H20	III	IIIa1, IIIa2, IIIb1, IIIb2	Site-wide

Geomodel uncertainties						
Item	Associated Uncertainty	Data Type	Horizon	Seismic Unit	Geotechnical Unit (s)	Extents
Till extents and thickness	<p>Till has been identified within the recently acquired geotechnical campaign, though within the seismic data it has not been possible to fully resolve clear till reflector interface (Section 6.2.3). Till geotechnical markers do not always align with the top of Unit IV (glacial) because it is likely that sediment deposits at the base of Unit III (glaciolacustrine) are locally characterized by similar geotechnical behaviour as the sediments at the top of Unit IV. Moreover, the top of Unit IV has been interpreted as regional surface corresponding to the last ice-contact surface and may not always represent the top of till deposits as sand outwash deposits may occur. Therefore, for the till deposits, minor discrepancies in the observed sediments changes may occur between the geotechnical data and seismic interpretation. Furthermore, multiple sub-units were identified within Unit IV (glacial) but not interpreted. Those subunits are likely to correspond to different till members recognized in the literature (GEUS, 2024), potentially separated by minor unconformities.</p> <p>Points above are remaining uncertainties in the current model and will require direct efforts to reduce in future studies.</p>	SBP	H25	IV	IVa, IVb	Site-wide
Possible gas	<p>Across the site, areas of seismic signal blanking have been observed, though unlike typical signal blanking associated with gas, the seismic signal is still visible both below, within and above areas of reduced amplitude/transparency. It is possible that this may be related to an acquisition set up issue, though the possibility of gas on the site cannot be fully ruled out.</p>	SBP	H20	III	N/A	Eastern and central part of the site
Lithified Chalk	<p>Unit V has been interpreted to be comprised of both Class-D, Unlithified Chalk and Class-A, Lithified Chalk. The Class-D, Unlithified Chalk was the most continuous surface which could be consistently picked and tied-in across the wide line spacing of the UHRS dataset. The Class-A, Lithified Chalk was visible only in discrete and widely dispersed areas, as such, consistently picking this reflector would not have been possible. Overall, H30 corresponds to the top of Class-D, Unlithified Chalk, but in discrete areas, the Class-D, Unlithified Chalk is not present, and H30 represents the interface between Unit IV (Glacial) and Class-A, Lithified Chalk.</p> <p>As Class-A, Lithified Chalk was not interpreted, it remains a large uncertainty in this revision of the geomodel and forms the basis of future investigation requirements.</p>	UHRS	H30	V	Vb	Site-wide
Gridding parameters	<p>The gridding parameters used were required to fully interpolate seismic data interpretation between main line spacings of 250 m (see Figure 5-2) and extrapolate to fill the site boundary with 3D interfaces. Gridded surfaces lose reliability away from the survey lines. This is particularly noticeable when the picked horizon shows greater spatial variation than the line spacing (i.e. if a picked horizon is steeply dipping or highly textured the gridding process is unable to capture the full detail and gridding artefacts are more significant).</p> <p>Because of the parameters used to account for the large line spacing on the URHS data, the values that intersect the interpretation (on the track lines) have good confidence levels (subject to outstanding interpretation uncertainty); interpolated and extrapolated areas (away from or between the track lines) are where the depth and elevation values are not as accurate and must be treated with extreme caution.</p>	UHRS	H30	V	N/A	Site-wide
Time-Depth conversion of SEGYS	<p>Bathymetry data was used as the vertical reference layer for the T-D conversion of SEGYS. Differences between the bathymetry and the UHRS seabed picks varies between 0 and 4.6 m at maximum, with an average of 0.11 m (99% of values below 0.47 m difference). Maximum differences are observed at wrecks locations, which are not visible in the UHRS seabed picks because they fall in between lines.</p> <p>Second source of uncertainties is related with the grid extent being limited to the site boundary and some seismic lines extending outside the site boundaries. Within the site boundaries, the T-D conversion model is constrained by the seismic unit grids. However, outside the site boundaries (18.75% of total UHRS dataset line distance), T-D conversion model layers have been extrapolated by the DDC tool to allow the T-D conversion of the full seismic sections. Because of the absence of geotechnical markers and seismic interpretation outside the site boundaries, uncertainties related with the extrapolated T-D conversion model cannot be quantified.</p>	UHRS	N/A	N/A	N/A	Site-wide

6.6 STATISTICAL CORRELATION OF GI WITH GEOPHYSICAL DATA

Correlation between the interpreted unit boundaries from geophysical data and geotechnical markers was assessed by quantifying the differences in depth. Statistics have been calculated on absolute differences, with minimum, maximum and average values, which are provided in Table 6-7.

Table 6-7 - Statistical correlation between GI and geophysical data

Statistical correlation between GI and geophysical data				
Unit Top	Minimum Difference (m)	Maximum Difference (m)	Average Difference (m)	Difference Standard Deviation (m)
Top Unit III	0.0	0.8	0.2	0.2
Top Unit IV	0.0	1.5	0.3	0.4
Top Unit V	0.0	0.5	0.2	0.1

For the northern site, correlation between the GI and geophysical data was assessed for the top of Unit III, top of Unit IV and top of Unit V with average differences of 0.2 m, 0.3 m and 0.2 m, respectively.

For the correlation between Unit III and the geotechnical markers, 14 out of the 20 locations have a geotechnical marker which can be correlated with the geophysical data. Out of the 8 locations, only location KFII_N_DCPT_18 shows a difference greater than 0.5 m, with a value of 0.75 m. This difference can be explained by the fact that the geotechnical marker corresponds to change of sediment type within the overlying marine unit (Unit I) and do not necessarily correspond the transition between Unit I and Unit III.

For the correlation between Unit IV and the geotechnical markers, 19 out of the 20 locations have a geotechnical marker which can be used for correlation. Out of the 19-locations used for testing the correlation, locations KFII_N_02_BH_A, KFII_N_20_DCPT and KFII_N_25_BH show differences greater than 0.5 m, with differences of 1.1 m, 1.5 m and 0.6 m, respectively. For location KFII_N_02_BH_A, the difference is explained by the fact that the top of Unit IV was picked at the seabed and included veneer of marine sediments, whereas the geotechnical unitization has those units separated. At location KFII_N_02_BH_A, it appears that the geotechnical marker is associated with an internal reflector at the base of seismic Unit III. This difference can be explained by the fact that the clays at the base of the glaciolacustrine can show similar geotechnical behaviour. Similarly, for location KFII_N_25_BH the geotechnical marker, corresponding to the top of glacial sediments, is associated with an internal boundary within the glacio-lacustrine unit (seismic Unit III).

For the correlation between the Unit V Chalk and the unlithified chalk markers (UL chalk), only one location (KFII_N_07_CPT_A) do not present a chalk geotechnical marker. For all 19 remaining locations, the difference between the geophysical interpretation and the unlithified chalk marker is consistently below 0.5 m difference.

Overall, the correlation between the geotechnical units and the seismic unit are fairly robust and the discrepancies are essentially explained by the intrinsic nature of the geotechnical and seismic data.

7 GEOTECHNICAL PARAMETERS

7.1 GENERAL

Geotechnical parameters were determined for each geotechnical unit identified at the site. The geotechnical unitisation was performed to capture the broad-based geotechnical properties identified based on the geophysical data, IGM and factual geotechnical data (Gardline, 2024). Table 6-2 summarises the geotechnical units and descriptions identified. It should be noted that different nomenclatures were used to differentiate between the seismostratigraphic units (e.g. SU I, SU II, etc.) and geotechnical units (e.g. GU Ia, GU Va, etc.).

7.2 GEOTECHNICAL SOIL PARAMETERS

This section presents the parameters included in this report that are relevant to foundation design. Soil parameters within different strata are graphically presented in Appendix C. Table 7-1 summarises the parameters presented in this report when characterising the geotechnical soil and rock properties.

Table 7-1 - Geotechnical soil and rock parameters determined

Geotechnical soil and rock parameters	
Soil Properties	Rock Properties
CPT measured parameters (q_c , f_s , u_2)	Unconfined compressive strength
CPT interpreted parameters (q_t , q_n , R_f , Q_t , B_q , F_r , I_c)	Young's modulus
Water Content	Poisson's ratio
Unit weight	RQD
Atterberg limits	
Particle density	
Chemical tests (CO_3 , Cl , SO_4 , pH , organic content)	
Undrained shear strength (undisturbed and remoulded)	
Soil sensitivity	
Relative density	
Friction angle (ϕ' , ϕ_{cs} , ψ)	
Interface friction angle (δ)	
Shear wave velocity	
Small strain shear modulus (G_0)	
Strain at half deviator stress (ϵ_{50})	
Preconsolidation stress	
Overconsolidation ratio (OCR)	
Lateral stress ratio (K_0)	
Thermal conductivity	

The strength, stiffness and cyclic behaviour of soil and rock were not derived as they are outside the scope of this IGM. However, cyclic test data has been presented by (Gardline, 2024) and should be considered by the geotechnical designer.

Unitised geotechnical parameters were derived from the available in situ and factual data. However, it should be noted that for certain soil and rock parameters, limited data was

available in the individual units. In such units, the parameters for different units were compiled together to provide representative derived parameters based on statistical and engineering judgement. Hence, this provided a general representation and characterisation of a broader group of units with similar properties.

7.3 RECOMMENDED PARAMETER BOUNDING FRAMEWORK

A bounding framework is commonly used to evaluate geotechnical soil parameters. Venterra adopted a best estimate (BE), lower estimate (LE), and high estimate (HE) approach, when applicable, to demonstrate data trends and quantify soil variability. The BE lines have been derived with due consideration of the soils and geotechnical parameters variability using statistical assessment and/or engineering judgement. The BE lines may be considered as characteristic values for engineering behaviour where ‘average’ properties are most relevant for the limit state under consideration. For independent parameters with sufficient data, the BE has been generally estimated as the mean of the measurements available for specific soil layers. Some additional conservatism on either side of the unbiased “Best Estimate” may be required in certain situation such as where localised behaviour governs (e.g. end bearing capacity of the pile).

Statistical assessment was performed following DNV-ST-207 (2012) recommendations. Where statistical assessment was performed, outliers were identified and removed from the dataset. The statistical assessment was then performed on a revised dataset without outliers. Where few data were available (e.g. only two data points) statistical assessment could not be performed. Therefore, engineering judgement was adopted to determine the geotechnical bounds.

The LE and HE lines have been derived using engineering judgement to provide a credible indication of the low and high distribution of the parameters, respectively.

BE soil profiles for CPT measurements and interpreted data, that is, qc, qt, qn, were determined considering the soil behaviour and adopting engineering judgement. In clay dominated soils, the BE may not consider the sand spikes with the profile biased towards the clay dominated units. In sand dominated units, thin to thick beds of clay may not be considered. The LE and HE profiles captured the peaks and troughs of the CPT measurements based on engineering judgement.

In some geotechnical units (GU) where varied soil properties were identified e.g. transitional soil units, GU IVa and GU IVb defined as clay and sand tills, variable soil units were observed consisting of predominantly sand or clay but also consisting of silt, sandy or clay, gravel. Engineering judgement was applied in determining the geotechnical bounds. The geotechnical behaviour of these units may vary, and these units should be considered with extreme caution by the geotechnical designer.

The LE and BE parameter profiles maybe considered applicable for settlement analysis and axial and lateral capacity assessments. The HE parameter profiles maybe considered applicable to installation and depending on the designer, natural frequency assessments. The geotechnical designer is ultimately responsible for determination of the applicable parameter profiles for design.

The geotechnical parameter bounds are presented in Appendix C.

The proposed indicative recommended lines may be amended by the designer for specific design purposes reflecting the geotechnical problem considered, to provide a more detailed assessment and/or as a result of consideration of complex soil-structure interaction.

7.4 INTERPRETATION STRATEGY

An in-depth analysis of borehole logs, CPT data, and soil profiles was conducted to provide information about soil and rock layers at varying depths. Locations and depths of soil samples were identified, facilitating the correlation of laboratory test results with specific subsurface conditions. Laboratory test results were comprehensively evaluated to discern crucial engineering properties of the soil. The interpretive analysis of these laboratory test results forms a foundational element in the comprehensive understanding of the engineering properties of the soil. The following interpretation strategy was followed:

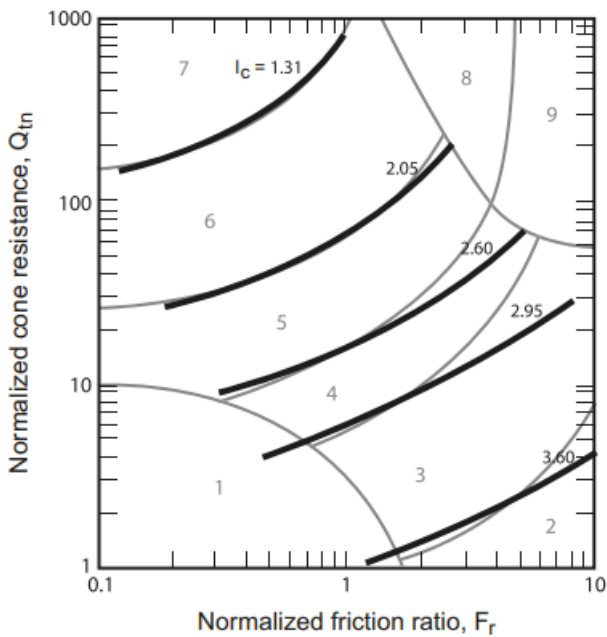
- Review of borehole information and any co-located CPT. Soil layer boundaries are established based on this review.
- Evaluation of the CPT measurements (tip resistance, sleeve friction, friction ratio, and excess pore pressure) to understand typical trends in soil response to CPT advancement.
- Confirm that variation in CPT trends match the initially established soil layer boundaries and adjust as needed.
- Review laboratory test results to corroborate the assigned soil classification and establish additional soil parameters.

Geotechnical units which were observed to behave as a transitional unit such as silt, both drained and undrained parameters have been presented.

7.5 SELECTION OF CPT CLASSIFICATION METHOD

7.5.1 GENERAL

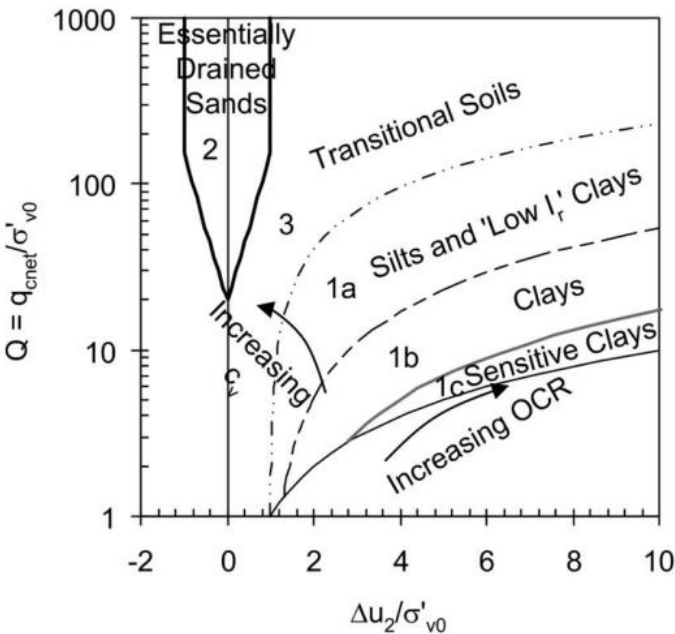
There are several CPT classification methods available. Each method was developed and calibrated for specific soil types and can have different levels of accuracy in identifying soil behaviour types. The soil behaviour type methods by Robertson (2009), Schneider et al. (2008) and Robertson (2016), were compared which related more to soil behaviour than classification, to the soil classifications presented in the final borehole logs. Appendix C presents the CPT classification based on Robertson (2016) and Schneider et al (2008). Figure 7-1 shows the soil classification according to Robertson (2009) and Figure 7-2 shows the soil classification according to Schneider et al (2008) used to assess pore pressure response.



Zone	Soil Behavior Type	I_c
1	Sensitive, fine grained	N/A
2	Organic soils – clay	> 3.6
3	Clays – silty clay to clay	2.95 – 3.6
4	Silt mixtures – clayey silt to silty clay	2.60 – 2.95
5	Sand mixtures – silty sand to sandy silt	2.05 – 2.6
6	Sands – clean sand to silty sand	1.31 – 2.05
7	Gravelly sand to dense sand	< 1.31
8	Very stiff sand to clayey sand*	N/A
9	Very stiff, fine grained*	N/A

* Heavily overconsolidated or cemented

Figure 7-1 - Robertson (2009) classification



Zone	Soil Type
1a	SILTS and 'Low I_r ' CLAYS
1b	CLAYS
1c	Sensitive CLAYS
2	Essentially drained SANDS
3	Transitional soils

Figure 7-2 - Schneider et al (2008) classification

7.5.2 SOIL CLASSIFICATION BASED ON CPT DATA

Table 7-2 summarises the CPT classification for each geotechnical unit based on the classification charts from both Robertson (2009) and Schneider et al. (2008).

Table 7-2 CPT classification

CPT classification			
GU	Robertson (2009) Chart Zone	Schneider et al. (2008) Chart Zone.	CPT Classification Description
Ia	5	2,3	sand mixtures consisting of silty sand to sandy silt behaving as drained or partially drained similar to a transitional soil
Ib	4 to 6	1a to 2	transitional soil and may behave as drained or undrained
II	4, 5	1b and 3	transitional unit behaving more as a clayey silt. Hence, further review of this unit should be performed based on lab data
IIIa1	4 with scattered data in zones 5 and 6	1b and 3	silty clay
IIIa2	6	2	clean sand
IIIb1	6, 5	3	silty sand which may behave as a transitional soil
IIIb2	5, scatter in zone 4	1b to 3	silty sand to sandy silt behaving between drained and undrained. This unit needs to be reviewed against lab data to ascertain its behaviour during design
IVa	8, 9	2, 3	heavily overconsolidated very stiff sand to fine grained which matches the BH description of very silty very sandy Clay (Clay Till). Hence, this unit should be assessed similar to a transitional unit by a competent geotechnical engineer to ascertain its geotechnical behaviour depending on the loading conditions, foundation type etc
IVb	6, 7	2	sand to gravelly sand which matches the BH description of fine to coarse, poorly sorted, clayey, very silty, very gravelly, Sand (Sand Till)
Va	6	2, 3	clean sand to silty sand. This may indicate that this chalk unit to behave as a cohesionless unit. This unit has been described as unlithified Chalk in the geotechnical logs. This will have to be further evaluated by a competent geotechnical engineer to ascertain its geotechnical behaviour depending on the loading conditions, foundation type, etc

7.6 SUMMARY OF LABORATORY TESTS

Table 7-3 summarises the types and number of tests that were available at the time of preparing this report as presented by (Gardline, 2024). The laboratory test quantities presented in Table 7-3 contain total quantities for the northern site as extracted from AGS data.

Table 7-3 - Types and number of tests available at time of reporting (Gardline, 2024)

Types and number of tests available at time of reporting ^a		
Classification Test Type	Lab	North Site
Water Content - Soil	Gardline	38
Water Content - Rock	Gardline	221
Bulk and Dry Density – Soil	Gardline	57
Bulk and Dry Density – Rock	Gardline	122
Particle Density	Gardline	7
Atterberg Limits (4 Point Method)	Gardline	13
Particle Size Distribution	Gardline	17
Angularity	Gardline	2
Maximum and Minimum Dry Density	Gardline	1
Carbonate Content	Gardline	3
Acid Soluble Sulphate	GEOLABS	4
Loss on Ignition	Gardline	1
Thermal Conductivity	Gardline	2
Acid Soluble Chloride	GEOLABS	7
Oedometer	Gardline	1
UUT	Gardline	0
UCS	GEOLABS	49
UCS with Young's Modulus	GEOLABS	49
Point Load ^b	Gardline	83
CIUc	GEO	2
CIDc	GEO	1
CAUc	GEO	1
CAUcyc	GEO	1
DSS	GEO	2
CSS ^c	GEO	2

Notes:

- a. The test quantities presented include total number for both North and South site
- b. Point load test numbers including tests conducted on cancelled UCS tests
- c. Each CSS allowed for a series of three tests

7.7 GEOTECHNICAL PROPERTIES

The soil and rock were classified in accordance with ISO 14688 and 14689 standards, respectively. The index testing used for classification of the soil samples included grain size distribution, Atterberg limits, moisture content, and unit weight. The summary of the results of these tests is tabulated in this section and presented graphically when applicable in Appendix C.

7.7.1 PARTICLE SIZE DISTRIBUTION

Particle Size Distribution tests (PSD) curves provide information about percentage of different grain sizes for a soil sample. The PSD testing was performed in accordance with ISO 17892-4: 2016. The PSD curves are presented in Appendix C.

The distribution of different soil fractions versus depth was analysed for the different geotechnical units. This parameter is important for understanding the composition of the subsurface and the likely engineering properties.

7.7.2 PLASTICITY

Atterberg Limits refer to specific moisture contents at which a soil undergoes changes in its physical properties. These limits are commonly used to classify fine-grained soils, such as silts and clays, based on their plasticity. The Atterberg limits include the following:

- Liquid Limit (LL): The moisture content at which the soil transitions from a plastic to a liquid state.
- Plastic Limit (PL): The moisture content at which the soil transitions from a plastic to a semi-solid state.

A plasticity chart divides soils into various zones or classes, each representing different engineering properties and behaviour. Atterberg's limits tests using the 4-point method were performed in accordance with ISO 17892-12: 2022 Standard. The plasticity chart and parameter bounds are presented in Appendix C. The results demonstrate that all geotechnical units can be classified as predominantly low to medium plasticity.

The geotechnical parameter bounds were determined by statistical assessment and engineering judgement.

7.7.3 MOISTURE CONTENT

The moisture content, w , is a parameter typically used for soil classification, estimation of void ratio and correlations to other soil parameters. Plot and parameter bounds of moisture content versus depth from offshore and onshore laboratory testing are presented in Appendix C. The moisture content at the northern site was observed to range between 8% and 29% across all units.

The geotechnical parameter bounds were determined by statistical assessment and engineering judgement.

7.7.4 UNIT WEIGHT

Unit weight was determined from bulk density and CPT-data. CPT derived unit weights were determined in accordance with Robertson and Cabal (2010) and compared to laboratory measurements (Appendix C). The CPT methods underestimate the unit weight especially for shallower soil layers where the overburden pressures are lower. This is not unusual as most unit weight correlations from CPT include a high degree uncertainty. CPT-derived values were not relied upon and presented when calculating representative geotechnical profiles unless there was insufficient bulk density data within the unit.

7.7.5 PARTICLE DENSITY

Particle density is a measure of the mass of solid particles per unit volume within a soil or sediment sample and provides information about packaging and arrangement of soil particles.

Particle density (G_s) measurements were performed following the fluid pycnometer method. Due to the limited number of particle density tests, all of the units were combined to determine a statistical assessment. Appendix C presents the particle density profiles and parameter bounds.

7.7.6 ORGANIC CONTENT

Organic content was measured by the loss on ignition method in accordance with BS1377-3:2018. Appendix C presents the parameter plots presenting the OC.

7.7.7 CARBONATE, SULPHATE, AND CHLORIDE CONTENTS

The carbonate content test was performed using the gasometric method. The results are reported as % CaCO₃ of soil dry mass.

The sulphate and chloride contents were performed using the acid and water-soluble method, whereas the chloride content tests were performed using the acid soluble method.

The carbonate, sulphate and chloride testing were performed following BS 1377-3:2018 recommendations.

7.7.8 THERMAL CONDUCTIVITY

Thermal conductivity (TC) tests have been performed using the transient heat method. TC was performed following ASTM D5334-22:2014 methodology. TC testing was performed on both undisturbed and reconstituted samples.

TC is highly influenced by saturation and dry density. An increase in either parameter will result in an increase in the soil's TC. Other factors of secondary importance include mineral composition, temperature, and time. Only a single TC test was performed at the northern site. Appendix C presents the TC profile versus depth.

7.8 ENGINEERING PROPERTIES

This section discusses the engineering properties of the sediments encountered during our field exploration program. The engineering properties are evaluated for each specific unit.

Section 7.3 discusses the bounding framework used to determine the engineering properties of fine-grained and coarse-grained sediments, respectively. Properties such as laboratory and field undrained shear strength (s_u), derived s_u from cone data, epsilon 50 (ϵ_{50}), consolidation properties and compressibility, and interpretation of stress history are discussed. The state of consolidation from laboratory and in-situ testing of fine-grained sediments is discussed. The state of consolidation of clayey soils was determined from incremental load consolidation tests, and empirically from correlations with CPT data. This coefficient is used to determine the depositional history of sediments and is used to predict the relative density and OCR.

7.9 CONE PENETRATION TEST PARAMETERS

7.9.1 GENERAL

The following cone penetration test (CPT) parameters are presented for each geotechnical unit.

- Measured cone resistance (q_c);
- Total cone resistance (q_t);
- Net cone resistance (q_n);

- Measured sleeve friction (f_s);
- Measured pore-water pressure (u_2);
- Friction ratio (R_f);
- Pore-water pressure ratio (B_q);
- Normalised cone resistance (Q_t);
- Normalised friction ratio (F_r);
- Soil behaviour type index (I_c);
- Relative density (D_r).
- Undrained shear strength (s_u)

The geotechnical parameter bounds for the above soil units were determined by engineering judgement considering the recommendations in Section 7.3. It should be noted that geotechnical profiles are only presented for q_c , q_t , f_s , D_r and s_u . Table 7-4 summarises the geotechnical profiles with depth and parameter calculations. Section 7.9.1.1 presents derivation of relative density (D_r).

Table 7-4 - Measured and derived CPT parameters

Measured and derived CPT parameters		
Parameter	Calculation	Geotechnical profiles
Measured cone resistance (q_c)	As measured in situ	LE, BE, HE
Total cone resistance (q_t)	$q_t = q_c + u_2(1 - \alpha)$	LE, BE, HE
Net cone resistance (q_n)	$q_n = q_t - \sigma_z$	LE, BE, HE
Measured sleeve friction (f_s);	As measured in situ	LE, BE, HE
Measured pore-water pressure (u_2)	As measured in situ	—
Friction ratio (R_f)	$R_f = f_s/q_t$	—
Pore-water pressure ratio (B_q)	$B_q = \Delta_u/q_n$ $\Delta_u = u_2 - u_0$	—
Normalised cone resistance (Q_t)	$Q_t = q_n/\sigma'_z$	—
Normalised friction ratio (F_r)	$F_r = f_s/q_n$	—
Soil behaviour type index (I_c)*	$I_c = [(3.47 - \log Q_t)^2 + (\log F_r + 1.22)^2]^{0.5}$	—
Notes: * = Soil behaviour type index (I_c) determined according to Robertson (2016) α = Cone area ratio Δ_u = Net pore pressure u_0 = hydrostatic pore pressure σ_z = Total vertical stress — = Geotechnical profiles not derived		

7.9.1.1 RELATIVE DENSITY

Relative density (D_r) was determined using the relationship proposed by (Jamiolkowski, et al., 2001) . It should be noted that this methodology for determining relative density is developed for clean silica sand. Hence, the D_r determined using this method maybe unrepresentative due the varying fines contents observed in the soils and should be considered with caution (Fioravante, et al., 2023). No adjustment for fines was performed.

7.9.2 STATIC UNDRAINED SHEAR STRENGTH

Field estimates of S_u were provided using Torvane (TV) and pocket penetrometer (PP) tests. The TV and PP were performed in the offshore laboratory immediately after sample recovery. These two methods provide quick, in-situ assessments of the soil's strength without requiring extensive laboratory testing. However, it's important to note that these are index test methods and may not provide accurate results. Therefore, these index strength tests were not considered in the geotechnical bounding.

Undrained shear strength (s_u) was determined from laboratory tests performed both offshore and onshore. s_u was determined from unconsolidated undrained triaxial (UU) tests performed both offshore and onshore. While, miniature lab vanes (MLV) and advanced laboratory strength tests including direct simple shear (DSS) tests, and consolidated triaxial (CIUc, CIDc, CAUc) tests were performed in the onshore laboratory.

s_u was also determined from CPT data using Equation 7-1.

$$s_u = q_n / N_{kt}$$

Equation 7-1

Where:

N_{kt} = Empirical factor relating net cone resistance to undrained shear strength

An assessment was performed to determine the appropriate N_{kt} empirical factor to be applied for each cohesive geotechnical unit. This was performed using the UU, CIUc, CAUc and DSS data within each geotechnical soil unit. The s_u determined from DSS, UU, CIUc were corrected to equivalent s_u from CAUc (suc) and then used in performing the N_{kt} assessments. There was only a single triaxial test data and 2 DSS tests at the northern site spread across different units. Hence, considering the limited data set, no N_{kt} assessment was performed and N_{kt} values of 15 to 20 were assumed.

7.9.3 REMOULDED UNDRAINED SHEAR STRENGTH

At the northern site, no remoulded undrained shear strength ($s_{u(R)}$) testing was performed. Hence $s_{u(R)}$ can be approximated directly from CPT data based on the recommendation below from Quiros and Young (1988) (Equation 7-2).

$$s_{u(R)} = f_s$$

Equation 7-2

7.9.4 SENSITIVITY

Soil sensitivity (S_t) is defined as the ratio of peak to the remoulded undrained shear strength. This parameter provides an indication as to how much strength loss should be expected upon sample disturbance, remoulding or when subjected to monotonic or cyclic loading that cause large deformations.

It was determined from CPT data as no remoulded laboratory tests were performed. S_t was determined using the method proposed by Schmertmann (1978) as described by Equation 7-3.

$$S_t = N_s / R_f$$

Equation 7-3

Where:

N_s = Empirical constant

The value of N_s is determined by various factors such as OCR and mineralogy. Therefore, for this assessment an N_s value of 7.1 was adopted.

7.9.5 STRESS HISTORY AND CONSOLIDATION

The state of consolidation is an important indicator of stress state and stiffness of soils, which are important design considerations. To compute the state of consolidation, Venterra used the incremental loading (IL) consolidation tests on selected, relatively undisturbed specimens. Those test results together with the CPT data provided important insight into the behaviour of the cohesive units.

7.9.5.1 OVERCONSOLIDATION RATIO

Overconsolidation ratio is determined as the ratio of maximum preconsolidation stress to the effective vertical stress as defined by Equation 7-4.

$$OCR = \sigma'_p / \sigma'_{vo}$$

Equation 7-4

Where:

σ'_p = preconsolidation pressure

In addition to OCR being determined from laboratory test data, OCR was also estimated from CPT tip resistance data using the empirical correlation by Kulhawy and Mayne (1990) (Equation 7-5).

$$\sigma'_p = k(q_t - \sigma_{vo})$$

Equation 7-5

Where:

q_t = cone tip resistance corrected for boundary effects

σ_{vo} = estimated in-situ total vertical stress

k = empirical factor equal to 0.33

OCR was also estimated indirectly estimated from s_u data determined from triaxial test data where available. The relationship proposed by Ladd (1970) as presented in Equation 7-6 was used.

$$OCR = \left(\frac{(s_u/\sigma'_{vo})_{OC}}{(s_u/\sigma'_{vo})_{NC}} \right)^{1/\lambda_0}$$

Equation 7-6

Where:

$(s_u/\sigma'_{vo})_{OC}$ = Ratio for overconsolidated soil

$(s_u/\sigma'_{vo})_{NC}$ = Ratio for normally consolidated soil of 0.25

$\lambda_0 = 0.85$

The preconsolidation pressure estimated from CPT data was used to develop OCR profiles and compared to laboratory test results. Geotechnical LE, BE and HE profiles were determined by engineering judgement. Appendix C presents the OCR profiles and parameter bounds.

7.9.6 COEFFICIENT OF LATERAL EARTH PRESSURE AT REST

The lateral earth pressure coefficient at rest (K_0) is defined as the ratio of horizontal effective stress to vertical effective stress (Equation 7-7).

$$k_0 = \sigma'_{ho} / \sigma'_{vo}$$

Equation 7-7

Where:

σ'_{ho} = horizontal effective stress

σ'_{vo} = vertical effective stress

This ratio is commonly used to quantify the lateral pressure a soil exerts on a structure when loaded vertically. This ratio is also important in evaluating the depositional history and consolidation state of the soil. A higher k_0 indicates an increase in consolidation state. k_0 can be determined for uncemented sands and clays of low to medium sensitivity as described in Equation 7-8.

$$k_0 = (1 - \sin\phi')OCR^{\sin\phi'}$$

Equation 7-8

Where:

OCR = over consolidation ratio

ϕ' = effective friction angle

Since k_0 is a function of ϕ' , the Kulhawy and Mayne (1990) expression was used. OCR was set to 1.0 for cohesionless soils. With increasing OCR, k_0 is limited by the passive earth pressure coefficient (k_p) where passive failure supersedes.

7.9.7 EFFECTIVE STRESS PARAMETERS

7.9.7.1 GENERAL

The following effective stress parameters were determined for both cohesive and cohesionless soils:

- Peak friction angle
- Interface friction angle
- Critical state friction angle

Effective stress parameters for cohesive soils were determined from CAUc and CIUc test data. For cohesionless soils were determined from CIDc test data. Engineering correlations were also considered in the derivation of effective stress parameters.

7.9.7.2 PEAK FRICTION ANGLE

The peak friction angle (ϕ') represents the resistance to sliding and shear deformation along a potential failure plane within a soil mass. It is a measure of the internal frictional resistance between soil particles and is one of the key factors governing the shear strength of soils. ϕ' was determined from CID test data.

ϕ' was also determined from CPT data using the strength and dilatancy framework proposed by Bolton (1986). A critical state friction (ϕ'_{cv}) angle of 32° was used in the assessment of ϕ' . It should be noted that the Bolton correlation has been developed for clean sand and should be considered with caution in sands with fines content. Appendix C presents the peak friction angles and the geotechnical profile bounds. The bounds were determined by engineering judgement.

It should be noted that only a single CID test was performed at this site. A good match was observed between the CID data point compared against the friction angle determined from CPT based on Bolton (1986). No further calibration was performed considering the limited dataset.

7.9.7.3 INTERFACE FRICTION ANGLE

Interface friction angle (δ) were determined based on API recommendation no test data was available. Equation 7-9 was used to determine δ .

$$\delta = \phi' - 5^\circ$$

Equation 7-9

7.9.7.4 CRITICAL STATE FRICTION ANGLE

Critical state friction angle (ϕ'_{cv}) was determined from available triaxial test data. Global; review of the ϕ'_{cv} was performed due to the limited triaxial test data available.

7.9.8 STIFFNESS PARAMETERS

Unit specific stiffness parameters consisting of small strain shear modulus (G_0) were determined and are presented in this section. G_0 was determined from:

- PS logging data
- Seismic CPT data
- CPT data

7.9.8.1 P-S LOGGING

P-S logging was performed at four BH locations from 70 m below seafloor (BSF) to between 4.0 m and 18.0 m BSF. Both P and S waves were picked and processed.

7.9.8.2 SEISMIC CPT

Seismic CPT's were performed at two locations across the entire site. The seismic shear wave values (V_s) as presented in the factual report were adopted.

7.9.8.3 CPT DATA

Shear wave velocities (V_s) were inferred from CPT data. The relationship proposed by Mayne (2006) was adopted to determine V_s . The V_s values determined from CPT data were calibrated against the P-S logging data. A calibration factor of 1.6 was applied for the sediments and 3.0 was applied for the unlithified Chalk.

7.9.8.4 SMALL STRAIN SHEAR MODULUS

Small Strain Shear Modulus (G_0) was determined using the V_s values determined from P-S logging, SCPT and as inferred from CPT data. Equation 7-10 was hence used to determine G_0 .

$$G_0 = \rho V_s^2$$

Equation 7-10

Where:

ρ = Bulk density of the soil [Mg/m^3]

V_s = Shear wave velocity [m/s^2]

Appendix C presents the G_0 values for each geotechnical unit. Geotechnical bounding was determined based on engineering judgement.

7.9.8.5 STRAIN AT 50% PEAK DEVIATOR STRESS

The strain at 50% of the maximum deviatoric stress, ε_{50} , is used in the formulation of traditional lateral load-deflection (p-y) curves in cohesive layers and is derived from triaxial test stress-strain plots. ε_{50} was determined from the CIUc, and CAUc test data. Appendix C presents the ε_{50} test data with depth and parameter bounds.

7.10 ROCK PARAMETERS

7.10.1 GENERAL

The rock identified at the northern site was Chalk with top to bedrock varying between -25.8 mMSL to -77.4 mMSL. The Chalk consisted of:

- Unlithified Chalk – Class Dm/Dc
- Lithified Chalk – Class A1 to B4

Design in Chalk should be considered with caution as it may lead to excessively long piles or premature refusal during installation. This will be dependent on the Chalk structure and properties.

CPTs were able to penetrate into the unlithified chalk but not into the lithified chalk. This is because the unlithified chalk is encountered as a structureless chalk slightly sandy silty gravelly to very gravelly. The thickness of the unlithified Chalk varied in thickness from less than 5m to greater than 25m. The unlithified Chalk was underlain by the structured lithified Chalk where CPTs terminated at top and were recovered by coring.

This section of the report discusses the characterisation of rock parameters in view of the laboratory test results, which included point load tests, unconfined compressive strength (UCS), and UCS with young's modulus. Appendix C presents the rock parameters and the tabulated parameter bounds.

7.10.2 RQD

Rock quality designation (RQD) is a measure of quality of rock cores recovered in a borehole. RQD is described as the ratio of solid core pieces longer than 100 mm length per core run. An RQD of 75% or greater indicates good quality rocks and 50% or less indicates poor quality rock cores. RQD was determined mainly for the lithified (structured) Chalk (GU Vb). Appendix C presents that RQD with depth. It can be observed that most of the rock cores had an RQD greater than 80% indicating a good quality structured Chalk.

In the unlithified structureless Chalk where coring was performed. RQD were predominantly 0% with few core runs with RQD at 100%. This shows the unlithified Chalk (GU Va) to be very variable consisting of both structureless and structured Chalk. This variability in GU Va should be considered with caution in the foundation design.

7.10.3 POINT LOAD TESTS

A total of 83 Point Load Tests have been performed to determine Point Load Index (PLI) for rock samples. PLI assesses the rock strength by applying a concentrated load at a specific point and measuring the applied load at failure. The shape of the rock selected for the PLI will determine if the test will be performed diametral (D), Axial (A), Irregular lump (I) or random (U). PLI observed to have failed early or incorrectly were not included.

7.10.4 UNCONFINED COMPRESSIVE STRENGTH

A total of 98 UCS tests were performed to determine the uniaxial compressive strength of rock samples. Out of the 98 tests, 49 included strain measurements to calculate Poisson's ratio

and Young's modulus. All the tests with strain measurements have been interpreted by using a secant method.

Several samples did not have an acceptable L/D ratio. For samples with L/D outside of the 2.0 to 2.5 range per ASTM or 2.5 to 3.0 range per ISRM, the results may therefore be biased. Venterra used the method recommended by Tuncay et al. (2019) to correct the UCS for samples with low L/D.

PLT tests were converted to an equivalent UCS value as described by Equation 7-11. It should be noted that only the axial PLT were considered which is representative of a similar failure condition to UCS.

$$UCS = I_{S50}k$$

Equation 7-11

Where:

I_{S50} = Adjusted point load value

k = conversion factor

Appendix C presents a comparison of PLT and UCS test results with bulk density. A review of this plots shows a k factor of 16 was determined to be applicable for converting PLT to equivalent UCS results. Geotechnical bounding has been presented based on engineering judgement biased towards the UCS results.

7.10.5 INTACT YOUNGS MODULUS

Intact young's modulus (E_i), tangential at 50% of the UCS failure mode, of the Chalk was determined from UCS strength tests with Youngs modulus. Appendix C presents the E_i plots where measured.

8 HAZARDS AND GEOHAZARDS

8.1 SEAFLOOR HAZARDS

A summary is provided below of the individual seafloor hazards identified by (GEOxyz, 2024). The associated risks to development are considered minimal as they have been previously investigated and are summarised here for a complete overview of the site. The level of risk for the described hazards is expected to be reduced further with the future site investigations required for the development of the site.

8.1.1 BOULDERS AND DEBRIS

A total of 12,478 targets were interpreted on the SSS (10843) and MBES (1635) data to be related to the presence of boulders. These vary in diameter between approximately 0.5 and 9.7 m, and in height between 0.0 and 3.3 m. A significant amount of scarring affects the seafloor and there is a possibility that some of the contacts interpreted as boulders represent just mounds of sediments developed during anchor-drag or trawl-related scarring. Additional targets were interpreted as debris, fishing equipment or unknown, with further comments on contacts potentially associated with known shipwrecks.

A total of 166 targets were interpreted on the SBP data, seen as hyperbolas on the seafloor which are not related to cables, wrecks, or other known features (Figure 8-1). These hyperbolas are most likely boulders or debris. Only isolated instances that had a strong amplitude were picked.

Boulder fields are present across the site, typically where Units III and IV outcrop. These fields have been digitized from the MBES and SSS datasets. On the SBP data, clusters of hyperbolas were interpreted at the seabed and interpreted as boulder fields. These boulder fields were cross checked with the MBES/SSS datasets to confirm the area boundaries align.

The site contains two levels of boulder field classification based on their density value for a 100 x 100 m area, that were provided and referenced by GEOxyz in their report (GEOxyz, 2024). However, the delivered shapefiles for these areas contain a variation in classification to that reported. The report describes classifications 1 and 2 representing a density of 40-80 boulders and >80 boulders, respectively.

Venterra highlights that GEOxyz interpreted additional preliminary areas classed as boulder fields, though these are based on the coverage of larger stones as a percentage in areas of seabed lithology consisting of SAND, GRAVEL, and pebbles. Given that this is not described in the GEOxyz report, only the extents of boulder fields based on the density criteria from their report, have been provided. The identification of the boulders and debris on site reduces their risk to development, though their positions should be taken into consideration for future planning of the site.

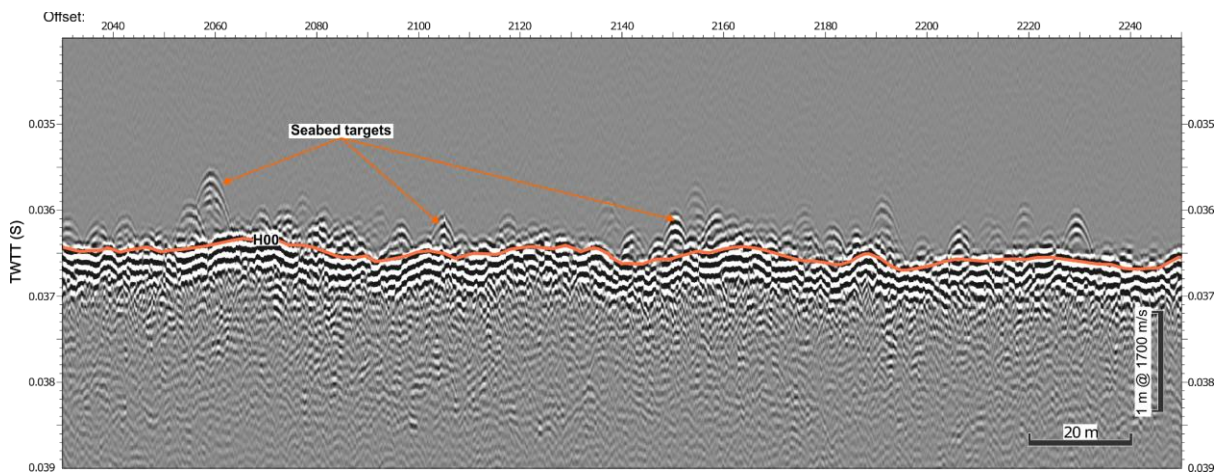


Figure 8-1 - Section of line '1437_C_KN_G06_L509V' seabed targets interpreted as boulders

8.1.2 DEPRESSIONS

Depressions were identified on the SSS and MBES data throughout the site and are similar in size and distribution, with denser areas located in the southern part of the site and labelled as 'pitted seabed'. These are shallow truncated channel features, with maximal localised depths up to 2.5 m deeper than the surrounding seabed. Given the density and spread of the features identified across the site, the risks related to this are considered minimal.

8.1.3 SEAFLOOR SCARRING

Extensive seabed scarring was found in the southern section of the site along the Baltic Pipe. These scars are interpreted to be associated with bottom scarring associated with the construction of the Baltic Pipe. There are numerous locations of disturbed seabed and anchor scars. These scars appear to be deeper and more erratic in their shape and positioning, comparing to others found within the site. They are located on both sides of the Baltic Pipe and extend up to 800 m on each side. Further south the scars are interpreted to be associated with fishing activity, the trawl marks are more equally spaced and shallower with defined paths across a wider area. As these areas are defined and the associated seabed slope values are low, the risks related to this are considered minimal.

8.1.4 SLOPE

Slopes across the site are generally not significant (under 1°), with an average of 0.55°, with the highest values at localised areas reaching up to 32°. Therefore, the risks related to this are considered minimal. The steepest slopes were reported within boulder fields or associated with scouring around seafloor features such as boulders, cable trenches (crossing southern part of the site) and shipwrecks.

8.1.5 WRECKS

There are eight elevated features observed on the SSS and MBES data, which were interpreted as shipwrecks and their associated debris. These features were not correlated with any publicly known shipwrecks in the area. Five of these wrecks were seen across six SBP track lines. They were seen as a significant disturbance to the seafloor reflection, which is not

geological in nature. As these wrecks and associated debris have been identified and mapped in the (GEOxyz, 2024) study, the risks related to this are considered minimal.

8.1.6 CABLES/PIPES

Five cables were identified in the south of the site on the MBES, SSS and SBP datasets. The Baltic Pipe, a High Voltage Cable and two Transmission Cables were seen on the SBP data, either on the seabed or just below, within Unit I. A fifth cable was seen in the south of the site on the MBES data, which runs northwards for approx. 1.3 km before becoming buried. The full extent of this cable is not seen on the SBP data. This known infrastructure has been identified and mapped and is therefore considered to be a reduced risk to development.

8.1.7 OTHER

Eight almost rounded shaped features have been identified in the southeastern part of the site. Features are aligned along northwest-southeast direction and are located approximately 300 m apart. Change of reflectivity on backscatter and SSS data suggests that the features are covered by coarser sediments than the surrounding material. The size and distribution indicate that the features are likely anthropogenic. Further examination revealed that the elevation change associated with the identified features is not substantial.

8.2 SUB-SEAFLOOR HAZARDS

8.2.1 BOULDERS AND COARSE SEDIMENTS

There were 639 buried contacts mapped within the site boundary, categorised as sub-seafloor targets (409) or areas of increased amplitude (230). The sub-seafloor targets were seen as hyperbolas beneath the seafloor (typically within Unit I) which are not related to cables, wrecks, or other known features. These hyperbolas are most likely boulders/drop stones or buried debris. Only hyperbolas that had a strong, clear amplitude were picked. Areas of increased amplitude seen beneath the seafloor (typically within Unit I) which were not related to cables, wrecks, or other known features were interpreted as areas where there was a change in lithology, possibly coarse sediment patches. Only isolated instances that had a strong amplitude were picked.

8.2.2 SHALLOW GAS

The water exchange with the North Sea is limited at the entrance by the shallow and narrow connections between Sweden and the Danish Islands. Together with the distinct thermo- and haloclines, this results in a highly stratified water column that is favourable for the preservation of organic carbohydrates. The Arkona Basin, which is located east off the site is characterized by shallow gas rich sediments with different levels of saturation. Geoacoustic investigations show gas accumulations in pockmark areas, and in regions with homogeneous deposited organic rich sediments. The gas present in Arkona Basin sediments is of biogenic origin and originates from the generation of methane by methanogenic bacteria. However, only little is known about heterogenous distribution of methane in the Arkona Basin (Mathys, et al., 2005).

In the literature, some common gas phenomena recognised on seismic profiles are acoustic turbidity, enhanced reflection amplitudes, inverse polarity of reflected wavelets and velocity-

pull-downs of reflectors. Acoustic turbidity is the most frequently cited evidence used to infer the presence of seafloor gas. It appears on profiles as amorphous echoes that cut across and mask the internal stratification of the sediment body (Mathys, et al., 2005). Gaseous sediments can be characterized by high acoustic impedance contrast and elastic contrast in relation to the surrounding medium such as—non-gaseous sediments, as seen on Figure 8-2, determining high acoustic energy scattering properties (Jaśniewicz, et al., 2019).

There are several instances of partial acoustic blanking observed on the SBP lines throughout the site. These areas are seen throughout Unit III. The extents of where H20 has been picked are the same as the extents of the partial acoustic blanking. This partial acoustic blanking is unlikely to be due to gas, as strong reflectors are observed beneath the blanked areas.

Areas of increased amplitude within the water column, extending from the seafloor and flaring up through the water column were observed across the site (Figure 8-3). Though this is possibly an indication of gas, in areas where possible flares were picked, there was no evidence of shallow gas within the seismic units.

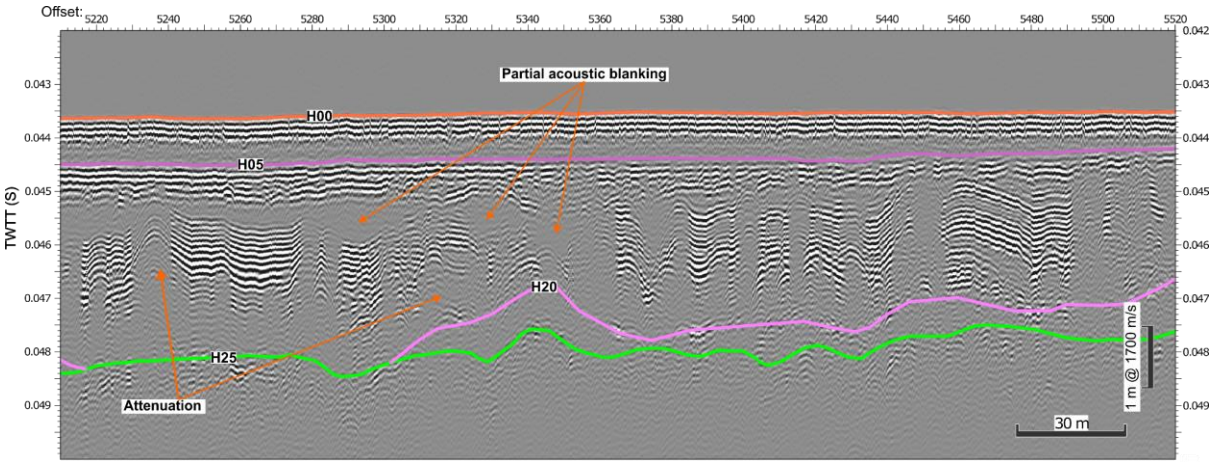


Figure 8-2 - Section of line '0041_A_KN_GO5_L033' showing partial acoustic blanking

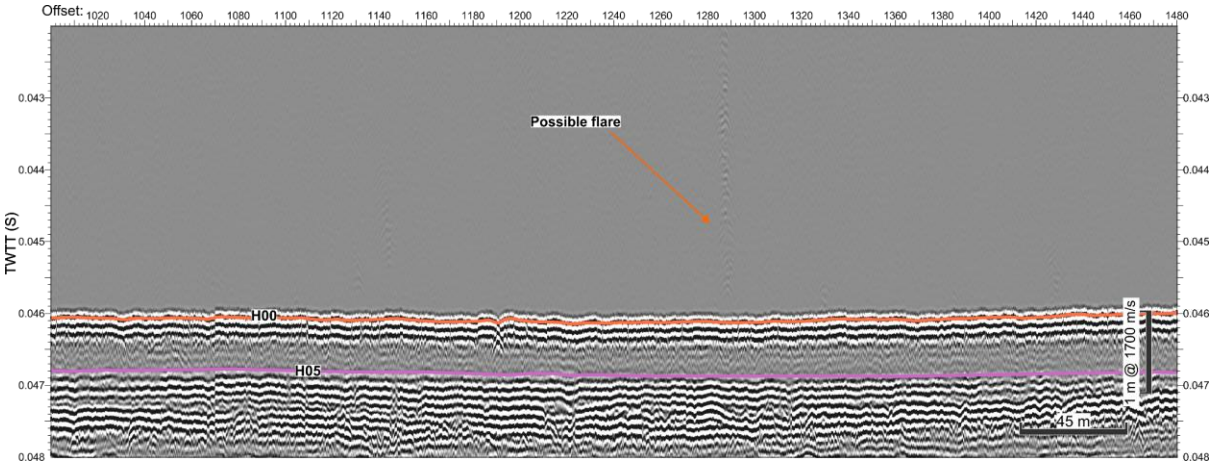


Figure 8-3 - Section of line '1185_C_KN_G06_L721V' showing a possible flare

8.2.3 CHANNELS AND CHANNEL INFILL

Evidence of channel incisions and infill is observable across the whole site area, within the Glacial and Chalk seismic units. These features were picked on the UHRS dataset, due to the greater depth of penetration and better visibility of the units.

312 features were picked within Unit IV (Glacial), these features were seen and picked on each of the UHRS in-lines. Most of these features relate to channels and incisions seen in the south of the site which can be tracked across each line spanning the width of the site. Further north, there are smaller channels and incisions which can only be tracked across <10 consecutive tracklines. Occasionally, small, isolated channels and incisions were seen and picked on one trackline only. Unit IV is comprised of complex structures, there are layers of strong reflectors seen on the UHRS dataset, which may relate to different sediment and till facies, and different glacial events, including series of overlying incisions and infilled channels at different depths. Capturing all features on the one horizon was not possible due to Kingdoms picking limitations. As such, only the largest features were picked in areas where there were multiple features in the one location at different depths. Unit IV is thickest in the central-south of the site, in the northeast-southwest trending channel feature present in the bedrock. Unit IV fills in this large bedrock channel, and within the glacial fill, there are series of glacial channels varying length and depth.

240 features were picked within Unit V (Chalk), these features were seen and picked on each of the UHRS in-lines. Most of these features relate to the northeast-southwest trending bedrock channel seen in the central-south of the site, which can be tracked across each line spanning the width of the site. This northeast-southwest trending bedrock channel is the largest channel seen within the site boundary. It starts as two main branches in the east, the southern branch being the smallest of the two and appearing to have a lateral branch of its own, which does not join the main channel feature. These two main branches join into one wide channel feature at the midway point of the site near the southern boundary. Further west again, the channel then forks into two separate branches, one continuing to the west, the other trending north-west until it is no visible at the western boundary of the site. Additional features were picks around this main northeast-southwest trending bedrock channel, but due to the UHRS line spacing, it is difficult to tell if these features are offshoots of the main channel, or isolated channels that are just in proximity to the main channel. The main northeast-southwest trending bedrock channel is 2.9 km at its widest point, and -47.8 mBSF at its deepest point. The second largest channel seen within the Chalk unit is found in the north of the site, trended east-west. It is 495 m at its widest point and 55 m at its thinnest point. This channel is less the 10 m in depth below seafloor. Occasionally, small, isolated channels and incisions were seen and picked on one track line only.

8.2.4 FAULTS AND FAULTING

GEOxyz, 2024 reported "The bedrock is likely to be Danian limestone (GEUS, 2024). Bedrock faults are not well imaged, though faults are almost certainly present. Some UHRS lines do show weak evidence for the position of fault planes. These ancient faults were reactivated during the Late Cretaceous/Early Palaeocene and, in this area, likely generated inversion. The high potential for erosion of the top of the bedrock (especially over the last 1.1 million years of

ice advances) makes it difficult to attribute features at the top bedrock surface to tectonic activity. The tectonic relief may well have been planned off by ice.

The top of the bedrock is generally 3 to 8 m below seabed, exceeding 25 m over a 500 m wide south-west to north-east trending zone, just south of the centre of the area. This feature may be related to faulting or erosion.

The upper surface of the bedrock is a truncation surface with an angular unconformity between the ~60 million-year-old limestones and their much younger overburden. The bedrock may have been subjected to numerous phases of erosion during early glaciations.”

During seismic interpretation, no major fault was evidence neither in SBP data nor in UHRS data.

8.2.5 GLACIAL FEATURES

The Quaternary geological evolution of the study area is defined by an alternation of glacial and interglacial periods. Scandinavian inland glaciers advanced several times through the Baltic area in the direction of Middle and Western-Europe (Mathys, et al., 2005). The nearby Arkona Basin has a complex geologic setting, with Cretaceous bedrock made of chalk successions, which were subsequently glacially overprinted and covered by glacial till, sands, and clays, fine-grained brackish to marine organic-rich deposits.

From literature in the Arkona Basin there are no traces of ice marginal forms. The only glacial feature encountered across the site area is a channel mentioned in Section 7.2.2, potentially it can be glacial-related and constitute tunnel valley. The infills can display similar physical and geotechnical properties to the adjacent units.

8.2.6 LOW STRENGTH SEDIMENTS

Low strength fine grained sediments have been sampled by the geotechnical data within seismic Units I to III. Unit I is comprised of marine sediments and exhibits a change in lithology from sands to silty sands, which are interpreted to be a low strength. The distribution of glacial sediment facies in Unit III is in general chaotic with alternating sections of clays and parallel-bedded, well sorted sands with laminated silt and clay interbeds. The sampled sediments from Unit III include very closely to closely spaced thin laminations of organic matter.

8.2.7 SHALLOW BEDROCK

The site is located at the margin of the Arkona Basin. Thus, the bedrock geology is represented by Upper Cretaceous chalk. The depth to bedrock (Unit V) varies from 1.4 mBSF to 47.8 mBSF, from the gridded surfaces (Figure 6-28). Most of the site area is characterised by depths to bedrock less than 7.2 mBSF, exceptions occurring in the southern channels and additional smaller scale incisions. Bedrock is not interpreted to crop out based on the available seismic data.

9 RISK REGISTER

A Risk Register is provided in Appendix D. Risks are graded by likelihood of occurrence and severity (pre-mitigation) based on the criteria and scoring system defined in the respective parts of the document. An overall risk level is determined from the risk matrix in Figure 9-1 (Vamanu, et al., 2016). The associated risks for the hazards identified on the site(s) are assessed and scored based on the available literature for risks within the marine environment and offshore renewable energy activities. These include:

- Documentation from the International Organization for Standardization (ISO) (International Organization for Standardization, 2017).
- Standards from the British Standards Institution (BSI) (British Standards Institute, 2003; British Standards Institute, 2013; British Standards Institute, 2021).
- Carbon trust risk assessment guidance (Carbon Trust, 2015).
- Documentation on Marine Geohazards from the European Marine Board (European Marine Board IVZW, 2021).
- Offshore wind farm risk management codes of practice from VdS (VdS, 2014).
- International Association of Oil & Gas Producers (IOGP) Risk management guidance for geophysical operations (International Association of Oil & Gas Producers, 2017).
- Offshore risk assessment guidance from the European Commission and the Joint Research Centre (Vamanu, et al., 2016).

The final risk classifications are graded with reference to the European Commission and Joint Research Centre report for offshore risk assessment (Vamanu, et al., 2016). The resultant Low, Medium, and High levels can be described as:

Low

"The risk of the occurrence of the event is acceptable, and no risk reduction/mitigation actions are required; the risk must however be part of the continuous risk management process, for further reduction."

Medium

"The risk should be monitored, yet at the current moment it is controlled as low as reasonable practicable (ALARP)."

High

"The risk is intolerable and risk reduction/mitigation actions must be put into place."

The identified foundation risks focus on selection and installation concerns relate specifically to the northern site. It should be noted that in most cases the identified levels of risk can be mitigated by acquisition of additional information or development of avoidance strategies: these measures are not necessarily required to inform conceptual foundation design. Timing of any mitigation measures should be determined based on the project development strategy. Survey-specific risks should be assessed as part of a project-specific survey strategy.

			Severity				
			Low	Minor	Moderate	Major	Severe
			1	2	3	4	5
Likelihood	Very Likely	5	Medium	Medium	High	High	High
	Likely	4	Medium	Medium	Medium	High	High
	Possible	3	Low	Medium	Medium	Medium	High
	Unlikely	2	Low	Low	Medium	Medium	Medium
	Very unlikely	1	Low	Low	Low	Medium	Medium

Figure 9-1 - Risk matrix

10 RECOMMENDATIONS

10.1.1 DESK STUDIES

A dedicated study for the identification of the wrecks identified on the MBES, SSS and seismic data would determine the need for UXO studies. There are no public records for the identified wrecks, therefore further investigation would be needed to confirm this.

A shallow gas hazard assessment would provide added benefit to the understanding of the site conditions. As discussed in Sections 6.2.2 and 8.2.2, the observed transparent facies (with reduced amplitude) does not exhibit typical behaviour of acoustic blanking attributed to the presence of gas. Mainly due to the fact that signal is still visible, above, below and often within these affected parts of the signal.

10.1.2 DATA RE-PROCESSING

Reprocessing of the UHRS dataset to provide improved visibility of reflectors for the sections of the data affected by the seabed de-multiple process. The current dataset provides a preliminary coverage of the site, though it is limited in that the remnant processing artefacts affect the continuity and interpretation of the H30 reflector of Unit V, within the northeast-southwest trending channel feature in the central-southern part of the site. Re-processing the existing data would reduce costs for immediate data acquisition and may provide improved results to constrain the associated uncertainty around the till and unlithified chalk interface, as well as inform on the behaviour of the deeper lithified chalk reflector.

10.1.3 FURTHER SURVEY AND INVESTIGATIONS

A significant source of uncertainty in the IGM is due to the current UHRS data line spacing of approximately 250 m. At this distance, significant extrapolation was required to create grids for the mapped seismic units. Where seismic units change significantly in depth between or along lines, the gridded surfaces can produce unrealistic trends that can give a false impression of changes in the depth of a unit. To alleviate this, additional seismic data should be acquired and added to the IGM to fill in gaps, reduce extrapolation distances, and subsequently improve reliability of unit depths. These additional surveys are advised to be undertaken with an adequate (narrower) line spacing for both 2D UHRS and SBP (e.g. Innomar) data, or even consider 3D UHRS. A revision to the IGM ought to follow each data acquisition milestone to address remaining knowledge gaps.

The acquisition of additional seismic and geotechnical data would allow for further improvements and refinement of the velocity model. If the unitisation of the subsurface changes based on new data, then the associated velocity model would need to account for this to allow for accurate conversion of the interpreted model.

The geotechnical and geophysical data has shown that the ground conditions vary both laterally and axially across the site. Hence, for detailed design, it is recommended to perform location specific geotechnical testing at each foundation location to determine the ground conditions.

A channel was observed at the south of the site. No geotechnical testing or sampling was performed within the channel. Geotechnical conditions could be variable both axially and laterally within the channel. Hence, it is recommended to target specific testing and boreholes within the channel to determine geotechnical properties.

Shallow bedrock consisting of unlithified (unstructured) and Lithified (structured) chalk was observed across the site. The testing at the site mainly targeted the lithified chalk with few classification testing performed within the unlithified chalk. However, considering the deep penetration of some of the CPTs into the unlithified chalk; this unit will be most critical for foundation design. The behaviour of chalk is very variable as noted by various authors such as Jardine et al and Buckley et al. Hence, additional targeted testing is recommended to determine the geotechnical properties of the unlithified (unstructured) chalk as well as the lithified (structured) chalk.

A limited geotechnical testing scope was performed at the northern site. Additional geotechnical testing is recommended to properly capture the geotechnical properties such as shear box testing, electrical resistivity, triaxial extension tests and permeability tests etc.

11 CONCLUSIONS

An IGM has been developed based on the integration of the recently acquired geophysical and geotechnical datasets, building on the results of the PGM (GEOxyz, 2024) and constraining the site as much as possible. Interpreted seismic units have been revised and correlated with independently interpreted geotechnical unit top markers. Based on this integration, a velocity model (appropriate to this stage of investigation) was developed and used for the depth conversion of the seismic dataset and interpretation. Though uncertainties remain, this model forms the basis of future detailed and targeted investigations required to further constrain the model and better understand the behaviour of the subsurface across the site.

Within the seismic data, four seismic units were differentiated based on their internal seismic facies and correlated with five geotechnical units (including 11 subunits). Seismic Unit I (marine sediments) consists of up to 2.22 m of surficial sands and clay, overlying the older glaciolacustrine deposits.

Seismic Unit II (not interpreted as part of this study and integrated within Unit III, see Section 6.2) corresponds to the post-glacial transition deposits. This transitional unit between Unit I and Unit III was observed across the whole site in seismic data but could not be identified in the geotechnical until later stage in the project. Because this unit shares geotechnical properties with GU Ib and GU IIIa1, it is expected to have limited impact on design.

Seismic Unit III has been interpreted as glacio-lacustrine deposits with two different facies separated by an internal boundary H20. Above this boundary, the seismic facies of Unit III show medium amplitude, chaotic, discontinuous reflectors and transition to low amplitude and occasionally transparent. This unit III is approximately 7.03 m in thickness and represents the glaciolacustrine unit as discussed by (GEUS, 2023; Jensen, et al., 1997). The base of the unit, along with the base of Unit I and the seabed, represents the top on the glacial unit - Unit IV. This unit is characterised by multiple subunits, which have been interpreted as multiple glaciations (GEUS, 2024). Each subunit is likely to correspond to a different till member, with each being separated by minor unconformities corresponding to erosional surfaces or ice-contact surfaces. The maximum thickness of this Unit IV reaches approximately 45.21 m, where paleochannels have been observed.

The base of Unit IV represents the top of Unit V, which is interpreted as unlithified chalk. The boundary between unlithified and lithified chalk was often described in geotechnical data but could not be tracked across the whole site in the seismic data. Further geotechnical investigations will be required to support the interpretation of this boundary in seismic data.

The current IGM presents limitations and uncertainties due to the coverage of the UHRS data and remnant processing artefacts, the limited number of geotechnical locations and retrieved samples. As a result, there is reduced accuracy between gridded UHRS lines, which is increased when there is more variability in interpretation along the survey line. The remnant processing artefacts in the seismic data prevent the tracking of otherwise continuous reflectors to inform on key surfaces and interfaces.

Hazards and geohazards were identified within the proposed site. They include boulders and debris, seafloor depressions and scarring, five wrecks, with three potential additional, five cables and a confirmed pipeline crossing the site. The subsurface hazards include boulders and coarse sediment patches, possible shallow gas (Unit III), incisions and channels within the glacial units (Unit IV) and at top of bedrock (Unit V), low strength sediment and shallow bedrock (Section 8.2.7).

Five geotechnical zones and 11 geotechnical units were identified across the site. The geotechnical zones represent broadly similar ground conditions laterally and vertical across the site. Geotechnical units represent similar geotechnical properties e.g. clay or sand.

Generally shallow bedrock of Chalk less than 10 m BSF is encountered across the site with the deepest bedrock encountered in the channel at the south of the site. Province 1 Chalk bedrock is less than 5 m BSF and covers approximately 35% of the site, Province 2 Chalk bedrock is between 5m and 10m and covers approximately 40% of the site. Provinces 3 to 5 defines the channel at the south of the site. Province 3 Chalk bedrock was encountered between 10 m and 20 m, Province 4 Chalk bedrock was encountered between 20 m and 30 m while in province 5 Chalk bedrock is considered greater than 30 m BSF. Design and installation of foundations in Provinces 1 and 2 may be challenging due to the shallow Chalk which may result in excessively long piles, difficulties in installation or the requirement for specialised installation techniques such as drive-drill-drive. In provinces 3 to 5, a large thickness of SU IV maybe encountered which consists of Silt, Sand Till and Clay Till. These soils may behave as transitional soils i.e. dependent on the loading conditions the soils may behave as drained or undrained. Hence should be considered with caution by the designer. Further, the high strength and gravelly nature of the soils may cause installation challenges.

The following should be considered when installing foundations within each of the provinces:

- Design and installation of foundations in Chalk may result in excessively long piles, increased risk of premature refusal during installation due to competent Chalk layers or flint beds, requirement of specialised installation techniques such as drive-drill-drive or drilled and grouted piles which may be expensive.
- Jack-up placement where low strength sediments are observed close to seafloor or at great depths should be considered with caution as they may result in excessive leg penetration, spudcan sliding, uneven leg penetration, punch through etc
- Very dense sands are observed overlying very low to low strength clays. Design of foundations in these soil layers should be considered with caution due to high risk of punch through, excessive length of piles being designed, pile run risks etc
- Very dense sands are observed close to seafloor and at shallow depths. Installation of foundations in these sands may be challenging due to limited penetration, early refusal etc.
- Transitional soils are observed across the site which may behave as drained or undrained dependent on the design conditions. Geotechnical units IIIb4, IIIb5, IIIb6 may behave as transitional soils and should be considered with caution by a geotechnical designer.

- Clay Till was observed overlying the Chalk bedrock. Installation of foundations in this unit may result in pile tip buckling, premature refusal or punch through into the lower strength unlithified Chalk considering the gravelly sandy very high to extremely high strength properties of the unit.

Unitised geotechnical parameters were determined to describe the geotechnical properties across the site. LE, BE and HE geotechnical profile bounds were assigned to some of the unitised geotechnical parameters. The geotechnical profile bounds were determined either statistically and/or by engineering judgement.

Shallow bedrock consisting of unlithified (structureless) and lithified (structured) chalk was observed across the site. The unlithified chalk varied laterally across the site with varying thicknesses. Limited testing was performed within the unlithified Chalk and it is recommended that additional testing is performed to fully characterise this unit.

This IGM presents the assessment of ground conditions at the Krieger's Flak II Northern OWF. Geophysical and geotechnical data acquired for the site were reviewed, integrated and analysed to develop an IGM with unitised geotechnical parameters. The main ground risk identified was shallow bedrock consisting of Chalk which was identified at its shallowest depth of less than 5 m BSF. The shallow bedrock will influence the foundation type of the OWF, foundation design and installation methodology. The site was split into five zones based on the depth to top of bedrock, geotechnical and geophysical data. The zones will aid in the initial planning of the turbine layout, foundation concept and design based on the engineering characteristics. Geotechnical parameters for each unit were also presented representing the range of engineering properties. It is recommended that the end user of this report performs an independent review of the IGM and parameters in respect to the proposed foundation typology and construction methodology.

12 REFERENCES

- Binzer, K., Lykke-Andersen, H. & Stockmarr, J., 1994. *Geological map of Denmark, 1:500 000. Elevation of the Pre-Quaternary surface.*, s.l.: GEUS Dataverse.
- Bolton, M., 1986. The strength and dilatancy of sands. *Géotechnique*, 36(1), p. 65–78.
- British Standards Institute, 2003. *BS EN ISO 19901 4:2003 - Petroleum and natural gas industries — Specific requirements for offshore structures — Part 4: Geotechnical and foundation design considerations*, London: British Standards Institute Limited.
- British Standards Institute, 2013. *BS 6349-1-1:2013-Maritime works –Part 1-1: General – Code of practice for planning and design for*, s.l.: BSI Standards Limited.
- British Standards Institute, 2021. *BS ISO 19901-10:2021-Petroleum and natural gas industries — Specific requirements for offshore structures-Part 10: Marine geophysical investigations.*, s.l.: BSI Standards Limited.
- Carbon Trust, 2015. *Cable Burial Risk Assessment Methodology-Guidance for the Preparation of Cable Burial Depth of Lowering Specification.*, London: Carbon Trust.
- DGU, 1992. *Geological map of the Danish underground.* s.l.:Varv.
- Emeis, K.-C., Endler, R. & Struck, U., 2002. The post-glacial evolution of the Baltic Sea. In: G. Wefer & W. Berger, eds. *Climate Evolution in NW Europe in the Holocene*. Berlin: Springer-Verlag.
- EMODnet, 2024. *EMODnet Central Portal*. [Online]
Available at: : <https://www.emodnet.eu/>
[Accessed 01 2024].
- Erlström, M. & Sivhed, U., 2001. Intra-cratonic dextral transtension and inversion of the southern Kattegat on the south-west margin of Baltica - Seismostratigraphy and structural development. *Sveriges geologiska undersökning*, p. 38.
- European Marine Board IVZW, 2021. *Marine Geohazards - Safeguarding society and the Blue Economy from a hidden threat.*, Ostend: European Marine Board IVZW.
- Expedition 347 Scientists, 2014. *Baltic Sea Basin Paleoenvironment: paleoenvironmental evolution of the Baltic Sea Basin through the last glacial cycle. IODP Prel. Rept., 347*, s.l.: Integrated Ocean Drilling Program.
- Fioravante, V. et al., 2023. *Calibration of cone resistance in a sand with fines by means of model testing*, s.l.: Offshore Site Investigation Geotechnics 9th International Conference Proceeding, Society for Underwater Technology.
- F. M. I., 2023. *Maritime Boundaries Geodatabase: Maritime Boundaries and Exclusive Economic Zones (200NM), version 12.*, s.l.: Marine Regions.
- Galsgaard, J., 2014. *Flint in the Danian København Limestone Formation*. [Online]
Available at: https://www.geo.dk/media/1951/flint-in-the-danian-koebenhavn-limestone-formation_jgalsgaard_2014.pdf
[Accessed 18 1 2014].
- Gardline, 2023. *Volume II: Measured and Derived Geotechnical Parameters and Final Results. Project: 53101 –Danish Offshore Wind 2030 - Lot 1 -Kriegers Flak II. Project No. 53101*, s.l.: s.n.
- Gardline, 2024. *Volume II: Measured and Derived Geotechnical Parameters (Report Ref: 53101)*, s.l.: Gardline.
- Gavin and Doherty Geosolutions Ltd., 2024. *Conceptual Ground Model, 24004-REP-001-00*, s.l.: s.n.
- GEOxyz, 2024. *Geophysical and Geological Survey Report For Kriegers Flak II North and South (BE5376H-711-03-RR)*, s.l.: GEOxyz.
- GEUS, 2022. *Geological Screening of Kriegers Flak North and South*, s.l.: s.n.
- GEUS, 2022. *Geological Screening of Kriegers Flak North and South*, s.l.: s.n.
- GEUS, 2023. *Screening of seabed geological conditions for the offshore wind farm areas Kriegers Flak II North and Kriegers Flak II South*, s.l.: s.n.

GEUS, 2024. *Denmark's Geology Portal*. [Online]

Available at:

<https://data.geus.dk/geusmap/?lang=da&mapname=denmark#baslay=&optlay=&extent=5296.602683329023,5932375.391217925,1107654.6090847922,6468052.484953636&layers=dkskaermkort>
[Accessed 18 01 2024].

Graversen, O., 2004. Upper Triassic - Cretaceous stratigraphy and structural inversion offshore SW Bornholm, Tornquist Zone, Denmark.. *Bulletin of the Geological Society of Denmark*, Volume 51, pp. 111-136.

Graversen, O., 2009. Structural analysis of superposed fault systems of the Bornholm horst block, Tornquist Zone, Denmark.. *Bulletin of Geological Society of Denmark*, Volume 57, pp. 25-49.

International Association of Oil & Gas Producers, 2017. *Risk management in geophysical operations - 432-02*, London: International Association of Oil & Gas Producers.

International Organization for Standardization, 2017. *ISO 19901-2:2017-Petroleum and natural gas industries — Specific requirements for offshore structures — Part 2: Seismic design procedures and criteria*, Geneva: International Organization for Standardization.

Jakobsen, P. R., Rohde, M. M. & Sheldon, E., 2017. Structures and stratigraphy of Danian limestone, eastern Sjælland, Denmark. *GEUS Bulletin*, Volume 38, pp. 21-24.

Jamiolkowski, M., LoPresti, D. & Manassero, M., 2001. Evaluation of Relative Density from Cone Penetration Test and Flat Dilatometer Test. In: *Soil Behavior and Soft Ground Construction (GSP 119)*. Reston, VA.: American Society of Civil Engineers, pp. 201-238.

Jardine, R., Chow, F., Overy, R. & Standing, J. R., 2005. *ICP design methods for driven piles in sands and clays*. London, p. 105: Thomas Telford Ltd.

Jaśniewicz, D., Klusek, Z., Brodecka-Goluch, A. & Bolątek, J., 2019. Acoustic investigations of shallow gas in the southern Baltic Sea (Polish Exclusive Economic Zone): a review.. *Geo-Marine Letters*, Volume 39, pp. 1-17.

Jensen, J. B. et al., 1997. The Baltic Ice Lake in the southwestern Baltic: sequence-, chrono- and biostratigraphy. *Boreas*, Volume 26, pp. 217-236.

Jensen, J. B., Kuijpers, A., Bennike, O. & Lemke, W., 2002. Balkat, the Baltic Sea without frontiers.. *Geologi, nyt fra GEUS*, Volume 4, p. 19.

Jensen, J. B., Moros, M., Endler, R. & Members, I. E. 3., 2017. The Bornholm Basin, southern Scandinavia: a complex history from Late Cretaceous structural developments to recent sedimentation. *Boreas*, Volume 46, pp. 3-17.

Jensen, J. B. & Nielsen, P. E., 1998. *Treasures hiding in the Sea Marine raw material and Nature Interests*, s.l.: s.n.

Karlsrud, K., Clausen, C. & Aas, P., 2005. *Bearing Capacity of Driven Piles in Clay, the NGI Approach*, Oslo, Norway: Norwegian Geotechnical Institute.

Kulhawy, F. H. & aMayne, P. W., 1990. *Manual on Estimating Soil Properties for Foundation Design*, s.l.: Electric Research Institute, EPRI.

Lemke, W., 1998. *Sedimentation und paläogeographische Entwicklung im westlichen Ostseeraum (Mecklenburger Bucht bis Arkonabecken) vom Ende der Weichselvereisung bis zur Litorinatransgression*. s.l.:IOW, Bibliothek.

Mathys, M., Thießen, O., Theilen, F. & Schmidt, M., 2005. Seismic characterisation of gas-rich near surface sediments in the Arkona Basin, Baltic Sea. *Marine Geophysical Researches*, Volume 26, pp. 207-224.

Mayne, P., 2006. *The 2nd James K. Mitchell Lecture: Undisturbed sand strength from seismic cone tests*. London, Intl. J. Geomechanics & Geoengineering, Taylor & Francis Group.

Michel, G. et al., 2023. Stratigraphic and palaeo-geomorphological evidence for the glacial-deglacial history of the last British-Irish Ice Sheet in the north-western Irish Sea. *Quaternary Science Reviews*, Volume 300, p. 107909.

- Mogensen, T. E. & Korstgård, J. A., 2003. Triassic and Jurassic transtension along part of the Sorgenfrei–Tornquist Zone in the Danish Kattegat.. *GEUS Bulletin*, Volume 1, pp. 437-458.
- Moreau, J. et al., 2016. Early diagenetic evolution of Chalk in eastern Denmark. *The Depositional Record*, 2(2), pp. 154-172.
- Moros, M. et al., 2002. Regressions and transgressions of the Baltic basin reflected by a new high-resolution deglacial and postglacial lithostratigraphy for Arkona Basin sediments (western Baltic Sea). *Boreas*, Volume 31, pp. 151-162.
- Pedersen, S. A. S., 1998. "Isrande.zip", *Kort over israndslinjer og lokaliteter i Skandinavien*. [Online] Available at: <https://dataverse.geus.dk/file.xhtml?persistentId=doi:10.22008/FK2/XOOWSR/HQ8T4F> [Accessed 02 01 2024].
- Robertson, P., 2009. Interpretation of cone penetration tests – a unified approach. *Canadian Geotechnical Journal*, Volume 43, pp. 1337-1355.
- Robertson, P., 2016. Cone penetration test (CPT)-based soil behaviour type (SBT) classification system – an update.. *Canadian Geotechnical Journal*, 53(12), p. 1910–1927.
- Robertson, P. & Cabal, K., 2010. *Estimating soil unit weight from CPT*, Huntington Beach, CA: 2nd International Symposium on Cone Penetration Testing.
- Rosentau, A., Bennike, O., Uścinowicz, S. & Miotk-Szpiganowicz, G., 2017. The Baltic Sea Basin. In: *Submerged landscapes of the European continental shelf: quaternary paleoenvironments*. s.l.:Johm Wiley & Sons Ltd., pp. 103-133.
- Schmertmann, J., 1978. *Guidelines for cone penetration test: Performance and design (Report no. FHWA-TS-78-209)*, s.l.: Federal Highway Administration, US Department of Transportation.
- Schneider, J., Randolph, M., Mayne, P. & Ramsey, N., 2008. Analysis of Factors Influencing Soil Classification Using Normalized Peizocone Tip Resistance and Pore Pressure Parameters. *Journal of Geotechnical and Geoenvironmental Engineering*, 134(11), pp. 1569-1586.
- Tuncay, E., Ozcan, N. T. & Kalender, A., 2019. An Approach to Predict the Length-to-Diameter Ratio of Rock Core Specimen for Uniaxial Compression Tests. *Bulletin of Engineering Geology and the Environment*, Volume 78, pp. 5467-5482.
- Vamanu, B., Necci, A., Tarantola, S. & Krausmann, E., 2016. *Offshore Risk Assessment - An overview of methods and tools.*, ISPRA: European Commission.
- VdS, 2014. *VdS 3549 2014-01 (01) International guideline on the risk management of offshore wind farms - Offshore code of practice.*, s.l.: Gesamtverband der Deutschen Versicherungswirtschaft.
- Vejbæk, O. V. & Britze, P., 1984. Top præ-Zechstein. *Danmarks Geologiske Undersøgelse Map series 45*.

13 APPENDICES

APPENDIX A – CHARTS AND DIGITAL DELIVERABLES

Charts and digital deliverables overview						
Type	File Type		File Name	Deliverable	Unit (if applicable)	Comment
Chart	PDF		24004-OVR-001-01-01	Site overview	N/A	
Chart	PDF		24004-BSF-002-05-01	Top of unit depth below sea floor	I	
Chart	PDF		24004-BSF-002-06-01	Top of unit depth below sea floor	III	
Chart	PDF		24004-BSF-002-07-01	Top of unit depth below sea floor	IV	
Chart	PDF		24004-BSF-002-08-01	Top of unit depth below sea floor	V	
Chart	PDF		24004-MSL-003-05-01	Top of unit elevation to MSL	I	
Chart	PDF		24004-MSL-003-06-01	Top of unit elevation to MSL	III	
Chart	PDF		24004-MSL-003-07-01	Top of unit elevation to MSL	IV	
Chart	PDF		24004-MSL-003-08-01	Top of unit elevation to MSL	V	
Chart	PDF		24004-ISO-004-04-01	Unit Isochore (thickness)	I	
Chart	PDF		24004-ISO-004-05-01	Unit Isochore (thickness)	III	
Chart	PDF		24004-ISO-004-06-01	Unit Isochore (thickness)	IV	
Chart	PDF		24004-HAZ-005-01-00	Site geohazards	N/A	
Chart	PDF		24004-Zon-007-01-01	Geotechnical zonation	N/A	
Chart	PDF		24004-BTH-008-01-00	Bathymetry	N/A	
Grid	ASCII	GeoTIFF	Top_Unit_I_mBSF	Top of unit depth below sea floor	I	
Grid	ASCII	GeoTIFF	Top_Unit_IIIa_mBSF	Top of unit depth below sea floor	III	
Grid	ASCII	GeoTIFF	Top_Unit_IIIb_mBSF	Top of unit depth below sea floor	IV	
Grid	ASCII	GeoTIFF	Top_Unit_Va_mBSF	Top of unit depth below sea floor	V	
Grid	ASCII	GeoTIFF	Top_Unit_I_mMSL	Top of unit elevation to MSL	I	
Grid	ASCII	GeoTIFF	Top_Unit_IIIa_mMSL	Top of unit elevation to MSL	III	
Grid	ASCII	GeoTIFF	Top_Unit_IIIb_mMSL	Top of unit elevation to MSL	IV	
Grid	ASCII	GeoTIFF	Top_Unit_Va_mMSL	Top of unit elevation to MSL	V	
Grid	ASCII	GeoTIFF	Unit_I_Isochore	Unit Isochore (thickness)	I	
Grid	ASCII	GeoTIFF	UnitIIIa_Isochore	Unit Isochore (thickness)	III	

Charts and digital deliverables overview						
Type	File Type		File Name	Deliverable	Unit (if applicable)	Comment
Grid	ASCII	GeoTIFF	Unit_IIIb_Isochore	Unit Isochore (thickness)	IV	
Grid	ASCII	GeoTIFF	Base_Unit_I_mBSF	Base of unit depth below sea floor	I	Venterra additional deliverable
Grid	ASCII	GeoTIFF	Base_Unit_IIIa_mBSF	Base of unit depth below sea floor	III	Venterra additional deliverable
Grid	ASCII	GeoTIFF	Base_Unit_IIIb_mBSF	Base of unit depth below sea floor	IV	Venterra additional deliverable
Grid	ASCII	GeoTIFF	Base_Unit_I_mMSL	Base of unit elevation to MSL	I	Venterra additional deliverable
Grid	ASCII	GeoTIFF	Base_Unit_IIIa_mMSL	Base of unit elevation to MSL	III	Venterra additional deliverable
Grid	ASCII	GeoTIFF	Base_Unit_IIIb_mMSL	Base of unit elevation to MSL	IV	Venterra additional deliverable
Geodatabase	.GDB		N/A		N/A	

APPENDIX B - SEISMIC CROSS SECTIONS

APPENDIX C - UNITISED GEOTECHNICAL PARAMETERS

APPENDIX D - RISK REGISTER

APPENDIX E – GEOTECHNICAL CROSS SECTIONS



We **develop** and **engineer** major global wind farm projects across the **entire** wind farm life cycle.



FIND OUT MORE

Environmental | **Advisory** | **Survey** | **Geoscience** | **Design**



Venterra Group,
3rd Floor, Standbrook House,
2-5 Old Bond Street,
London, W1S 4PD



venterra-group.com



Follow us